Spreading waves of invasive species

by

Andriamihaja Ramanantoanina

Dissertation presented for the degree of Doctor of Philosophy at Stellenbosch University

Department of Mathematical Sciences,
University of Stellenbosch,
Private Bag X1, Matieland 7602, South Africa.

Promoters:

Dr. C. Hui
Dr. A. Ouhinou

April 2014

Declaration

By submitting this dissertation electronically, I declare that the entirety of the work contained therein is my own, original work, that I am the owner of the copyright thereof (unless to the extent explicitly otherwise stated) and that I have not previously in its entirety or in part submitted it for obtaining any qualification.

Signature: .....
A. Ramanantoanina

Date: April 2014 .....

Abstract

Spreading waves of invasive species

A. Ramanantoanina

Department of Mathematical Sciences,
University of Stellenbosch,
Private Bag X1, Matieland 7602, South Africa.

Dissertation: PhD

April 2014

Invasive species are well known to harm economy as well as ecological assets and impair ecosystems functioning around the world. Timely control and management of new incursions of invasive species necessitate predictive tools that can anticipate areas that are susceptible to the invasion as well as the rate of the species spread. Early models predicted that a single species invading a homogeneous landscape advances its range at a constant rate which is determined by the population's growth and dispersal rate. Although this result has been successfully used in numerous cases, it leaves unanswered different patterns of range expansion that have been observed in nature. The purpose of this thesis was to model and investigate different factors that can influence the spread of a species, with an emphasis on the rate of spread.

First, we investigated the influence of an initial population with mixed dispersal abilities. In a first case, we assumed that all individuals have the same dispersal ability with the exception of few individuals which are significantly better dispersers. In a second case, we assumed that the dispersal abilities in the initial population are log-normally distributed. A system of integrodifference equations was used to model the spatiotemporal dynamics of the population. We found that the dispersal abilities were spatially sorted. The instantaneous rate of spread was found to be fully determined by the growth and dispersal abilities of the population at the advancing edge of the invasion.

The results therefore suggest that data collected from the core of the invasion may underestimate the spread of the population. Finally, our results suggest that the three patterns of range expansions presented by Shigesada and Kawasaki in 1997 can be alternatively explained by the mixture of individuals with different dispersal abilities in the initial population.

Second, we studied the influence of environmental heterogeneity on the spread of a population using integrodifference model in which growth and dispersal parameters are functions of habitat quality. Two environmental structures were considered. The first structure consists of a fragmented environment in which the habitat quality is given by step functions. This environment was used to investigate the influence of landscape fragmentation on the rate of spread. In the second environment structure, the habitat quality varies sinusoidally in space. This case was used to examine the influence of the amplitude of environmental variations. Lower and upper bounds of the asymptotic rate of spread was derived and verified using numerical simulations. In the case of fragmented environment, we further investigated the proportion of favourable habitat that is optimal for the spread of the population. The results suggest that the presence of unfavourable habitats can act to accelerate the spread of a population. Finally, an increase in the variability of the growth or dispersal processes can accelerate or decelerate the spread of a population depended on whether growth and dispersal parameters oscillate in or out of phase.

Lastly, we investigated how two density-dependent dispersal behaviours, namely prey evasion (PE) and predator pursuit (PP), shape the dynamics of a predator-prey system. PE portrays the tendency of prey avoiding predators by dispersing into adjacent patches with fewer predators, while PP describes the tendency of predators to pursue the prey by moving into patches with more prey. We used a spatially explicit metapopulation model to capture the dynamics of the species. Local populations were modelled based on the Beddington predation model, and different locations were linked by dispersal which incorporate PE and PP. Exhaustive numerical simulations were used to investigate the effects of PE and PP on the spatial synchrony, the persistence of metapopulation as well as the rate of spread. Results show that both PE and PP can alter spatial synchrony although PP has a weaker desynchronising effect than PE. The predator-prey system without PE and PP expanded in circular waves. The effect of PE can push prey to distribute in a circular ring front, whereas the effect of PP can change the circular waves to anisotropic expansions. The effects of PE and PP further enhanced the population size, broke down spatial synchrony and promoted the persistence of populations. Finally, weak PE and PP can accelerate the spread of prey while strong and disproportionate intensities slow down the range expansion.

Uittreksel

Versprei golwe van indringerspesies

("Spreading waves of invasive species")

A. Ramanantoanina

Department van Wiskundige Wetenskappe,
Universiteit van Stellenbosch,
Privaatsak X1, Matieland 7602, Suid Afrika.

Proefskrif: PhD

April 2014

Indringerspesies is alom bekend om beide ekonomiese en ekologiese sisteme te benadeel en die funksionering van ekosisteme regoor die wêreld negatief te beïnvloed. Gepaste monitering en bestuur van nuwe aanvalle van indringerspesies vereis gereedskap wat kan voorspel watter areas is vatbaar vir indringers sowel as die tempo van die verspreiding van spesies. Vroeë modelle het voorspel dat 'n enkele spesie wat 'n homogeniese landskap binne treë versprei teen 'n konstante tempo wat bepaal word deur die spesie bevolking se groeikoers en verspreidings tempo. Alhoewel hierdie resultaat suksesvol gebruik was in menigte gevalle, laat dit verskillende patrone van reeks uitbreiding wat waargeneem word in die natuur steeds onbeantwoord. Die doel van hierdie tesis was om die verskillende faktore wat die verspreiding van 'n spesie beïnvloed te modelleer en te ondersoek, met die klem op die tempo van verspreiding.

Eerstens, het ons die invloed van 'n oorspronklike bevolking met gemengde verspreidings vermoëns ondersoek. In 'n eerste geval, het ons aanvaar dat alle individue dieselfde verspreidings vermoëns besit met die uitsondering van enkele individue wat aansienlik beter versprei. In 'n tweede geval, het ons aanvaar dat die verspreidings vermoëns in die aanvanklike bevolking log-normaal versprei . 'n Stelsel van integro-verskil vergelykings was gebruik om die tydruimtelike

dinamika van die bevolking te modelleer. Ons het gevind dat die verspreiding vermoëns ruimtelik gesorteer was. Die oombliklike tempo van verspreiding was gevind om ten volle bepaal te word deur die groei en verspreiding vermoëns van die bevolking op die bevorderings rand van die inval. Die resultate dui dus daarop dat data wat versamel is vanuit die kern van die inval kan die verspreiding van die bevolking onderskat. Ten slotte, ons resultate dui daarop dat die drie patrone van reeks uitbreidings aangebied deur Shigesada en Kawasaki in 1997 kan alternatiewelik verduidelik word deur die mengsel van individue met verskillende verspreiding vermoëns in die oorspronklike bevolking.

Tweedens, het ons die invloed van heterogeniteit van die omgewing op die verspreiding van 'n bevolking bestudeer deur 'n integro-verskil model te gebruik waarin groei en verspreiding veranderlikes funksies is van habitat kwaliteit. Twee omgewings strukture was oorweeg. Die eerste struktuur het bestaan uit 'n gefragmenteerde omgewing waar die habitat kwaliteit deurgegee word as trap funksies. Hierdie omgewing was gebruik om die invloed van die landskap versnippering op die tempo van verspreiding te ondersoek. In die tweede struktuur omgewing, het die habitat kwaliteit sinusoïdaal gewissel in die ruimte. Hierdie saak was gebruik om die invloed van die amplitude van die omgewing variasies te ondersoek. Onderste en boonste grense van die asimptotiese tempo van verspreiding was afgelei en geverifieer deur gebruik te maak van numeriese simulasies. In die geval van 'n gefragmenteerde omgewing, het ons verdere ondersoek ingestel oor die verhouding van gunstigde habitat wat optimaal is vir die verspreiding van die bevolking. Die resultate dui daarop dat die teenwoordigheid van ongunstige habitatte kan optree om die verspreiding van 'n bevolking te versnel. Ten slotte, 'n toename in die wisselvalligheid van die groei of verspreiding prosesse kan die verspreiding van 'n bevolking versnel of vertraag afhangende of die groei en verspreiding parameters ossilleer binne of buite fase.

Laastens, het ons ondersoek hoe twee digtheids-afhanklike verspreidings gedrag, naamlik prooi ontduiking (PE) en roofdier strewe (PP), die dinamika van 'n roofdier -prooi stelsel vorm. PE beeld die neiging van die prooi om die roofdiere te vermy deur te versprei na aangrensende gebiede met minder roofdiere, terwyl PP beskryf die neiging van roofdiere om prooi na te streef deur te beweeg na gebiede met meer prooi. Ons het 'n ruimtelik eksplisiete meta populasie model gebruik om die dinamika van die spesies vas te vang. Plaaslike bevolkings was gemodelleer deur middel van die Beddington roofdiere model, en verskillende plekke was verbind deur verspreiding wat beide PE en PP inkorporeer. Vele numeriese simulasies was gebruik om die gevolge van PE en PP op die ruimtelike sinkronie, die voortbestaan van die meta populasie sowel as die tempo van verspreiding te ondersoek. Resultate toon dat beide PE en PP die ruimtelike sinkronie kan verander hoewel PP het 'n swakker desinkronie effek as PE. Die roofdier -prooi stelsel sonder PE en PP het uitgebrei in sirkelvormige golwe.

Die effek van PE kan prooi forseer om te versprei in 'n ring, waar die effek van PP die sirkelvormige golwe kan verander na anisotrope uitbreidings. Die gevolge van die PE en PP verder versterk die grootte van die bevolking, breek die ruimtelike sinkronie en bevorder die voortbestaan van bevolkings. Ten slotte, swak PE en PP kan die verspreiding van die prooi versnel, terwyl sterk en oneweredige sterkte vertraag die uitbreidings reeks.

Acknowledgements

Conducting a PhD is never the work of anyone alone. The contributions of different people have made this possible. I would like to extend my appreciation especially to the following.

My supervisors Dr. Cang Hui and Dr. Aziz Ouhinou. This thesis would not have been possible without their guidance during the research and their valuable comments on the manuscripts. While working with them I have learned quite a lot.

The Center for Invasion Biology (C.I.B) for their financial support during this Ph.D. I also gratefully acknowledge the use of the services and facilities of the African Institute for Mathematical Sciences (AIMS). I am appreciative of the staff members of both institutions for their academic, administrative and logistic supports.

My friends for their encouragements and advices. I am especially thankful to pt for proofreading the manuscripts and Marinel for the Afrikaans translation of the abstract. I am also thankful the participants to the "Theoretical Ecology Journal Club" of C.I.B for the knowledges they shared and the inspiring discussions on Ecology and Mathematical Ecology.

The Rabenantoandro family for their ceaseless support and prayers ... and for all the pecto, mofobaolina, voanjobory etc hihi.

My family for everything. To my father, Manerana. To mother, Mitady Anao. To Zoky sy Zandry, Hanina Anareo. To Andry, Kilome.

Last, but not least, thank you Heavenly Father for the countless blessings You poured into my life, specially since some August 2009.

Dedications

Ho an'i Dada tiako indrindra (To my father)

Contents

List of Figures

List of Tables

Chapter 1

Introduction

The applications of theoretical ecology range from the understanding of the natural world to explaining ecological phenomena and predicting the future behaviour of populations. In particular the spread of invasive organisms such as infectious diseases poses major worldwide problems in terms of ecology, health and economic impacts (the latter, estimated into the billions of dollars) (With, 2002; Pimentel *et al.*, 2005). Examples of invasive species are diverse, including mammals such as muskrats (*Ondatra zibethica*) in Europe, and birds such as the European starling (*Stumus vulgaris*) and house finch (*Carpodacus mexicanus*) in the USA (reviewed by Shigesada and Kawasaki (1997)). Insect invasions are also well documented as they often generate extensive agricultural damages (Liebhold and Tobin, 2008).

The invasion process is often divided into a series of stages. Common stages of invasions are identified as the transportation (from the species native range), introduction, establishment and the spread into an exotic location (Hastings, 1996; Blackburn *et al.*, 2009). All stages of the invasion are important and have been the subject of numerous investigations (Blackburn *et al.*, 2009; Davis, 2009). The goals of such investigations include the identification of potential invaders and susceptible regions, the estimation of the progress of the invasion and the prediction of its ecological impact (Andow *et al.*, 1990; Shigesada and Kawasaki, 1997). In particular, understanding the spread of invasive species has always been one of the main issues in Ecology.

The understanding of the spread of invasive species is of twofold interest. On the one hand, the term "invasive species" commonly refers to a group which, when introduced into a new environment, is likely to become environmental, ecological or economic pests, or on occasion human health impairment (see for example Savidge (1987); Seward *et al.* (2004); Blackburn *et al.* (2009) and references therein). The comprehension of their spread, both in terms of

rate and manner, is crucial for timely management as it can unravel different mechanisms and factors that affect the dynamics of species' geographical range (expansion or retraction) (Liebhold and Tobin, 2008; Sattenspiel, 2012). On the other hand, populations' spread has been speculated to play a role in shaping native and invasive species distributions and community compositions, and influence a population's persistence (Levine and Murrell, 2003; Zalewski and Ulrich, 2006; Flinn *et al.*, 2010).

A population's spread starts at individual level by each organism's need to disperse in order to promote their survival. From this rather instinctive motive of individuals' dispersal however emerged complex collective effects. Namely the population's spread and geographic range remain a major debate as different patterns of range dynamics have been observed in nature. For instance, Shigesada and Kawasaki (1997) reported three patterns of range expansion. The first type of pattern consists of a linear range expansion during which the population expands its range at a constant rate. The second type of pattern is characterised by a break of slope in the range versus time curve. Namely the invasion starts with a linear slow expansion followed by another linear expansion which occurs at a faster rate. The third pattern involves continuously increasing rate of spread, that is continuously accelerating range expansions.

The rate and direction of a population's spread rely on two components, namely the growth of local populations and the dispersal of individuals (Clark *et al.*, 2001; Coulson and Godfray, 2007). Dispersal plays an important role on the population's spread as it allows individuals to locate new habitats and occupy the extent of the available environment. Different types of dispersal have been identified, namely secular migrations, diffusions and long-distance dispersals (Pielou, 1979). Secular migrations involve slow migration accompanied by adaptation, sometimes speciation, and can yield range expansion or range shift over long time intervals (thousands or millions of years). Diffusion is concerned with individual movements based on random walk, yielding a normal distribution of the dispersal distance during a given period of time (Pielou, 1969; Lewis, 1997). There are however empirical evidences of fat-tailed distributions of dispersal distance (Hengeveld, 1989; Veit and Lewis, 1996; Clark *et al.*, 1998). Such movements are the subjects of long distance dispersals. As opposed to secular migrations, diffusion and long distance dispersals take place as the population grows.

Fields and laboratory observations have shown that a multitude of processes, ranging from species-based mechanisms to environment-based phenomena, can influence the two last types of dispersals. Immediate causes include crowding and the availability of food in the local habitat. In some cases, active dispersal was observed to be density-dependent, that is, the magnitude of dispersal depends on the local population size for example when competition in a

crowded area forces individuals to emigrate (positive density-dependence) or when crowding effects impair dispersal abilities (negative density-dependence) (See Ims and Andreassen (2005); Matthysen (2005) and Nowicki and Vrabec (2011)). Range expansions are also particularly noticeable when juveniles leave their natal sites and do not return (Savidge, 1974; Gaines and Bertness, 1993). Environmental conditions also contribute to different dispersal behaviours as individuals in quest for more favourable habitats may emigrate (Pärn *et al.*, 2012).

In addition to dispersal, the spread of a population is also highly correlated to the population growth (Veit and Lewis, 1996; Neubert and Caswell, 2000). Indeed, the oldest branch of Mathematical Ecology focuses on the increase and decline of populations, as all populations fluctuate in size (Malthus, 1798; Pielou, 1977). Population growth is clearly linked to the surrounding environments, including the population size itself. For instance, as the population grows, the population size is bound to eventually exceed the available resource and thereby induces a lower birth rate or higher mortality rate (Coulson and Godfray, 2007). Furthermore, there are also evidences of populations which grow slower when the population density is low. This phenomenon is commonly known as the Allee effect (Allee and Bowen, 1932; Veit and Lewis, 1996).

Mathematical and computational modelling have been powerful approaches for predicting species' range dynamics. Theoretical studies of ecological spread started with the seminal works of Skellam (1951). In his studies, Skellam (1951) used reaction-diffusion models based partial differential equations (PDE), which had initially been developed by Fisher (1937) (see also Kolmogorov *et al.* (1991)) for the spread of an advantageous allele in a population, in order to investigate the spread of muskrats in Europe. Early spread models, which incorporated the movements of individuals in reaction-diffusion models using a constant diffusion term and described the growth dynamics of the population using the most simple growth functions, lead to a robust and well known prediction of a constant rate of spread in the long term. As more field data have become available, more versatile models have also been developed from the Skellam's initial case to investigate the effects of different assumptions such as density-dependent diffusion (Sanchez-Garduno and Maini, 1994; Sanchez-Garduno *et al.*, 1997), spatially varying growth and diffusion (Shigesada *et al.*, 1986; Kinezaki *et al.*, 2006), density-dependent growth functions such as Allee effects (Lewis and Kareiva, 1993) and interactions with other species (Dunbar, 1983, 1984; Shigesada and Kawasaki, 1997; Hosono, 1998). An early review presented by Holmes *et al.* (1994) showed that reaction-diffusion models in the PDE framework could successfully depict numerous features of ecological phenomena and interactions. Traditional reaction-diffusion models however suffer from one major limitation, as their uses are inherently confined to populations

for which demographic processes and individuals movements can continuously occur in time and space, and individuals possess normally-distributed dispersal distances over a fixed period of time (Skellam, 1951; Holmes *et al.*, 1994).

Another line of spread models explicitly incorporates the distribution of dispersal distance to describe individuals' movement in the system. These classes of models have the advantage that the distribution of dispersal distance over a given period of time (also known as the dispersal kernel) is not necessarily a normal distribution (Kot *et al.*, 1996). Furthermore, dispersal kernel models are available in the literature in continuous (Mollison, 1977) as well as in discrete-time (Kot *et al.*, 1996). Like reaction-diffusion models, dispersal kernels models were used in population genetics (Weinberger, 1982) prior to their applications to population ecology. In discrete-time dispersal kernel models (known as integrodifference equations), population growth is assumed to occur during a sedentary stage whereas individual movements take place during the dispersal stage. The models are therefore suitable for organisms with non-overlapping generations and separated growth and dispersal stages. Classic examples of such populations include annual plants and seasonal insects (Liebhold and Tobin, 2008). Depending on the shape of the dispersal kernel, integrodifference models have yielded different range expansion patterns and have led to an attribution of the accelerating nature of range expansion to considerable long-distance dispersal (Kot *et al.*, 1996). Like reaction-diffusion models, dispersal kernel models have been extended to incorporate density-dependent dispersal (Veit and Lewis, 1996; Lutscher, 2008), spatially varying dispersal kernels (Kawasaki and Shigesada, 2007; Weinberger *et al.*, 2008), Allee effects (Wang *et al.*, 2002) and biotic interactions (Hosono, 1998; Li and Li, 2012).

A third line of models for spatial spread consists of stochastic and spatially explicit models (that is models that use geographical space to incorporate habitat features). Rapid advances in computer technology have allowed for extensive use of spatially explicit models for ecological spread. These are particularly powerful when incorporating demographic stochasticity as well as different landscape features such as dispersal barriers (Dunning Jr. *et al.*, 1995). Although the complexity of the resulting models often does not allow mathematical investigations, computational experiments have led to momentous highlights for instance on the role of long-distance dispersal (Pearson and Dawson, 2005). Recent uses of spatially explicit models suggest the evolution of dispersal strategies as an alternative explanation of the accelerating nature of range expansion (Phillips *et al.*, 2008; Travis *et al.*, 2009).

Although giant strides have been made with mathematical and computational models for the spread of invasive species, the theory of spatial spread is not complete. First, major contributions to the understanding of the rate of spread

tend to ignore details on the initial population or the propagule pressure. The propagule pressure, also known as introduction effort, is a composite measure of the initial population and commonly includes the number of individuals released in an alien environment and the number of releases (Lockwood *et al.*, 2005). There are significant empirical and theoretical evidences that propagule pressure promotes the success of species' establishment in the novel environment (Lockwood *et al.*, 2005; Mikheyev *et al.*, 2008; Simberloff, 2009; Gertzen *et al.*, 2011). Speculations also have emerged that propagule pressure influences to the rate of spread of a population (Wilson *et al.*, 2007). However, there has been a lack of theoretical investigations into the role of the propagule pressure to the dynamics of invasive species beyond a successful establishment. This issue will be approached in the third chapter of this thesis. Namely, we will construct a model in which the initial population consists of individuals with different dispersal abilities. We further assume the dispersal abilities are determined by inherited traits of an asexual species (Jenkins *et al.*, 2007; Talavera *et al.*, 2012). We consider different distributions of the dispersal abilities in the initial popualation and investigate their effects on the rate of spread.

Secondly, the spread of invasive species in heterogeneous environments has not been fully investigated. Spread models in a periodic environment were pioneered by Shigesada *et al.* (1986) in the PDE framework. Spatial spread in heterogeneous environments has since known great progresses. While some works focus on the investigation of the spread of organisms with different assumptions (Shigesada *et al.*, 1986; Kawasaki and Shigesada, 2007), others made previous results more clear for applied and theoretical purposes (Weinberger *et al.*, 2008). In the fourth chapter of this thesis, integro-difference equations (IDE) are used to investigate the spread of a population in a heterogeneous environment. In addition to the assumptions in earlier models that the population growth and dispersal kernels vary with the environment, we consider that, depending on the local habitat quality, a part of the population remains sedentary during the dispersal phase. Fragmented as well as sinusoidally varying environments are considered. While the fragmented environment is related to the geographical locations of favourable and unfavourable habitats, the sinusoidally varing environment emphasizes the difference between habitat qualities. In both context, we derive approximations of the asymptotic rate of spread.

Finally this thesis contributes to the understanding of the role of inter-specific interactions on the range expansions. Classic models that consider inter-specific often do not emphasize dispersal behaviours that result from species interactions (Dunbar, 1983, 1984; Hosono, 1998). Species interactions however have been observed to influence individual dispersal behaviours (Madsen and Shine, 1996; Morse, 2006; Weng *et al.*, 2007). In the fifth chapter of this thesis, we construct a model in which interactions between prey and predator species

are not limited to growth functions but also affect individuals movements in either species. We highlight the importance of dispersal behaviours in the spatiotemporal distribution of the spreading species as well as their rate of spread.

The remainder of this thesis is organised as follows. In the second chapter, we provide a review of existing mathematical spread models. In the third chapter, investigate the spread of a population from a mixed initial propagule. In the fourth chapter, we study the spread of a population in heterogeneous environments. The fifth chapter is devoted to the spatio-temporal dynamics of a predator-prey system with density-dependent dispersal behaviours, namely prey evasion and predator pursuit. In the last chapter, we discuss the models presented in Chapters 3, 4 and 5 with an emphasis on possible extensions of the models.

Chapter 2

Spread models for invasive species

The study of the spread of invasive species can be traced back to the work of Skellam (1951). It has ever since made great theoretical progresses, mainly through different assumptions on the growth and dispersal processes. In this chapter, we review major developments in the study of spread of invasive species. A summary of the rates of spread derived from different models is provided in Table 2.1 and a summary of modelling frameworks is presented in Table 2.2.

2.1 Single species growth models

Different investigations have demonstrated a correlation between the population growth rate and the rate of spread (Veit and Lewis, 1996; Neubert and Caswell, 2000). Population growth is usually modelled in discrete or continuous time frameworks depending on whether the species under investigation has non-overlapping generations.

The earliest growth model was due to Malthus (1798). The model suggests that the rate of change in the population growth is proportional to the population size. For continuous growths, the model can be phrased as an ordinary differential equation

$$\frac{\mathrm{d}u}{\mathrm{d}t} = ru \tag{2.1.1}$$

where $u(t)$ is the population size at time t and $r \geq 0$ is the intrinsic growth rate. The Malthusian model yields an exponentially increasing population size

$$u(t) = u_0 e^{rt},$$

where $u_0 > 0$ is the initial population size. For species with non-overlapping generations, the exponential growth is modelled by the difference equation

$$u(t+1) = ru(t) \tag{2.1.2}$$

and solves into

$$u(t) = u_0 r^t,$$

which grows exponentially whenever r is larger than 1. The Malthusian growth assumes that the population grows without external influence and is most accurate for a short time interval.

For longer time interval, demographic processes are subject to different external factors such as the availability of resource. These growth constraints were modelled by Verhulst in the 19th century by introducing a term that slows the population growth as the population size increases (Verhulst, 1838). A model resulting from such correction is commonly known as a logistic model. A commonly used logistic model for a continuous growth takes the form

$$\frac{\mathrm{d}u}{\mathrm{d}t} = ru\left(1 - \frac{u}{K}\right). \tag{2.1.3}$$

The number $K \geq 0$, referred to as the carrying capacity of the environment, depicts the maximal population size that the environment can support. A discrete logistic growth was due to Ricker (1954) and is phrased as

$$u(t+1) = u(t)e^{r(1-\frac{u(t)}{K})}. \tag{2.1.4}$$

The Ricker model describes an overcompensatory growth, that is the population growth is exponentially constrained by the environment when the population size is large. A less dramatic decline of reproduction at high population size was introduced by (Beverton and Holt, 1957) and takes the form

$$u(t+1) = \frac{ru(t)}{1 + (r-1)u(t)/K}. \tag{2.1.5}$$

Typically, the population size increases below the carrying capacity and decreases above it. However, it is worth to note that the carrying capacity

consists of a different concept from the equilibrium of a population. In particular, the carrying capacity of an environment may change over time (Meyer and Ausubel, 1999).

The per-capita growth rate can also be altered by low population size due to different mechanisms such as a reduced mating probability or less collective defence (Boukal and Berec, 2002; Kramer *et al.*, 2009). More clearly, there are evidences that the population size and the per-capita growth rate are positively correlated. This phenomenon is commonly known as the Allee effect after the observation by its namesake (Allee, 1931). Numerous models have been used to depict the dynamic of a population subject to Allee effect (Boukal and Berec, 2002), including the model by Lewis and Kareiva (1993)

$$\frac{\mathrm{d}u}{\mathrm{d}t} = ru\,(u-\alpha)\left(1-\frac{u}{K}\right) \tag{2.1.6}$$

where α is a threshold density under which the population growth rate is negative (See also Gruntfest *et al.* (1997)).

2.2 Spread models for single species

In addition to the population growth, the spread of a population also relies on dispersal processes which allow individuals to move from their birth place into new locations. Dispersal can be of diffusive nature and happens gradually in the extent of the environment (Okubu, 1988), or feature long distance jumps and yields more patchily distributed population (Mollison, 1977). Dispersal processes, combined with growth models form the core of spread models for invasive species.

2.2.1 Partial differential equations

Partial differential equations (PDE) are commonly used to model the spread of a population with a diffusive dispersal. In one dimensional habitats, classical PDE models for the spread of a population are of the form

$$\frac{\partial u}{\partial t} = D\frac{\partial^2 u}{\partial x^2}u + g(u) \tag{2.2.1}$$

where $u(x,t)$ is the population size at location x and time t, D and g indicate the diffusion rate and the population growth respectively. In the Skellam

(1951) model, the population undergoes Malthusian growth, whereas in the Fisher (1937) model, a logistic population growth is used. Both models lead to a constant asymptotic rate of spread

$$c = 2\sqrt{g'(0)D}. \tag{2.2.2}$$

The derivation of rate of spread relies on the linearisation of Eq. 2.2.1 when the population size is low, and the prediction of the rate of spread (Eq. 2.2.2) holds when the maximal growth rate is associated to low population size ($g(u) \leq g'(0)u$).

In the presence of Allee effects, that is the population growth is reduced at low density (Eq. 2.1.6) (Allee, 1931; Allee and Bowen, 1932; Kramer *et al.*, 2009), Lewis and Kareiva (1993) showed that a successful invasion occurs only if the Allee effect is less than half the carrying capacity ($\alpha < K/2$). In this case the rate of spread is given by

$$c = \sqrt{2rD}(K/2 - \alpha). \tag{2.2.3}$$

Similar to the population growth, dispersal can also be influenced by the population size (Krebs *et al.*, 1973; Bengtsson *et al.*, 1994)(See also Matthysen (2005); Denno and Peterson (1995) for evidence of density-dependent dispersals.) Density-dependent dispersal was introduced by Gurney and Nisbet (1975) to regulate population size along with density dependent growth rates. Sanchez-Garduno and Maini (1994) later showed that the spread of a population with density-dependent dispersal can be modelled by

$$\frac{\partial u}{\partial t} = \frac{\partial}{\partial x}\left(D(u)\frac{\partial u}{\partial x}\right) + g(u). \tag{2.2.4}$$

The existence of a travelling wave solution has been established for different classes of diffusion functions both when $D(u) > 0$ or non-degenerate (Hadeler, 1981) and when $D(0) = 0$ or degenerate case (Sanchez-Garduno *et al.*, 1997). In the latter case, different shape of travelling waves were observed, namely sharp-type or front-type, depending on whether $D'(0)$ vanishes or not.

2.2.2 Dispersal kernel models

One major pitfall of the PDE models discussed above is their limitation to neighbouring dispersal. The models assume that the distance an individual

achieves during a dispersal stage follows a Gaussian distribution. This limitation can be overcome by the use of integrodifference or integrodifferential equations which feature a probability function to model dispersal distances (Hui *et al.*, 2011). Such function, commonly referred to as *dispersal kernel* or *redistribution kernel*, gives the probability density function for the location x to which an individual at y disperses during the dispersal phase. In addition to their ability to incorporate different dispersal kernels, integrodifference models are also commonly used to model a population which undergo growth and dispersal phase in separate stages (Lutscher and Petrovskii, 2008).

Let $k(x, y)$ denote the dispersal kernel and $u(x, t)$ the population size at time t. The population size at location x after the growth and dispersal stages is given by

$$u(x, t+1) = \int k(x, y) g(y, u(y, t)) \mathrm{d}y. \tag{2.2.5}$$

In a homogeneous landscape, that is $g(x, u) = g(u)$ and $k(x, y) = k(|x - y|)$, Mollison (1991) gathered conditions, commonly referred to as the *linear conjecture*, under which non-linear models such as Eq. 2.2.5 result into the same rate of spread as their linear approximation, here given by

$$u(x, t+1) = \int k(|x - y|) g'(0) u(y, t) \mathrm{d}y. \tag{2.2.6}$$

The linear conjecture holds whenever (i) the non-linear model is bounded by its linearisation and (ii) individuals only have influence on nearby locations. The first condition is verified for example when the growth rate is highest in newly discovered habitats, that is $g(u) \leq g'(0)u$ (Mollison, 1991). The second condition is the case for instance when there is no long-distance density dependence. The Ricker (1954) and the Beverton and Holt (1957) models, which are logistic models, are common examples of such growth functions.

When the linear conjecture holds, Kot *et al.* (1996) thoroughly investigated the IDE 2.2.5 and found that the rate of spread is highly influenced by the shape of the dispersal kernel k, more particularly by its moments. The authors established that

- If the dispersal kernel it admits a moment generating function

$$M(s) = \int k(z) e^{sz} \mathrm{d}z \tag{2.2.7}$$

for some $s > 0$ (k is exponentially bounded), the population governed by Eq. 2.2.5 expands its range at a constant rate of spread

$$c = \min_{s \in I} \frac{1}{s} \ln \left[g'(0) M(s) \right], \tag{2.2.8}$$

where I is the interval in which the moment generating function is defined.

In particular, when only a part of the population migrates during the dispersal phase, the population can be modelled by

$$u(x, t+1) = \int dk(x, y) g(u(t, y) \mathrm{d}y + (1 - d) g(u(t, x)) \tag{2.2.9}$$

where d is the dispersal probability. The asymptotic rate of spread is given by

$$c = \min_{s \in I} \frac{1}{s} \ln \left[g'(0)(dM(s) + (1 - d)) \right]$$

and increases with the dispersal probability d Lutscher (2008).

- If the dispersal kernel does not have a moment generating function but the moments

$$\mu_n = \int k(z) z^n \mathrm{d}z$$

are finite for all n (k is heavy-tailed), the population expands at polynomially increasing rate;

- If the dispersal kernel has infinite moments (k is fat-tailed), the population expands at exponentially increasing rate.

Although the linear conjecture does not hold for species exhibiting Allee effect and no explicit formula have not been derived for the rate of spread for IDE models in this case, Wang *et al.* (2002) established necessary and sufficient conditions for the success of an invasion and it is speculated that the presence of Allee effect has the potential to reduce the rate of spread (Kot *et al.*, 1996).

Similar to PDE models, IDE models have been extended to incorporate density-dependent dispersals. Veit and Lewis (1996) introduced density-dependent

dispersal in the IDE framework to model the invasion of house finch. Lutscher (2008) established a framework for more general cases of IDE.

$$u(x,t+1) = \int k(x,y)D[g(u(y,t)]g(u(y,t))\mathrm{d}y + (1 - D[g(u(x,t))])g(u(x,t)). \tag{2.2.10}$$

In Eq. 2.2.10, an individual will emigrate from its location with probability $D(u)$ and will remain with probability $1 - D(u)$. It is worth noting that the growth and dispersal processes occur separate in time, so that the post-reproduction dispersal rate is given by $D(g(u))$. The resulting rate of spread however remains an open problem as the linear conjecture does not hold for density-dependent IDE.

2.2.3 Stratified diffusion

Diffusive and long distance dispersals can occur simultaneously. The joint dispersal pattern is termed *stratified diffusion* (Hengeveld, 1989). While the long distance aspect of a stratified diffusion allows the formation of new colonies ahead of the population front, the diffusive dispersal drives the range expansion of individual colonies. Eventually, different colonies coalesce and form a large block of invaded region.

Shigesada *et al.* (1995) modelled stratified diffusions by assuming that individual colonies expand their ranges at a constant rate c (Skellam (1951)), and new colonies establish at a rate $\lambda(r)$ from a colony of radius r. The authors established that the total area occupied by the population is given by

$$A(t) = \int_0^\infty 2\pi r\rho(r,t)\mathrm{d}r \tag{2.2.11}$$

where $\rho(r,t)$ is the distribution of colony size at time t; in other words $\rho(r,t)\mathrm{d}r$ gives the number of colonies with radius between r and $r+\mathrm{d}r$. The distribution of colony size is governed by the von Foester equation

$$\frac{\partial\rho}{\partial t} + c\frac{\partial\rho}{\partial r} = 0 \tag{2.2.12}$$

with

$$\rho(r,0) = \delta(r)$$

which represents the initially introduced population; and

$$c\rho(0,t) = \int_0^\infty \lambda(r)\rho(r,t)\mathrm{d}r$$

which depicts the number of newly formed colonies (with radius $r = 0$) at time t.

The model yields an initial slow range expansion, which is determined by the diffusion of the initial population, followed by an accelerating range expansion (Andow *et al.*, 1993; Shigesada *et al.*, 1995). The acceleration of the later phase of the invasion depends on the colonisation rate $\lambda(r)$.

2.2.4 Metapopulation models

The concept of mepatopulation finds its origin from Levins (1969). Levins (1969) compared a metapopulation to a population of local populations which grow in discrete patches and can be unstable. The "birth" of a local population consists of the colonisation (or re-colonisation) of an unnocupied patch, whereas the "death" process corresponds to the extinction of the local population. As opposed to the PDE and dispersal kernel models, metapopulation models often assume that space is discrete. Metapopulation models are frequently used to investigate the effects of local dynamics population and migration among patches on the regional dynamics, namely the persistence of the overall population (Hanski, 1998). Levins'occupancy model however can be used to study the spread of a population.

Levins'model simplifies the local population dynamics and considers only whether a patch is populated or not. The model is phrased by the ordinary differential equation

$$\frac{\mathrm{d}P}{\mathrm{d}t} = \kappa P(1-P) - \epsilon P \tag{2.2.13}$$

where κ and ϵ denote the colonisation and extinction rates respectively. Assuming that the occupied area is circular, the rate of spread can be approximated by

$$c(t) = \frac{1}{\sqrt{2\pi P}}\frac{\mathrm{d}P}{\mathrm{d}t}.$$

Clearly the model depicts the logistic dynamics of species occupancy and predicts an increasing rate of spread when the occupancy is low. The rate of spread

decreases as the occupancy approaches the equilibrium value $\hat{P} = 1 - \frac{\epsilon}{\kappa}$. The model further predicts that the available environment can be fully occupied at equilibrium only when $\epsilon = 0$, that is the local populations do not go extinct (Hui *et al.*, 2011).

2.3 Environmental heterogeneity

The spread models presented in the previous sections were constructed on homogeneous landscapes in which growth and dispersal functions do not depend explicitly on the quality of the habitats. Skellam (1973) however noted that the dispersal of the population can be influenced by external factors such as the distribution of food or attracting and repelling substances. A review by With (2002) pointed that both demographic and dispersal processes can be affected by environmental heterogeneity (See also Hastings *et al.* (2005)).

Different mathematical models have been used to elucidate the role of landscape features and to estimate the spread of a species in a heterogeneous environment. The use of PDE models to investigate the effects of environmental heterogeneity was pioneered by Shigesada *et al.* (1986) (See also Berestycki *et al.* (2005)). The one-dimensional landscape consisted of alternating "favourable" and "unfavourable" patches with different growth and dispersal parameters. The model has the form

$$\frac{\partial u}{\partial t} = \frac{\partial}{\partial x}\left(D(x)\frac{\partial u}{\partial x}\right) + r(x)u(1-u) \tag{2.3.1}$$

where

$$D(x) = D_1 \text{ if } x \text{ is a favourable habitat and } D_2 \text{ otherwise,} \tag{2.3.2}$$

and

$$r(x) = r_1 \text{ if } x \text{ is a favourable habitat and } r_2 \text{ otherwise.} \tag{2.3.3}$$

The model was later extended by Kinezaki *et al.* (2006) to study the invasion of sinusoidally varying environments. From both models, it was shown that although the range expansion accelerates or decelerates depending on the habitat quality at the front location, the average rate of spread can be approximated by

$$c = 2\sqrt{< r >_A < D >_H} \tag{2.3.4}$$

where $< r >_A$ and $< D >_H$ denote the arithmetic mean of the growth rate and the harmonic mean of the dispersal rate respectively.

Spatial heterogeneities have also been implemented in IDE frameworks. Kawasaki and Shigesada (2007) established the rate of spread of a population following an IDE model with Laplace dispersal kernel and periodically varying growth rates. Weinberger *et al.* (2008) and Dewhirst and Lutscher (2009) extended the model to include spatial heterogeneity in the dispersal kernel. The population density in the next generation arises mathematically as

$$u(x, t+1) = \int k(x, y) g(u, y) \mathrm{d}y. \tag{2.3.5}$$

For a Ricker (1954) growth, g is given by

$$g(u, y) = u e^{r(y)u(1-u)}$$

where r is the same as in Eq. 2.3.3. The spatial dependence of the dispersal kernel was reflected in its variance, which varies with the quality of the origin of dispersal events. Dewhirst and Lutscher (2009) showed that when the habitat consists of alternating "favourable" and "unfavourable" patches, the population spreads if the spatial average of the growth rate satisfies

$$pe^{r_1} + (1-p)e^{r_2} > 1$$

where p is the proportion of "favourable" habitats. In this case, the rate of spread is given by

$$c = \min_{s \in I} \frac{1}{s} \left(pe^{r_1} M_1(s) + (1-p)e^{r_2} M_2(s) \right) \tag{2.3.6}$$

if the dispersal kernels in favourable and unfavourable patches admit moment generating function M_1 and M_2 respectively on the interval I. Although no theoretical proof has been completed, numerical simulations suggest that this result is still valid when the environment is formed by randomly tallying favourable and unfavourable patches of length p and $1-p$ respectively (Kawasaki and Shigesada, 2007; Dewhirst and Lutscher, 2009).

2.4 Biotic interactions

The models that we have presented so far assume that invading organisms are isolated in the region and do not interact with other species. Different fields data however have demonstrated that interspecific interactions can, not only promote local extinctions and shape the species distribution (Bengtsson, 1989; Okubo *et al.*, 1989), but also influence the rate of the spread (Ferrer *et al.*, 1991; Fraser and Gilliam, 1992).

The spatiotemporal dynamics of two interacting species u_1 and u_2 can be depicted by

$$\frac{\partial u_1}{\partial t} = D_1 \frac{\partial^2 u_1}{\partial x^2} + g_1(u_1, u_2) \tag{2.4.1}$$

$$\frac{\partial u_2}{\partial t} = D_2 \frac{\partial^2 u_2}{\partial x^2} + g_2(u_1, u_2). \tag{2.4.2}$$

For competing species, Okubo *et al.* (1989) used the relations

$$g_1(u_1, u_2) = u_1(r_1 - \mu_{11}u_1 - \mu_{12}u_2) \tag{2.4.3}$$

$$g_2(u_1, u_2) = u_2(r_2 - \mu_{21}u_1 - \mu_{22}u_2). \tag{2.4.4}$$

In a region that is occupied by a resident species u_1, the success of an invasion by a competitor u_2 is fully determined by its competitive strength (Shigesada and Kawasaki, 1997; Hosono, 1998). Namely if $r_1\mu_{21} < r_2\mu_{11}$, the invading species u_2 spreads at rate

$$c_2 = 2\sqrt{r_2 D_2 \left(1 - \frac{r_1\mu_{21}}{r_2\mu 11}\right)}. \tag{2.4.5}$$

The expression of the rate of spread indicates that the rate of spread of the invading species is negatively influenced by its native competitor. Such phenomenon has been observed in nature for the example in the case of European starling as reported by Ferrer *et al.* (1991).

For a predator-prey interaction, the growth functions are given by

$$g_1(u_1, u_2) = r_1 u_1 (1 - \frac{u_1}{K}) - \mu_{12}u_1u_2 \tag{2.4.6}$$

$$g_2(u_1, u_2) = -\mu_{22}u_2 + \mu_{21}u_1u_2. \tag{2.4.7}$$

In a region that is homogeneously inhabited by the prey population (u_1), the success of the predator invasion has been thoroughly examined by (Dunbar, 1983, 1984). It was established that the predator spreads at rate

$$c_2 = 2\sqrt{D_2(\mu_{21}K - \mu_{22})}. \tag{2.4.8}$$

The last formula indicates that the predator species can successfully invade the region when $K > \frac{\mu_{22}}{\mu_{21}}$. Furthermore, the rate of spread of the predator species increases with the prey carrying capacity.

2.5 Spatially explicit models

Spatially explicit models (SEM) have become important tools for ecological modelling due to the rapid development of computer technology. A model is said to be spatially explicit when it uses landscape map that describe the habitat feature in addition to population simulator (Dunning Jr. *et al.*, 1995). SEM can be individual-based or population-based.

Individual-based models (IBM) consider discrete individuals as the building blocks for modelling ecological phenomena. The concept of "individuals" does not necessarily describe specific organisms, but also a population unit such as ant colonies (Berec, 2002). Each individual has at least one feature and acts under biologically relevant rules. The primary feature of individuals consists of their spatial location, but individuals can also differ in age, sex, body size, and other growth and dispersal relevant traits (Berec, 2002; Phillips *et al.*, 2008; Travis *et al.*, 2009). Recent uses of IBM for the spread of invasive species have suggested the evolution of dispersal strategies as an alternative explanation of the accelerating nature of range expansions (Travis and Dytham, 2002; Phillips *et al.*, 2010).

For population-based SEM, space is considered as a tessellation of cells containing a population and connected by dispersal processes. Although hexagonal cells have been considered in some studies, square grid cells are commonly used because it permits easier switch between different spatial scale and implementation of GIS rasters (Birch *et al.*, 2007). Demographic processes (such as reproduction and mortality) occur within individual cells and can be dependent of the cell's type. Each cell is assumed to be homogeneous and is characterised by specific demographic properties (See for example Hassell *et al.* (1991); Taylor and Hall (2012)). Dispersal on the other hand involves immigration and emigration processes and thus rely on the status of other neighbouring cells (Dunning Jr. *et al.*, 1995).

Both classes of SEM allow the implementation of difficult landscape features such as dispersal barrier and habitat boundaries or hostile habitat (Dunning Jr. *et al.*, 1995). However population-based models are more suitable for heterogeneous landscape specially if the extent of the landscape as well as the population size are large (Hassell *et al.*, 1991). On the other hand, IBM are recommended when the population is rare as it permits the integration of stochastic demographic and dispersal events (Travis and Dytham, 2002; Phillips *et al.*, 2010).

SEM allow the implementation of numerous details, including habitat heterogeneity and stochasticity, individual characteristics and demographic stochasticity (Pearson and Dawson, 2005). Due to the amount of details included in the models, SEM can be complicated and deriving theoretical insight are often equally complex if not impossible. However, the use of SEM cannot be undermined as simulations have shed light on different ecological phenomena, for example the role of long-distance dispersal in fragmented habitats (Pearson and Dawson, 2005), and provided alternative explanations accelerating invasions (Phillips *et al.*, 2010).

Table 2.1: Summary of spread models in invasion ecology.

Highlights	Models	Asymptotic rate of spread	References
Linear range expansion results from a constant diffusion and exponential or logistic growth.	PDE, Eq. 2.2.1	$2\sqrt{rD}$	Fisher (1937); Skellam (1951)
An invading predator can spread only when the environment can sustain enough prey population. In this case, the rate of spread of an invading predator increases with the native prey's carrying capacity.	PDE, Eq. 2.4.1 with Eq. 2.4.6	$2\sqrt{D_2(\mu_{21}K - \mu_{22})}$	Dunbar (1983, 1984)
Allee effect reduces the rate of spread and can explain the initially slow rate of spread observed in many invasions.	PDE, Eq. 2.2.1 with Eq. 2.1.6	$\sqrt{2rD}(1/2 - \alpha)$ when $0 < \alpha < 1$	Lewis and Kareiva (1993)
The rate of spread is highly dependent on the distribution of dispersal distances (dispersal kernel).	IDE, Eq. 2.2.5	$\min_s \frac{1}{s} \log g'(0)M(s)$, when the dispersal kernel admits a moment generating function M.	Kot *et al.* (1996)
Invading competitor can only spread if it is competitively stronger than the native species. Furthermore, the rate of spread is slowed down by the presence of the native competitor.	PDE, Eq. 2.4.1 with Eq. 2.4.3	$2\sqrt{r_2 D_2 \left(1 - \frac{r_1 \mu_{21}}{r_2 \mu_{11}}\right)}$	Shigesada and Kawasaki (1997); Hosono (1998)
The rate of spread increases with the dispersal probability.	IDE, Eq. 2.2.9	$\min_{s \in I} \frac{1}{s} \ln\left[g'(0)(dM(s) + (1-d))\right]$	Lutscher (2008)
The rate of spread in a periodically fragmented environment can be obtained via a spatial averaging technique.	PDE, Eq. 2.3.1	$c = 2\sqrt{< r >_A < D >_H}$ where $< r >_A$ and $< D >_H$ denote the arithmetic mean of the growth rate and the harmonic mean of the dispersal rate respectively.	Shigesada *et al.* (1986); Kinezaki *et al.* (2006)
	IDE, Eq. 2.3.5	$\min_s \frac{1}{s}(pe^{r_1}M_1(s) + (1-p)e^{r_2}M_2(s))$, where p is the proportion of favourable habitats.	Dewhirst and Lutscher (2009)

Table 2.2: Frameworks of spread models.

Population	Time	Space	Modelling framework	References
Continuous	Continuous	Continuous	PDE	Fisher (1937); Skellam (1951); Holmes *et al.* (1994)
Continuous	Continuous	Discrete	System of ODE	Li *et al.* (2005); Ramanantoanina *et al.* (2011)
Continuous	Discrete	Discrete	System of difference equations	Hassell *et al.* (1991)
Continuus	Discrete	Continuous	IDE	Kot *et al.* (1996); Dewhirst and Lutscher (2009)
Discrete	Continuous and discrete	Continuous and discrete	IBM, governed by set of rules	Berec (2002); Hui *et al.* (2011)

Chapter 3

Propagule pressure and the spread of a mixed population

3.1 Introduction

The ability to estimate the rate of spread of an invasive species is important for the success of its management and control (Mack *et al.*, 2000). Early theories suggested that the velocity at which a species expands its range depends on the population growth and dispersal rates (Skellam, 1951). Models based on partial differential equations, such as the reaction-diffusion (RD) model that assume a normal distribution of species' dispersal distances (i.e. dispersal kernel), have yielded a widely-used formula which depicts a constant asymptotic rate of spread ($c = 2\sqrt{rD}$, where r and D denote the intrinsic growth and diffusion rates respectively) (Fisher, 1937; Skellam, 1951). However, a growing body of evidence suggests that the rate of spread of species may not be constants (Cohen and Carlton, 1998). Shigesada and Kawasaki (1997) presented three patterns of range expansions, namely linear expansion with a constant rate of spread; bi-phase expansion which has a break between linear expansions, with the second phase expansion having a higher rate; accelerating expansion with a continuously increasing rate of spread.

To fully comprehend the accelerating nature of range expansion, different dispersal strategies have been incorporated into RD models. In particular, fat-tailed dispersal kernels (i.e. movements with a substantial portion of long-distance dispersal) have been shown to be capable of boosting up the range expansion and are, thus, an appropriate mechanism for explaining the accelerating range expansion (Kot *et al.*, 1996). However, this explanation suffers from two pitfalls (Phillips *et al.*, 2008). First, the rate of spread predicted from a fat-tailed dispersal kernel can increase to infinity, an obvious exaggeration of

the reality. Second, the parameters of fat-tailed dispersal kernels are difficult to estimate due to the rarity of observed long-distance dispersal events (Hastings *et al.*, 2005) and often require a substantial amount of recapturing records (Hui *et al.*, 2012). Shigesada *et al.* (1995) tackled the conundrum of biphasic and accelerating range expansion patterns by using a combined dispersal kernel (a probability of p to move a short distance and a probability of $1 - p$ to move a long distance) (See also Shigesada and Kawasaki (1997) and Clark *et al.* (1998)). This combined dispersal kernel can lead to a budding pattern of stratified range expansion, with the expansion speeding up when the buds of founding populations merge into a super-colony. However, little evidence exists for this combined, stratified dispersal kernel in nature.

Two recent breakthroughs in invasion biology suggest new alternative concepts that could explain the range expansion that accelerates to a limited speed. First, propagule pressure (i.e, introduction effort, which incorporates the frequency of releases and the number of individuals released into a non-native region) has been identified as one key factor of invasion success (Lockwood *et al.*, 2005; Colautti *et al.*, 2006; Simberloff, 2009). Studies further show that the initial propagules often consist of a suite of individuals with different selective performance (Korsu and Huusko, 2009). Therefore, instead of assuming identical individuals in the initial population, it is more reasonable to conceptualize the initial population as a group of individuals with inherent differences. Indeed, assuming only one dispersal ability in the population often leads to an underestimation of the rate of spread in animals (Skalski and Gilliam, 2000). Second, during the range expansion, individuals will be sorted spatially according to their dispersal abilities (Phillips *et al.* (2010); Shine *et al.* (2011) and references therein) so that individuals with stronger dispersal abilities will be more likely to locate at the advancing range front (e.g. Cane toad (*Bufo marinus*) in Australia, Phillips *et al.* (2007); Indian myna (*Acridotheres tristis*) in South Africa, Berthouly-Salazar *et al.* (2012); Bush cricket Simmons and Thomas (2004)). The range expansion could, thus, be accelerating due to a dynamic dispersal kernel driven by this process of spatial sorting for stronger dispersers at the range front. It is necessary to incorporate both propagule admixture and spatial sorting into spreading models and to examine how these two factors affect the dynamic forms of dispersal kernels and the velocity of range expansion.

Here, we present a mathematical model that incorporates different dispersal abilities of individuals in the initial propagules. Unlike the effect of propagule pressure on the success of establishment (Mikheyev *et al.*, 2008; Gertzen *et al.*, 2011), its effect on the rate of spread has not been thoroughly investigated. We examine how the variation of dispersal ability in the initial propagule shape the range expansion and the rate of spread.

3.2 The model

The model has two parts. In the first part, we present a spread model for the spread of a mixed population. In the second part, we describe the distribution of dispersal abilities in the initial propagule.

3.2.1 Reproduction and dispersal

We consider the invasion of a one-dimensional habitat by an mixed population which consists of n groups of individuals with different dispersal abilities. Each group of individuals undergoes two separated phases: reproduction and dispersal. Let, $u_i(x,t), i = 1,\ldots,n$ denote the population size of group i at location x and time t.

The dispersal of type i individuals is modelled by the dispersal kernel $k_i(x,y)$ (i.e. the probability that an a type i individual moves from location y to x during a time step (Kot *et al.*, 1996)). We assume that the habitat is homogeneous; that is, the dispersal kernel $k_i, i = 1,\ldots,n$ depends only on the distance between the locations ($z = |x-y|$). The dispersal kernel k_i can be identified by its variance

$$d_i^2 = \mathrm{Var}(k_i).$$

For a Gaussian kernel, k_i is given by

$$k_i(x-y) = \frac{1}{\sqrt{2\pi d_i^2}} e^{-\frac{(x-y)^2}{2d_i^2}}, \tag{3.2.1a}$$

and for a Laplace kernel,

$$k_i(x-y) = \frac{1}{\sqrt{2d_i^2}} e^{-|x-y|\sqrt{\frac{2}{d_i^2}}}. \tag{3.2.1b}$$

Hereafter, d_i^2 will be referred to as the dispersal ability of type i individuals.

We assumed that the dispersal ability of an individual is determined by an inherited trait of an asexual population (See, for example, Jenkins *et al.* (2007);

Talavera *et al.* (2012)). The reproduction phase of the individuals with dispersal ability d_i^2 is depicted by a non-negative function $g_i(u_1, \ldots, u_n)$ satisfying

$$g_i(u_1, \ldots, u_n) = 0 \text{ whenever } u_i = 0, \tag{3.2.2a}$$

and

$$g_i(u_1, \ldots, u_n) \leq R_i u_i \tag{3.2.2b}$$

where

$$R_i = \frac{\partial g_i}{\partial u_i}(0, \ldots, 0). \tag{3.2.2c}$$

In what follows, we assume that there is no trade off between growth and dispersal ability. More precisely, we assume that individuals with different dispersal abilities are equally reproductive, that is $R_1 = R_2 = \ldots = R_n = R$. Eq. 3.2.2a indicates that only individuals with dispersal ability d_i^2 can have offspring with the same dispersal ability. Eq. 3.2.2b and Eq. 3.2.2c imply that individuals are more productive when the population density is low (there is no Allee effect). Examples of such growth functions include the Ricker (1954) model

$$g_i(u_1, \ldots, u_n) = u_i e^{r - u/K}, r \geq 0 \tag{3.2.3a}$$

and the Beverton and Holt (1957) model

$$g_i(u_1, \ldots, u_n) = \frac{R u_i}{1 + (R-1)u/K} \tag{3.2.3b}$$

where $u = \sum_{j=1}^{n} u_i$ is the total population. Note that for the Ricker model 3.2.3a, $R = e^r$.

Given the population size $u_i(x,t)$ at time t, the population size at time $t+1$ is depicted by

$$u_i(x, t+1) = \int k_i(x-y) g_i(u_1(y,t), \ldots, u_n(y,t)) \mathrm{d}y, \ 1 \leq i \leq n. \tag{3.2.4}$$

When there is no trade off, an equation generating the total population

$$u(x,t+1)=\sum_{i=1}^{n}\int k_i(x-y)g_i(u_1(y,t),\ldots,u_n(y,t))\mathrm{d}y$$

can be derived. For the Ricker model for instance, we deduce that

$$u(x,t+1)=\int\sum_{i=1}^{n}k_i(x-y)u_i(y,t)e^{r-u(y,t)/K}\mathrm{d}y.$$

When the total population $u(y,t)$ is non-zero, we can write

$$u(x,t+1)=\int\left(\sum_{i=1}^{n}k_i(x-y)\frac{u_i(y,t)}{u(y,t)}\right)u(y,t)e^{r-u(y,t)/K}\mathrm{d}y.$$

Consider

$$\mathcal{K}(x,y;t)=\sum_{i=1}^{n}k_i(x-y)p_i(y,t) \tag{3.2.5}$$

and

$$p_i(x,t)=\frac{u_i(x,t)}{u(x,t)}. \tag{3.2.6}$$

The total population is governed by

$$u(x,t+1)=\int\mathcal{K}(x,y;t)g(u(y,t))\mathrm{d}y. \tag{3.2.7}$$

It is worth noting that p_i is the proportion of the total population at location x which have dispersal kernel k_i (when $u(x,t)>0$). $\mathcal{K}(x,y;t)$ is referred to as the *expected kernel* at location y and time t. Eq. 3.2.7 is similar to an integrodifference model (Kot *et al.*, 1996) with dispersal kernel $\mathcal{K}$. Evidently, the expected dispersal kernel K depends not only on the dispersal distances but also on the starting location and time of the dispersal event and time (i.e. it is a dynamic dispersal kernel; Phillips *et al.* (2008)).

3.2.2 The initial propagule

Let the initial propagule consist of U_0 individuals with different dispersal abilities. Hereafter, U_0 will be referred to as the *propagule size*. We considered two specific scenarios of probability distribution of dispersal abilities in the initial propagule.

First, we assumed that the population consists of individuals with two different dispersal abilities d_1^2 or d_2^2 (where $d_1^2 < d_2^2$). The majority of the initial propagule are individuals with dispersal ability d_1^2, and there is only a small fraction of individuals with dispersal ability d_2^2. In this case, the initial condition ($u_1(x,0)$ and $u_2(x,0)$) of the model Eq. 3.2.4 satisfies

$$\begin{cases} u_1(0,0) + u_2(0,0) = U_0 \text{ and } u_2(0,0) \ll u_1(0,0), \\ u_1(x,0) = u_2(x,0) = 0 \text{ for } x \neq 0. \end{cases} \tag{3.2.8}$$

The second scenario assumes a population with many more dispersal abilities in the initial propagule. Motivated by the growing evidence that species' relative abundances follow a log-normal distribution (Limpert *et al.*, 2001; May and McLean, 2007), we generated dispersal abilities in the the initial propagule as follows.

- For each individual in the initial propagule, a dispersal ability d^2 was drawn from the continuous log-normal distribution $\ln N(\mu, \sigma)$. Hereafter, σ will be referred to as the *propagule diversity*. The parameter e^{μ} gives the median dispersal ability of the initial propagule.
- Individuals with closely similar dispersal abilities were grouped together. Namely, we divided the population into n groups where the group i consisted of individuals with dispersal ability between $(i-1)\delta$ and $i\delta$, for some $\delta > 0$. The number of groups n is the smallest integer such that the maximal dispersal ability is bounded by $n\delta$.
- A unique dispersal ability was assigned to all individuals in a group, namely, individuals in the group i were given the dispersal ability

$$d_i^2 = (i-1)\delta + \frac{\delta}{2}, \ i = 1, \ldots, n.$$

The initial condition $u_i(x,0), i = 1, \ldots, n$ of the model Eq. 3.2.4 is therefore given by

$$u_i(x,0) = \begin{cases} \text{Number of individuals with dispersal ability } d_i^2 & \text{if } x = 0 \\ 0 & \text{otherwise.} \end{cases} \tag{3.2.9}$$

A list and description of the parameters are provided in Table 3.1.

Variable / Parameter	Description
R	Intrinsic growth rate
K	Carrying capacity
U_0	Propagule size: size of the total population at $t = 0$
σ	Propagule diversity
d_i^2	Dispersal ability of type-i individuals
k_i	Dispersal kernel of type-i individuals
$u_i(x,t)$	Size of the type-i population at location x and time t
$u(x,t)$	Size of the total population at location x and time t
$p_i(x,t)$	Proportion of type-i population at location x and time t
$\overline{d^2}(x,t)$	Mean dispersal ability at location x at time t
$x^*(t)$	Location of the front of the invasion at time t

Table 3.1: Description of parameters and variables for the spread of a mixed population.

3.2.3 Tests

Model 3.2.4 was solved using Fast Fourier Transform (FFT) routines from the SciPy library in Python.

To visualise the dynamics of different groups in the population with many dispersal abilities, the population was classified into three categories according to individuals' dispersal ability. An individual with dispersal ability d_i^2 was classified as

$$\begin{cases} \text{Slow disperser} & \text{if } d_i^2 < d_1^2 + \frac{d_n^2 - d_1^2}{3}, \\ \text{Intermediate disperser} & \text{if } d_1^2 + \frac{d_n^2 - d_1^2}{3} \leq d_i^2 < d_1^2 + 2\frac{d_n^2 - d_1^2}{3}, \\ \text{Fast disperser} & \text{if } d_1^2 + 2\frac{d_n^2 - d_1^2}{3} \leq d_i^2. \end{cases} \tag{3.2.10}$$

The shape of the expected dispersal kernel (Eq. 3.2.5) was investigated along with the mean dispersal ability of the population at location x and time t. The mean dispersal ability was defined by

$$\overline{d^2}(x,t) = \sum_{i=1}^{n} d_i^2 p_i(x,t). \tag{3.2.11}$$

The instantaneous rate of spread from time t to time $t+1$ and the average rate of spread were computed respectively as

$$c_I(t) = x^*(t+1) - x^*(t) \tag{3.2.12}$$

and

$$c(t) = \frac{x^*(t) - x^*(0)}{t} \tag{3.2.13}$$

where $x^*(t)$ is the location of the front defined for a certain threshold of detection u^* by

$$x^*(t) = \max_{x \geq 0} \{x, u(x,t) > u^*\}. \tag{3.2.14}$$

Recall that we are interested in the spread of the total population $u = \sum_{i=1}^{n} u_i$.

3.3 Results

3.3.1 Spread of a population with two dispersal abilities

When the initial propagule was as described in Eq. 3.2.8, Fig. 3.1a shows that at the beginning of the invasion, the sub-population with dispersal ability d_2^2 remained low in number. At this stage of the invasion, the total population, like the initial propagule, consisted in majority of individuals with dispersal ability d_1^2. The individuals with dispersal ability d_2^2 however did not go extinct and eventually reached the front of the invasion (Fig. 3.1a, $t = 10$ and $t = 20$). After attaining the front of the invasion, individuals with dispersal ability d_2^2 increased in number and a spatial sorting of the dispersal abilities was observed. Namely, the front of the invasion was occupied by individuals with

the stronger dispersal ability d_2^2 whereas the core of the invasion was dominated by individuals with dispersal ability d_1^2 (Fig. 3.1a, $t = 30$ and $t = 40$).

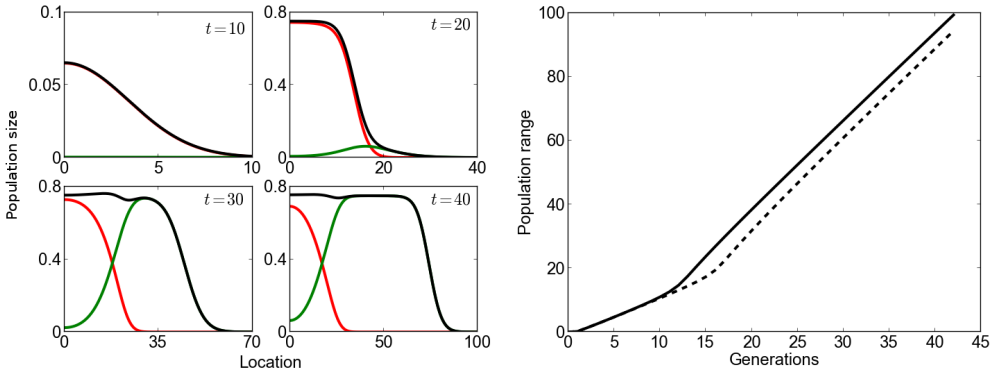

(a) Population dynamics. (b) Range expansion.

Figure 3.1: Spread of a population with two dispersal abilities, with Gaussian dispersal kernels and Ricker growth. Parameter values are $R = e^{0.75}$, $d_1^2 = 1$, $d_2^2 = 5$. (a) Population size at different time with the initial populations $u_1(0,0) = 0.99$ and $u_2(0,0) = 0.01$. The colors red, green and black correspond to the sub-populations with dispersal ability d_1^2, d_2^2 and the total population respectively. (b) Population range at different generations when the initial propagule are $u_1(0,0) = 0.99$ and $u_2(0,0) = 0.01$ (solid line) and $u_1(0,0) = 0.999$ and $u_2(0,0) = 0.001$ (dashed line).

A break of slope was observed during the population's range expansion (Fig. 3.1b). The invasion consisted of a slow initial expansion followed by a linear expansion at faster rate. Furthermore, we observed that the time at which the increase in the rate of spread was shortened by increasing the fraction of the initial population with dispersal ability d_2^2. However, the slope of the population range, that is the rate of spread was not affected by the distribution of dispersal abilities in the initial propagule (Fig. 3.1b).

Asymptotic rate of spread

The asymptotic rate of spread, that is the rate of spread in the later phase of the invasion, was heuristically derived as follows. First, we note that behind the front of the invasion (defined in Eq. 3.2.14) the population densities are small ($u_i \leq u^* < 1$), and the model Eq. 3.2.4 can be approximated by

$$u_i(x, t+1) = \int R k_i(x-y) u_i(y,t) \mathrm{d}y, \quad i = 1, 2. \tag{3.3.1}$$

Previous results (Kot *et al.*, 1996) have shown that when the initial population $u_i(x,0)$ has compact support, the solution of Eq. 3.3.1 tends to a travelling wave solution of the form

$$u_i(x,t) = e^{-\lambda_i(x-c_it)}, \quad i = 1,2 \tag{3.3.2}$$

which spreads at rate c_i defined by

$$c_i = \frac{1}{\lambda_i}\log(RM(d_i,\lambda_i)) = \min_{\lambda\in I}\frac{1}{\lambda}\log(RM(d_i,\lambda)) \tag{3.3.3}$$

when the moment generating function of the kernel k_i

$$M(d_i,\lambda) = \int k_i(z)e^{-\lambda z}\mathrm{d}z$$

exists. For Gaussian and Laplace kernels, the interval I is given by $I = (0,\infty)$ and $I = \left(0, \frac{\sqrt{2}}{d_i}\right)$ respectively.

Recall that we are interested in the spread of the total population $u = u_1 + u_2$. Using Eq. 3.3.2, we have

$$u(x,t) = e^{-\lambda_1(x-c_1t)} + e^{-\lambda_2(x-c_2t)}. \tag{3.3.4}$$

One can show for Gaussian and Laplace kernels that

$$\lambda_2 < \lambda_1 \text{ and } \lambda_1c_1 = \lambda_2c_2. \tag{3.3.5}$$

The derivation of Eq.3.3.5 is presented at the end of this section. From Eq.3.3.5 and Eq. 3.3.4, we have

$$\begin{aligned} u(x,t) &= e^{-\lambda_1(x-c_1t)} + e^{-\lambda_2(x-c_2t)} \\ &= e^{\lambda_2c_2t}(e^{-\lambda_1x} + e^{-\lambda_2x}). \end{aligned}$$

We conclude that at the front wave,

$$u(x,t) \propto e^{-\lambda_2(x-c_2t)} \text{ as } x \text{ tend to } +\infty. \tag{3.3.6}$$

Eq. 3.3.6 indicates the total population $u(x,t)$ of the linearised model (Eq. 3.3.1) spreads at rate bounded by c_2. Therefore the rate of spread of the total population u of the non-linear model Eq. 3.2.4 satisfies

$$c \leq \min_{\lambda \in I} \frac{1}{\lambda} \log(RM(d_2, \lambda)).$$

The equality

$$c = \min_{\lambda \in I} \frac{1}{\lambda} \log(RM(d_2, \lambda)) \tag{3.3.7}$$

holds for monotonically increasing growth function (Weinberger, 1982; Kot, 1992). An approximation of c can be obtained following the line of (Lutscher, 2007) as follows. Using the expansion

$$M(d_2, \lambda) = 1 + \frac{d_2^2}{2}\lambda^2 + \frac{\gamma_2 d_2^4}{24}\lambda^4$$

where γ_2 represents kurtosis of the dispersal kernel k_2, then the expansion

$$\log(1+x) = x \text{ for } |x| < 1$$

one can approximate c by

$$c \approx \min_{\lambda \in I} \frac{1}{\lambda} \left(\log R + \frac{d_2^2}{2}\lambda^2 + \frac{\gamma_2 d_2^4}{24}\lambda^4 \right). \tag{3.3.8}$$

By finding the minimum of the function

$$f(\lambda) = \frac{1}{\lambda} \left(\log R + \frac{d_2^2}{2}\lambda^2 + \frac{\gamma_2 d_2^4}{24}\lambda^4 \right)$$

one can establish that (Lutscher, 2007)

$$c \simeq \sqrt{2\log(R) d_2^2} \left(1 + \frac{\log(R)}{12}\gamma_2 \right). \tag{3.3.9}$$

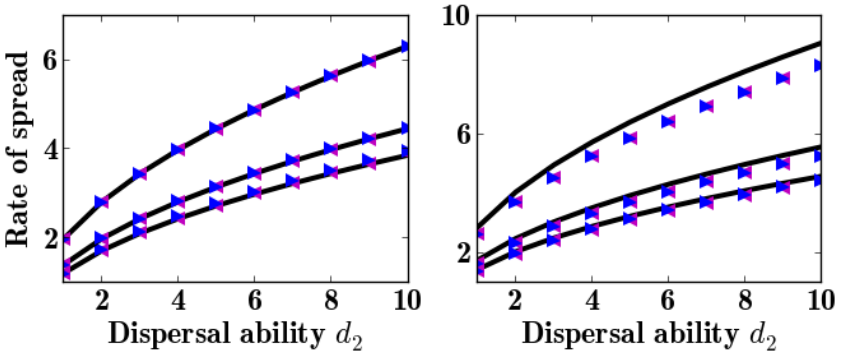

Figure 3.2: Theoretical and computed rate of spread when two dispersal abilities are present in the population. Blue triangle: with the initial values $(0.9, 0.1)$. Magenta triangle: with initial values $(0.99, 0.01)$. Solid lines: Estimation from Eq. 3.3.10a (left) and Eq. 3.3.10b (right). $d_1 = 1$, $R = e^{0.75}, e^1$ and e^2

In particular, when Gaussian kernels (Eq. 3.2.1a) are used

$$c_{\text{Gauss}} \simeq \sqrt{2\log(R)d_2^2} \tag{3.3.10a}$$

and in the case of Laplace (Eq. 3.2.1b) dispersal kernels

$$c_{\text{Laplace}} \simeq \sqrt{2\log(R)d_2^2}\left(1 + \frac{\log(R)}{4}\right). \tag{3.3.10b}$$

Intensive numerical simulations suggest that while Eq. 3.3.10a fit well with the asymptotic rates of spread obtained with Gaussian dispersal kernels, Eq. 3.3.10b provides an upper bound of the rate of spread from Laplace dispersal kernels (Fig. 3.2).

Establishing the relations 3.3.5 for Gaussian and Laplace kernels

Consider the function f defined on I by

$$f(d_i, \lambda) = \frac{1}{\lambda}\log(RM(d_i, \lambda))$$

and let λ_i satisfy

$$c_i = f(d_i, \lambda_i).$$

We know from Eq. 3.3.3 that

$$\frac{\partial}{\partial \lambda} f(d_i, \lambda_i) = 0.$$

For Gaussian kernels,

$$M(d_i, \lambda) = e^{\frac{1}{2} d_i^2 \lambda^2},$$

$$f(d_i, \lambda) = \frac{1}{\lambda} \left(\log R + \frac{1}{2} d_i^2 \lambda^2 \right),$$

$$\frac{\partial}{\partial \lambda} f(d_i, \lambda) = \frac{1}{\lambda^2} \left(\frac{1}{2} d_i^2 \lambda^2 - \log R \right).$$

From $\frac{\partial}{\partial \lambda} f(d_i, \lambda_i) = 0$, we deduce that

$$\lambda_i = \sqrt{\frac{2 \log R}{d_i^2}} \text{ and } c_i = \sqrt{2 d_i^2 \log R}.$$

Given that $0 < d_1^2 < d_2^2$, we deduce for Gaussian kernels that

$$\lambda_2 < \lambda_1 \text{ and } \lambda_1 c_1 = \lambda_2 c_2.$$

For Laplace kernels, the moment generating kernel M, f and f' are given by

$$M(d_i, \lambda) = \frac{1}{1 - d_i^2 \lambda^2 / 2},$$

$$f(d_i, \lambda) = \frac{1}{\lambda} \left(\log(2R) - \log(2 - d_i^2 \lambda^2) \right),$$

and

$$\frac{\partial}{\partial\lambda}f(d_i,\lambda)=\frac{1}{\lambda^2}\left(\frac{2d_i^2\lambda^2}{2-d_i^2\lambda^2}-\Big(\log(2R)-\log(2-d_i^2\lambda^2)\Big)\right).$$

Since $\frac{\partial}{\partial\lambda}f(d_i,\lambda_i)=0$ we have

$$\frac{2d_i^2\lambda_i^2}{2-d_i^2\lambda_i^2}-\big(\log(2R)-\log(2-d_i^2\lambda_i^2)\big)=0 \text{ for } i=1,2. \tag{3.3.11}$$

Consider the function h defined for $d>0$ by

$$h(d)=\frac{2d^2\lambda^2(d)}{2-d^2\lambda^2(d)}-\big(\log(2R)-\log(2-d^2\lambda^2(d))\big).$$

Along the curve $\frac{\partial}{\partial\lambda}f(d,\lambda)=0$ we have $h'(d)=0$ that is

$$\frac{2(d^2\lambda^2(d))'}{(2-d^2\lambda^2(d))^2}-\frac{(d^2\lambda^2(d))'}{(2-d^2\lambda^2(d))}=0$$

where $(d^2\lambda^2(d))'$ is the derivative of $d^2\lambda^2(d)$ with respect to d, and deduce that

$$\big(d^2\lambda^2(d)\big)'(d^2\lambda^2(d))=0.$$

Since λ and d are strictly positive, we have

$$(d^2\lambda^2(d))'=0.$$

The last equation implies that

$$d\lambda(d)=\log\left(\frac{2R}{2-d^2\lambda^2(d)}\right)$$

is constant, and $\lambda(d)$ is a decreasing function of d.

Since $d_1<d_2$, $\lambda(d_1)=\lambda_1$ and $\lambda(d_2)=\lambda_2$ we conclude that

$$\lambda_2<\lambda_1 \text{ and } \lambda_1c_1=\lambda_2c_2$$

for Laplace kernels.

3.3.2 Spread of a population with many dispersal abilities

To understand the more general case where n dispersal abilities were present in the initial propagule, we investigated the occurrence of spatial sorting and the evolution of dispersal kernel then we studied the instantaneous and asymptotic rate of spread.

Spatial sorting and the expected dispersal kernel

We run intensive numerical simulations to study the dynamics of the population when many dispersal abilities are present in the initial propagule. Namely we have used different combinations of $\sigma \in (0, 0.5)$ and $10 \leq U_0 \leq 1000$.

When many dispersal abilities were present in the population, slow dispersers abounded at the beginning of the invasion and fast dispersers remained low in number. Eventually , fast dispersers reached the invasion front, leaving the slow dispersers behind (see for example Fig. 3.3c). As this process was repeated at each generation, a gradient of dispersal abilities formed in the invaded region. This phenomena is commonly known as spatial sorting. Namely, at different generations, slow dispersers abounded at the core of the invasion whereas faster dispersers occupied the invasion front.

Spatial sorting was also detected using the mean dispersal abilities (Eq. 3.2.11) which was found to vary along the direction of range expansion at each generation (Fig. 3.4, Top). Habitats that were invaded at the early stage of the invasion remained with low mean dispersal ability. Newly occupied habitats on the other hand were characterised by a larger mean dispersal ability. Extensive numerical simulations suggest that spatial sorting was more pronounced at large propagule size (U_0) and high propagule diversity (σ). As the mean dispersal ability varied with generation and location, it was also the case for the expected dispersal kernel. We observed that the dispersal kernel at the core of the invasion was narrower than that at the front (Fig. 3.4, Bottom). In other words, populations from the front were more likely to travel longer distance compared to populations from the origin. Furthermore, the expected dispersal kernel was found to be close to the dispersal kernel associated to the mean dispersal ability, that is the expected dispersal kernel (Eq. 3.2.5) can be approximated by

$$K_{\text{approx}}(x, y; t) = \frac{1}{\sqrt{2\pi \overline{d^2}(y, t)}} e^{-\frac{(x-y)^2}{2\overline{d^2}(y,t)}} \tag{3.3.12a}$$

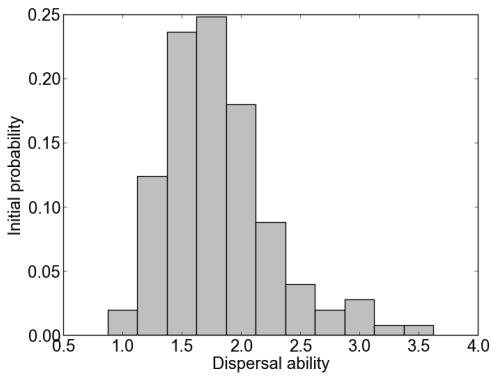

(a) Initial propagule.

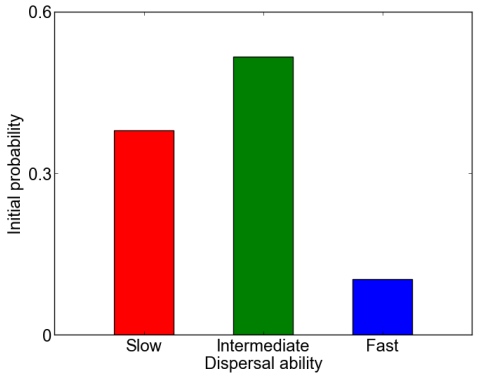

(b) Performance of the initial propagule.

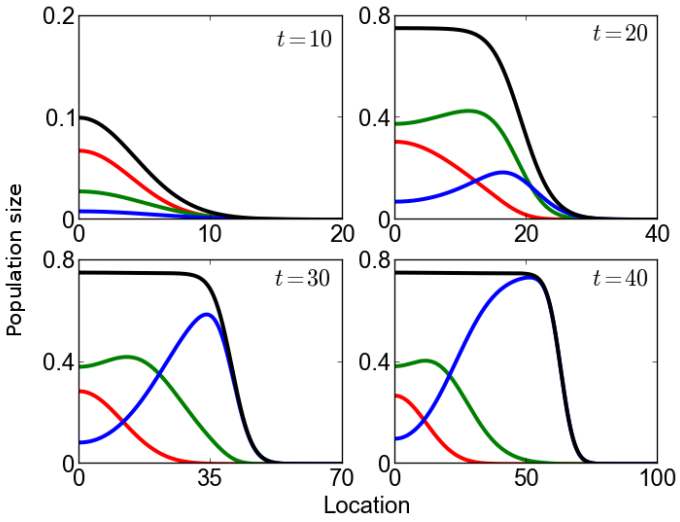

(c) Invasion.

Figure 3.3: A propagating population resulting from Eq. 3.2.4 with Ricker growth (Eq. 3.2.3a) and Gaussian dispersal kernel (Eq. 3.2.1a). Parameters were chosen as follows: $R = e^{0.75}$, $\mu = .5, \sigma = 0.25$, $U_0 = 100$ and $K = 500$. (a) Distribution of dispersal abilities in the initial propagule.(b) Classification of the initial propagule as slow, intermediate and fast dispersers (Eq. 3.2.10). (c) Population size at different time. The colors red, green and blue correspond respectively to slow, intermediate and fast dispersers whereas black lines represent the total population.

and

$$K_{\text{approx}}(x, y; t) = \frac{1}{\sqrt{2\overline{d^2}(y,t)}} e^{-|x-y|\sqrt{\frac{2}{\overline{d^2}(y,t)}}} \tag{3.3.12b}$$

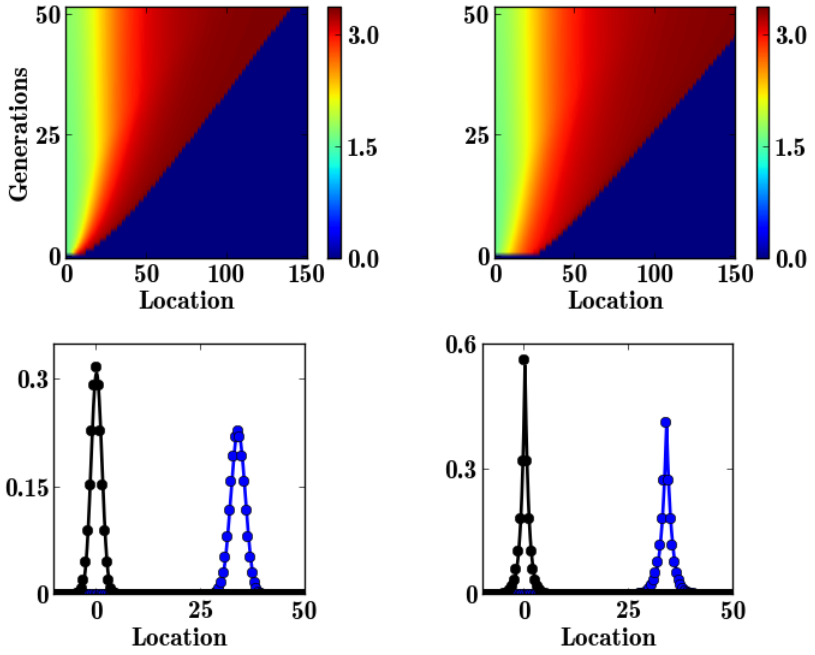

Figure 3.4: Evolution of dispersal ability and dispersal kernels. **Top:** Mean dispersal ability. During the invasion, dispersal ability at the front is higher than the dispersal ability at the core of the invasion. The region in blue indicates habitats that have not been invaded at each generation. **Bottom:** The expected dispersal kernel at the core of the invasion (in black) is narrower than at the front (blue). In both cases, the expected dispersal kernel (Eq. 3.2.5)(full circles) can be approximated by the kernel with mean dispersal ability (Eq. 3.3.12) (solid line). Figures in the left and the right were obtained using Gaussian and Lapalce dispersal kernels respectively.

when Gaussian and Laplace kernels were used respectively, where $\overline{d^2}(y,t)$ is the mean dispersal ability (as defined in Eq. 3.2.11) at the location y at time t.

Accelerating range expansion

We observed two distinct phases during the spread of the mixed population from Eq. 3.2.4. The first phase consisted of an accelerating range expansion. During this phase the instantaneous rate of spread (Eq. 3.2.12) increased with generations. In the example shown in Fig. 3.5, the rate of spread increased for almost 40 generations. After the accelerating phase, we observed that the population continued to expand its range but at a constant rate, that is a linear range expansion, signaling the end of spatial sorting..

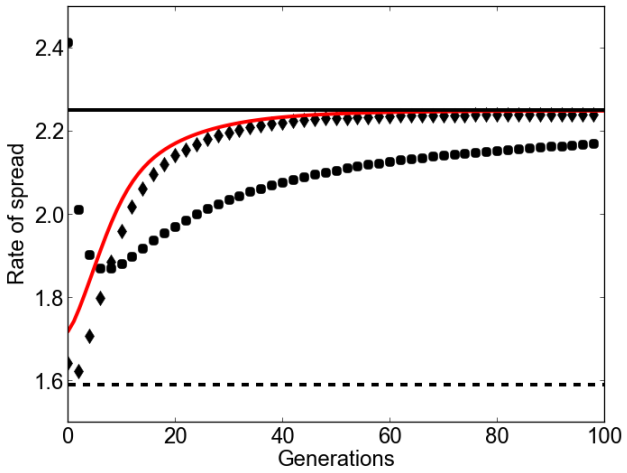

Figure 3.5: Rate of spread of a mixted population with $R = e^{0.75}, \mu = .5, \sigma = 0.25, U_0 = 100$. Diamonds: Instantaneous rate of spread (Eq. 3.2.12). Circle: Average rate of spread (Eq. 3.2.13). Solid black line: Asymptotic rate of spread (Eq. 3.3.10a). Solid red line: Rate of spread of the frontal population (Eq. 3.3.13). The dashed line shows the asymptotic rate of spread predicted by a single population.

The instantaneous rate of spread depicts the rate at which the population expands its range at a given generation (t). Numerical simulations suggested that the instantaneous rate of spread can be determined by the dispersal ability of the frontal population (Fig. 3.5). Namely, the rate of spread can be approximated by the rate of spread of a single species with dispersal kernel $K_{\text{approx}}(x^*(t), y)$ and rate of spread

$$c^*(t) = \sqrt{2\log(R)\overline{d^2}(x^*(t), t)} \tag{3.3.13}$$

where $\overline{d^2}(x^*(t), t)$ is the mean dispersal ability at the front $x^*(t)$ of the invasion at time t. Furthermore, both the instantaneous and average rate of spread tended to an asymptotic rate of spread

$$c = \min_{\lambda \in I} \frac{1}{\lambda} \log(RM(d_n, \lambda)) \tag{3.3.14}$$

which was obtained with similar methods as for the model with two dispersal abilities, where d_n^2 is the maximal dispersal ability in the population.

Median rate of spread

At this stage, we recall that the dispersal rates of the individuals were drawn from a log-normal distribution $\log N(\mu, \sigma)$. As a consequence, the maximal dispersal level d_n^2 is a random number. Consider the random variable D_{U_0} consisting of the maximal dispersal rate of an individual in an initial propagule of size U_0. The aim of this section is to find the median value of D_{U_0}, thus, equivalently, the median rate of spread.

The cumulative distribution function of the r.v. D_{U_0} is given by

$$F(x, U_0) = P(D_{U_0} \leq x) = (\Phi(x))^{U_0} \tag{3.3.15}$$

where $\Phi(x)$ is the cumulative distribution function the log-normal $\log N(\mu, \sigma)$ distribution:

$$\Phi(x) = \frac{1}{2} + \frac{1}{2} \operatorname{erf}\left(\frac{\log(x) - \mu}{\sqrt{2\sigma^2}}\right). \tag{3.3.16}$$

Let $\widetilde{d}_n^2$ denote the median value of D_{U_0}. $\widetilde{d}_n^2$ satisfies $F(\widetilde{d}_n^2, U_0) = \frac{1}{2}$. From Eq. 3.3.15 and Eq. 3.3.16, we have

$$\left(\frac{1}{2} + \frac{1}{2} \operatorname{erf}\left(\frac{\log(\widetilde{d}_n^2) - \mu}{\sqrt{2\sigma^2}}\right)\right)^{U_0} = \frac{1}{2}$$

and

$$\operatorname{erf}\left(\frac{\log(\widetilde{d}_n^2) - \mu}{\sqrt{2\sigma^2}}\right) = 2^{1-\frac{1}{U_0}} - 1.$$

Solving the last equation for the median value $\widetilde{d}_n^2$ yields

$$\widetilde{d}_n^2 = \exp\left(\mu + \sqrt{2\sigma^2}\, \operatorname{erf}^{-1}\left(2^{1-\frac{1}{U_0}} - 1\right)\right). \tag{3.3.17}$$

For Gaussian kernels, the median rate of spread of the invasion governed by Eq. 3.2.4 with initial propagule of size U_0 is given by

$$\widetilde{c} = \sqrt{2\log(R)\widetilde{d}_n^2}. \tag{3.3.18}$$

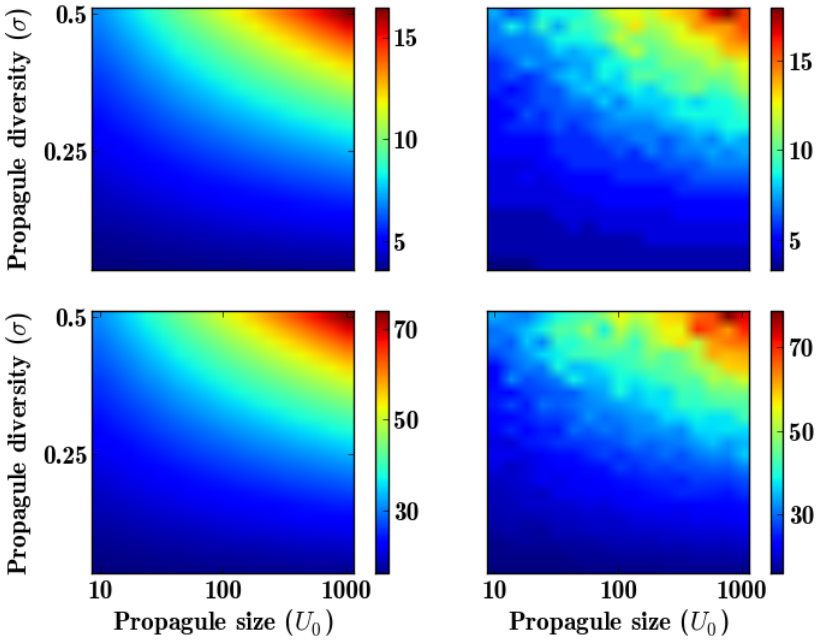

Figure 3.6: Median of the asymptotic rate of spread for $R = e^{0.75}$. The theoretical median of the rate of spread was derived in Eq. 3.3.18 and the computed median rate of spread was obtained from 15 simulations for each set of parameter values. **Top:** $e^{\mu} = e^{1}$. **Bottom:** $e^{\mu} = e^{2.5}$. **Left:** Theoretical rate of spread. **Right:** Computed rate of spread.

A parameter plane showing the median rates of spread is given in Fig. 3.6. Lower rates of spread were observed when either the propagule size or propagule diversity was low. It is worth noting that as the diversity parameter becomes smaller (that is there a less dispersal differential in the population and the individuals have the same dispersal rate D), the rate of spread is equal to that obtained with the RD model ($c = 2\sqrt{rD}$). The rate of spread increases with the propagule size and diversity.

The median rate of spread (Eq. 3.3.18 with Eq. 3.3.17) was tested by solving Eq. 3.2.4 numerically for different propagule size (U_0) and propagule diversity (σ). For each pair (U_0, σ) the rate of spread was computed as the median rate of spread from 15 simulations. Fig. 3.6 shows that the predicted rate of spread agreed with the median rate of spread obtained from numerical simulations for different values of μ.

We found that as σ tends to 0, the rate of spread becomes independent of the propagule size. Indeed, this case corresponds to an initial propagule with single dispersal ability. Furthermore, we found that increasing the propagule size and the propagule diversity both result to faster spread of the population.

3.4 Discussion

The role of propagule pressure in the introduction and establishment success has a rich background in the literature (Simmons and Thomas, 2004; Lockwood *et al.*, 2005). In this work, we went further and investigated the contribution of propagule pressure in the actual rate of spread and the shape of the range expansion pattern. Two properties of the propagule were incorporated in the models, namely the propagule size (i.e. number of individuals in the propagule) and the propagule dispersal diversity (i.e. distribution of the dispersal rates of the individuals in the propagule). Different dispersal abilities were incorporated in our model using a system of integrodifference equations (IDE). IDEs have been used to model the invasion of species with non-overlapping generations such as insects (Miller and Tenhumberg, 2010) and plants (Allen *et al.*, 1996; Neubert and Caswell, 2000). IDEs are particularly powerful due to their flexibility to incorporate different dispersal kernels.

Most studies that investigate the effects of propagule pressure consider only two aspects, namely the number of release of non-native species and the number of individuals released (Korsu and Huusko, 2009; Gertzen *et al.*, 2011). Recent studies, however, have speculated that the difference in performance of the individual propagules can affect the success and the rate of invasion by providing better adapted individuals (Geller *et al.*, 2008; Simberloff, 2009; Lawrence and Cordell, 2010). In particular, different dispersal abilities have been observed in the propagule of different species (Rabinowitz, 1978; Morse and Schmitt, 1985; Korsu and Huusko, 2009).

We considered two distributions of dispersal abilities in the initial propagule. In the first case, we examined the importance of a small number of individuals with stronger dispersal ability in the initial propagule. A linear range expansion was observed during the initial phase of the invasion, which was followed by another linear expansion with higher rate of spread. The expression of the asymptotic rate of spread (Eq. 3.3.9) shows that the long-term range expansion is determined by the dispersal ability of the fast dispersers, however rare they were in the initial propagule. this phenomenon is expected when the fast dispersers do not go extinct, for example as result of demographic stochasticity which are important in population at low density (Lande, 1993; Allen, 2003). Furthermore, the time at which the break of slope in the population range was observed depends on the number of fast individuals in the initial propagule as well as the threshold of detection of the population.

In the second case, we considered the case where the dispersal ability of the initial propagule are log-normally distributed. Unlike most models that incorporate different dispersal abilities (see for example Murrell *et al.* (2002); Travis and Dytham (2002); Phillips *et al.* (2008) and Béchinou *et al.* (2012)), our

model does not take into account the possible mutation of dispersal-relevant traits. Dispersal abilities have been observed to be subject to spatial selection pressure during range expansion (Shine *et al.*, 2011; Berthouly-Salazar *et al.*, 2012). More clearly, the expanding edge is inhabited by individuals with a higher dispersal ability than the core population. Our results suggest that even when evolutionary processes are not taken into account, the different dispersal in the original propagule can lead to a spatial sorting of dispersal ability. Furthermore, spatial sorting was more apparent for more heterogeneous propagules. We found that the frontal population was less heterogeneous and consisted of fast dispersers, compared the population at the core of the invasion where all dispersal abilities were present, as predicted by competition models in which dominant species win and limit weaker individuals' invasion (Allen *et al.*, 1996; Shigesada and Kawasaki, 1997).

The spatial sorting of dispersal ability was reflected in the mean dispersal rate of the population. At the beginning of the invasion, individuals with better dispersal abilities are low in number as their growth is limited by the individuals with weaker dispersal abilities. However, fast dispersers do not go extinct as they are as competitive as the slow dispersers. As individuals with better dispersal ability reach the front of the invasion, they can grow in number in the open space without any competition against the slow dispersers. The mean dispersal ability at the frontal population therefore increases. This process occurs at every generation during range expansion and results into an increasing dispersal ability on the expanding edge. The increasing dispersal rate in turn yields an increasing rate of spread, that is an acceleration of the range expansion. Numerical simulations suggested that the rate of spread between two generations can be approximated using the dispersal ability of the frontal population only. This result is consistent to the findings of Bouin *et al.* (2012). This result suggests that (1) empirical quantifications of the dispersal ability, such as the mean dispersal rate for all individuals are only accurate for a short period of time and may underestimate the long-term rate of spread of the population (dashed line in Fig. 3.5) and (2) empirical predictions based on dispersal abilities obtained from the core population can depreciate the real rate of spread.

The rate of spread, however, is bounded as the dispersal rates are bounded. After the initial acceleration, the population expands at constant rate. A close formula for the asymptotic rate of spread was derived for the constant asymptotic rate of range expansion (Eq. 3.3.18 and 3.3.17). First, it is worth recalling that the rate of spread was obtained with the assumption that the dispersal ability of the propagule is log-normally distributed. This assumption was used due to different evidences that species-abundance relationships follow a log-normal distribution (Preston, 1962; Magurran, 1988; Bell, 2000; Limpert *et al.*, 2001). The rate of spread, however, can be derived for different

propagule distributions simply by using the corresponding cumulative probability function in Eq. 3.3.16. For instance, for a normally distributed initial propagule, Eq. 3.3.16 becomes

$$\Phi(x) = \frac{1}{2} + \frac{1}{2}\,\mathrm{erf}\left(\frac{x-\mu}{\sqrt{2\sigma^2}}\right) \tag{3.4.1}$$

and the asymptotic rate of spread is given by

$$\widetilde{c} = \sqrt{2\log(R)\widetilde{d}_n^2} \tag{3.4.2}$$

with

$$\widetilde{d}_n^2 = \mu + \sqrt{2\sigma^2}\;\mathrm{erf}^{-1}\left(2^{1-\frac{1}{U_0}} - 1\right). \tag{3.4.3}$$

Second, the obtained rate of spread is similar to the approximation for RD model ($c = 2\sqrt{rD}$). Moreover, the RD result is obtained when a common dispersal rate is shared by all individuals, by letting σ tend to 0. Finally, the expression Eq. 3.3.17) suggests that the rate of spread increases with the propagule pressure. This results is in line with the speculation that increasing the propagule size can improve the species spread by providing better suited individuals for invasion (Wilson *et al.*, 2007; Simberloff, 2009). Furthermore, our results are consistent with the findings of (Skalski and Gilliam, 2000) and (Yamamura, 2002) who explored different models to elucidate the important of the dispersal ability in a population.

To conclude, our results suggest that the variety of dispersal abilities in the initial propagules plays an important role in shaping the range versus time pattern during a population's spread. A biphasic invasion, which consists of two linear range expansions with different rates, resulted from a propagule with two dispersal levels. When the initial propagule was more heterogeneous, the invasion started at a slow rate and then accelerated until a maximal rate of spread was attained. In addition, our results emphasize the importance of census time and locations when estimating the parameters of reaction-dispersal models.

Chapter 4

Spread in heterogeneous landscape

4.1 Introduction

Environmental conditions may influence the invasion process at different stages. In particular, the rate of spread was found to be environmentally dependent for different species (With, 2002). A number of empirical investigations have speculated that the spatial heterogeneity of the landscape can influence the rate of spread of invasive species (Hastings *et al.*, 2005, and references therein). Indeed, spatial heterogeneity can influence demographic as well as dispersal processes which are the keys to determining the spread of the population (With, 2002; Hui *et al.*, 2012).

The theory of invasion in heterogeneous environments has a rich background in the continuous time framework (using PDEs). Namely, two implementations of spatial heterogeneity have been investigated theoretically. Shigesada *et al.* (1986) first proposed the spatial heterogeneity by alternating homogeneously favourable and unfavourable patches on an infinite one-dimensional environment. The growth rate and diffusion coefficient were given by periodic step functions of the locations. Another environment structure was investigated by Kinezaki *et al.* (2006) by allowing the growth and dispersal parameters to vary sinusoidally in space in response to a sinusoidally distributed habitat quality. In both models, a population introduced at a local point propagated into periodic travelling waves. Estimations of the rate of spread were derived as $c = 2\sqrt{\langle r(x)\rangle_A \langle D(x)\rangle_H}$ when the period of environmental change was sufficiently small, where $\langle r(x)\rangle_A$ and $\langle D(x)\rangle_H$ denote the spatial arithmetic mean of the growth rate and spatial harmonic mean of the diffusion coefficient respectively. The first model put an emphasis on the influence of the sizes of favourable and unfavourable patches on the rate of spread of the population.

The later model on the other hand elucidated the role of the amplitude and wave length of the growth and dispersal parameters.

In this work, we investigate how a population with non-overlapping generations expands its range under the influence of environmental heterogeneity. integrodifference equations are commonly used to model spatiotemporal dynamics of such populations (Kot *et al.*, 1996). The spatial arrangement of habitats have also attracted interest in this context. While some authors constructed more general and robust mathematical formulae of the asymptotic rate of spread (Weinberger *et al.*, 2008), others investigated different assumptions on the spatial heterogeneity and their influence on the population's spread (Kawasaki and Shigesada, 2007; Dewhirst and Lutscher, 2009).

Kawasaki and Shigesada (2007) first proposed the patchy environments which consists of alternating favourable and unfavourable patches. The model was built with exponentially damping (Laplace) dispersal kernel. It was assumed that the spatial heterogeneity affects only the growth processes and did not influence the dispersal kernel. One important outcome of this work suggests that the presence of unfavourable patches can decrease the rate of spread dramatically. However, the population can always spread when the favourable habitats are wide enough regardless of the quality and sizes of unfavourable patches. Dewhirst and Lutscher (2009) later investigated a more general case for the same environment structure. Namely, in addition to location-dependent growth, they considered that individual dispersal behaviours are also affected by the environment for example when individuals from unfavourable locations may disperse far in an attempt to find more favourable habitats. Such dispersal behaviours were incorporated in the model by allowing the variance of the dispersal kernels to vary in space. Similar to the work of Shigesada *et al.* (1986), their approach also put an emphasis on the availability of favourable habitats, that is the proportion of favourable habitats in the environment rather than the actual sizes of the patches. A minimal proportion of favourable habitat to ensure a successful invasion as well as the asymptotic rate of spread were derived.

In this work, two environment structures are considered, namely the alternating favourable and unfavourable patches and the sinusoidally varying environment which were used by Shigesada *et al.* (1986) and Kinezaki *et al.* (2006) respectively in the PDE framework. In addition to location-dependent population growth, individual dispersal behaviours are affected by the environment in two ways. First, the dispersal distance of migrating individuals are affected by the habitat quality of their locations, for example when individuals from unfavourable locations may disperse far in an attempt to find more favourable habitats. Second, we assume that depending on the quality of the local habitat, only a fraction of the local population emigrates while the other

individuals remain sedentary. Such dispersal behaviour are incorporated by using location-dependent dispersal probability.

We first focus on the spread of a population in a patchy environment. This environment structure is used to study the effects environment fragmentations on the rate of spread. We conduct numerical simulations to investigate the instantaneous rate of spread, and derive an estimation of the asymptotic rate of spread. The asymptotic rate of spread is also tested for randomly generated (non-periodic) patchy environments. Then we discuss the proportion of favourable habitat which is optimal to the spread of invasive species. The optimal favourable habitat is illustrated as a function of the growth and dispersal parameters in favourable and unfavourable patches.

The sinusoidally varying environments are used in this work to emphasize the effects of the amplitude of growth and dispersal oscillations on the spread of a population. As for the patchy environment, we use numerical simulations to investigate the instantaneous rate of spread and find an approximation of the asymptotic rate of spread.

4.2 Model formulation

In this section, we model the spatiotemporal dynamics of a population in a heterogeneous environment, then develop the spatial dependence of the growth and dispersal processes.

4.2.1 Modelling the spatiotemporal dynamics of the population

We consider a population which undergoes growth and dispersal stages separated in time. Such spatiotemporal dynamics of population are commonly modelled using integrodifference equations (IDE). In the simplest scenario which consists of a homogeneous environment, that is the growth and dispersal processes do not depend on the location, IDE models take the form

$$u(x, t+1) = \int k(|x-y|)g(u(y,t))\mathrm{d}y$$

where $u(x,t)$ denotes the population size at location x and time t. The function g models the growth of the population, and the dispersal kernel k gives the

probability distribution that an individual from a location y disperses to a location x.

In this work we analyse the IDE model with spatial heterogeneity, that is the growth and dispersal processes depend explicitly on the quality of the local habitat.

The spatial dependence of the growth process is described by a non-negative function $g(u, x)$ satisfying

$$g(u, x) \leq g_u(0, x)u \tag{4.2.1}$$

for all (u, x) where u denotes the population size and $g_u(0, x) = \frac{\partial g}{\partial u}(u = 0, x)$ is the intrinsic growth rate. In what follows, the intrinsic growth rate is denoted by $R(x) = g_u(0, x)$. A commonly used growth function is the Ricker (1954) model given by

$$g(u(x, t), x) = u(x, t)e^{r(x)-u(x,t)}, \tag{4.2.2}$$

and we have $R(x) = e^{r(x)}$.

The dependence of the dispersal process on the spatial heterogeneity can manifest in different ways (Fahrig, 2007; Lutscher, 2008). First, the distance effected by an individual during a dispersal event can be influenced by the habitat quality (Klaassen *et al.*, 2006; Fahrig, 2007). In this case, the spatial dependence of the dispersal process is reflected in the dispersal kernel. More clearly, the dispersal kernel does not only depend on the distance from the source and target location during a dispersal event, but also depends explicitly on the origin of the dispersal. In this case, the dispersal process is described by

$$\hat{u}(x, t) = \int k(|x - y|, y)u(y, t)\mathrm{d}y. \tag{4.2.3}$$

It is worth noting that the second variable of the dispersal kernel models the origin of the dispersal event. We assume that the nature of the dispersal kernel is the same at different locations, *only the parameters of the kernels vary in space*. For example, if Gaussian kernels are used, the dispersal kernels are given by

$$k(|x - y|, y) = \frac{1}{\sqrt{2\pi\sigma^2(y)}} e^{-\frac{(x-y)^2}{2\sigma^2(y)}}. \tag{4.2.4a}$$

Similarly, for Laplace kernels the dispersal kernels are given by

$$k(|x-y|,y) = \frac{1}{\sqrt{2\sigma^2(y)}} e^{-|x-y|\sqrt{\frac{2}{\sigma^2(y)}}}. \tag{4.2.4b}$$

Secondly, spatial heterogeneity can also influence the proportion of the local population that emigrates from the patch or the *dispersal probability*. This phenomenon has been observed for example in European starling and was referred to as the *good-stay, bad-disperse* rule (Hui *et al.*, 2012). In this case, if the pre-dispersal population is given by $u(x,t)$, the dispersal process can be described as

$$\tilde{u}(x,t) = \int \Big[d(y)k(|x-y|) + (1-d(y))\delta(x-y)\Big]u(y,t)\mathrm{d}y. \tag{4.2.5}$$

Here $d(x)$ gives the proportion of the local population that emigrates from the location x, and therefore $1-d(x)$ gives the proportion of the population which remains sedentary.

Taking into account the spatial heterogeneity of the growth process (Eq. 4.2.1), the dispersal probability (Eq. 4.2.5) and the dispersal kernel (Eq. 4.2.3), we consider the following reaction-dispersal model

$$u(x,t+1) = \int \Big[d(y)k(|x-y|,y) + (1-d(y))\delta(x-y)\Big]g(u(y,t),y)\mathrm{d}y \tag{4.2.6}$$

where

$$\delta(x-y) = \begin{cases} 1 & \text{if } x = y \\ 0 & \text{Otherwise.} \end{cases}$$

4.2.2 Modelling the spatial dependence of the growth and dispersal parameters

Two kinds of spatial heterogeneity structures were considered in this work. In the first case, we assume that the environment is periodically fragmented. In this case the habitat consists of alternating "favourable" and "unfavourable" patches with lengths L_1 and L_2 respectively (Shigesada and Kawasaki, 1997).

The habitat is then periodic with a period $L = L_1 + L_2$ with a proportion $p = L_1/L$ favourable patches. The intrinsic growth rate is modelled by

$$R(x) = \begin{cases} R_1 & \text{in favourable habitats} \\ R_2 & \text{in unfavourable habitats.} \end{cases} \tag{4.2.7a}$$

Naturally, R_1 and R_2 are non-negative and we assume that the population can grow in the favourable habitats, that is $R_1 > 1$. For the Ricker model (Eq. 4.2.2), we use $R(x) = e^{r(x)}$ with

$$r(x) = \begin{cases} r_1 & \text{in favourable habitats} \\ r_2 & \text{in unfavourable habitats} \end{cases} \tag{4.2.7b}$$

with $r_2 < r_1$ and $0 < r_1$.

Similarly the dispersal parameters d and σ^2 are respectively given by

$$d(x) = \begin{cases} d_1 & \text{in favourable habitats} \\ d_2 & \text{in unfavourable habitats} \end{cases} \tag{4.2.7c}$$

with $0 \leq d_1, d_2 \leq 1$, and

$$\sigma^2(y) = \begin{cases} \sigma_1^2 & \text{if } y \text{ is a favourable habitat} \\ \sigma_2^2 & \text{otherwise.} \end{cases} \tag{4.2.7d}$$

The second type of heterogeneity consists of a sinusoidally varying environment with wave-length L. We assume that the growth and dispersal processes vary with habitat quality, so that parameters R, d and σ^2 are respectively given by

$$R(y) = R_m + R_a \sin\left(\frac{2\pi}{L} y\right), \tag{4.2.8a}$$

$$d(y) = d_m + d_a \sin\left(\frac{2\pi}{L} y\right), \tag{4.2.8b}$$

and

$$\sigma^2(y) = \sigma_m^2 + \sigma_a \sin\left(\frac{2\pi}{L} y\right). \tag{4.2.8c}$$

The parameters $R_m > 0$, $d_m \geq 0$ and $\sigma_m^2 \geq 0$ denote the spatial mean of growth, dispersal probability and variance of the dispersal kernels respectively. On the other hand, $|R_a|$, $|d_a|$ and $|\sigma_a|$ denote the amplitude of the processes. It is worth to note that the parameters R_a, d_a and σ_a can take negative values. Furthermore, the growth and dispersal probability (resp. dispersal kernel) oscillate in or out of phase, depending on whether $R_a d_a > 0$ or $R_a d_a < 0$ (resp. $R_a \sigma_a > 0$ or $R_a \sigma_a < 0$). Out of phase oscillations indicate trade-off between the two underlying processes.

The parameters are chosen such that R, d and σ^2 are non-negative. Therefore, the mean and amplitude of R, d and σ^2 satisfy $R_m - |R_a| \geq 0$, $d_m - |d_a| \geq 0$ and $\sigma_m^2 - |\sigma_a| \geq 0$. Furthermore, the dispersal probability d satisfies $0 \leq d(y) \leq 1$ for all y, that is $d_m + |d_a| \leq 1$.

A list of the parameters in this Section and the rest of this Chapter is given in Table 4.1.

Variable / Parameter	Description
$u(x,t)$	Population size at location x and time t
k	Dispersal kernel
σ^2	Variance of the dispersal kernel k (function of the location x)
σ_1^2	Value of σ^2 in favourable habitats
σ_2^2	Value of σ^2 in unfavourable habitats
σ_m^2	Mean of σ^2 in sinusoidally varying habitats
σ_a	Amplitude of σ^2 in sinusoidally varying habitats
d	dispersal probability (function of the location x)
d_1	dispersal probability from favourable habitats
d_2	dispersal probability from unfavourable habitats
d_m	Mean dispersal probability in sinusoidally varying habitats
d_a	Amplitude of the dispersal probability in sinusoidally varying habitats
R	Intrinsic growth rate (function of the location x)
R_1	Growth rate in favourable habitats
R_2	Growth rate in unfavourable habitats
R_m	Mean growth rate in sinusoidally varying habitats
R_a	Amplitude of the growth rate in sinusoidally varying habitats
L	Period (wave length) of habitat variation

Table 4.1: Description of parameters and variables.

4.2.3 Quantities of interests

In the numerical simulations, the range of a population at time t is given by

$$x^*(t) = \max\{x, u(x,t) \geq u^*\} \tag{4.2.9}$$

for a threshold of detection u^*, and the corresponding instantaneous and average rate of spread are given by

$$c_I(t) = x^*(t+1) - x^*(t) \tag{4.2.10}$$

and

$$c_A(t) = \frac{x^*(t)}{t} \tag{4.2.11}$$

for $t > 0$.

The time lag before the species range expansion is defined as the first time when the population was detected after its introduction:

$$T(u^*) = \min\{t > 0, x^*(t) > 0\}. \tag{4.2.12}$$

4.3 Results

4.3.1 Time lags in a periodically fragmented environment

To examine whether a population can expand its range in a periodically fragmented environment, we carried out numerical simulations of Eq. 4.2.6, where the spatial dependence of the growth and dispersal processes are as in Eq. 4.2.7, for various sets of parameter values.

We observed that when the population did not go extinct, it expanded its range in both directions from the introduction location. The population range was influenced by different parameters. In some cases, a time lag was observed

before the population's range expansion, often when the population was introduced in an unfavourable patch. Fig. 4.1b shows the range of a population which only started to expand after nine generations. We investigated the length of the time lags for various sets of parameter values. In this section, the populations were introduced only in unfavourable patches as time lags were observed more often in this case.

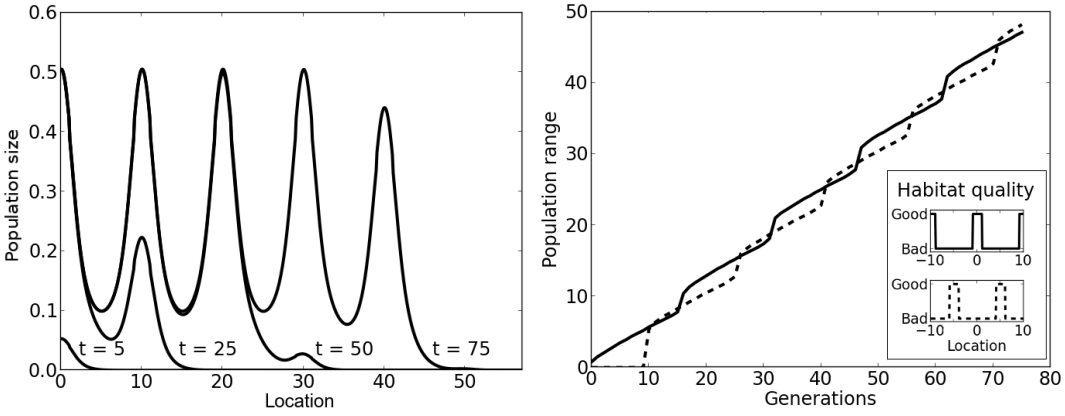

(a) (b)

Figure 4.1: (a) Population density in a periodically fragmented landscape. The initial population was introduced in a good patch. (b) The population range when the initial population was introduced in a good patch (solid line) and in a bad patch (dashed line). In both figures, parameter values were as follows: patches width $L_1 = 2$ and $L_2 = 8$, growth rates $R_1 = e^1$ and $R_2 = 1$, emigration rates $d_1 = d_2 = 1$, variance of dispersal kernels $\sigma_1^2 = \sigma_2^2 = 1$. The threshold of detection was set to $u^* = 0.005$.

Fig.4.2a shows a parameter plane of the time lag as a function of the initial population size (u_0) and the threshold of detection (u^*). The time lag decreased with the size of the initial population and increased with the threshold of detection. Persistent time lags were noticed even for low threshold of detection when the initial population size was very low. On the other hand, the time lags were short or absent when a large population was introduced and the threshold of detection was low.

The time lag was also observed to vary with the growth rate (R_2) and emigration rate (d_2) from unfavourable patches. Fig. 4.2b shows the time lag was shortened by increasing growth and emigration rates. The time lags were longer when unfavourable patches were characterised by declining population size ($R_2 < 1$). However, time lags were still noticed when the population was able to grow in unfavourable patches ($R_2 > 1$) and were more pronounced when only a small proportion of the population migrates.

Fig. 4.2c shows the effects of the width of unfavourable patches (L_2) and the variance of the dispersal kernels (σ_2^2) on the time lags. The time lags were lengthened by the width of unfavourable patches. The variance of the dispersal kernel on the other hand had negative effects on the time lags. Moreover, the time lags were less affected by the dispersal kernel when the width of unfavourable patches were small. In particular in Fig. 4.2c, no time lags observed when the habitats consisted entirely of favourable patches ($L_2 = 0.$).

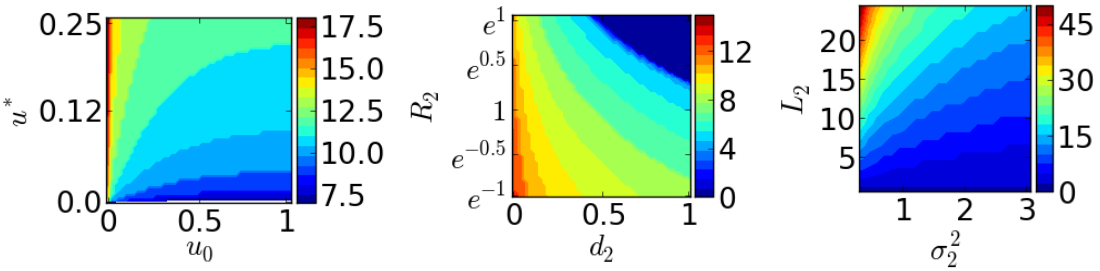

(a) (b) (c)

Figure 4.2: Parameter plans showing the time lag before the range expansion of populations introduced in unfavourable patches. Unless mentioned otherwise, the parameter values are $L_{1,2} = 5$, $R_1 = e^1$ and $R_2 = e^{-0.5}$, $d_{1,2} = 1$, $\sigma_{1,2}^2 = 1$, $u^* = 0.005$ and $u_0 = 0.25$. (a) Time lag as a function of the initial population size (u_0) and the threshold of detection (u^*).u_0 runs from 0.001 to 1 at a step of 0.02 and u^* runs from 0.005 to 0.25 at a step of 0.005. (b) Time lag as a function of the growth rate (R_2) and emigration rates (d_2) in unfavourable patches. R_2 runs from e^{-1} to e^1 at a step of 0.04 and d_2 runs from 0.02 to 1 at a step of 0.02. (c) Time lag as a function of the width of unfavourable patches (L_2) and the variance of dispersal kernels (σ_2^2). L_2 runs from 0 to 25 with a step of 1 and σ_2^2 runs from 0.25 to 3 at a step of 0.125.

4.3.2 Spread in a periodically fragmented environment

Population size and instantaneous rate of spread

Intensive numerical simulations suggested a similarity between the range dynamics of a propagating population that was introduced in a good and bad patch (see for example Fig. 4.1b). Therefore the population ranges and rate of spread in the remainder of this chapter were computed for populations introduced in a favourable patch.

First we investigated the effects of changing period L of environment variation and the width of the patches, that is L_1, L_2. To this end, we undertook numerical simulations for various period of the landscape L and set the width of favourable and unfavourable patches respectively to $L_1 = pL$ and $L_2 = (1-p)L$ for some p between 0 and 1. We recall that p corresponds to the proportion of good habitat in the environment. We observed that the population size oscillated with the environment. Furthermore, for a fixed proportion of good habitat p, the oscillations of the population size were more pronounced, with larger amplitude and longer wave length, for longer period of the environmental variation L (Fig. 4.3, left). More precisely, the wave length of the population size matched the period of environmental variations.

The period of the environmental variations also affected the rate of spread of the population. When the period of the environment was short, we observed that the instantaneous rate of spread fluctuated with small amplitude. As the period environmental variations increase, the fluctuations of the rate of spread became more evident with greater amplitude (Fig. 4.3, middle). On the other hand, the time averaged rate of spread was less affected by the period of the environmental variations. Less fluctuations were observed in the temporal dynamics of the average rates of spread. Moreover, we observed that the average rate of spread tend to the same value for populations invading environments with different period propagate when the same proportion of good habitats were available.

These observations also manifested in the range dynamics of the populations. Namely, consecutive accelerations and decelerations of the population's range expansion were observed, specially for long period of the environmental variations. In a broader view however, we observed that the trend of range expansions remained the same for populations propagating in environment with different period but sharing a common proportion of favourable habitats (Fig. 4.3, right). To see this effect in a wider perspective, we calculated the asymptotic rate of spread.

Asymptotic rate of spread

The asymptotic rate of spread is derived hereafter. The main results are given in Eq.4.3.7 and Eq.4.3.12.

First, we assume that the population is small at the front of the invasion and consider the linearisation

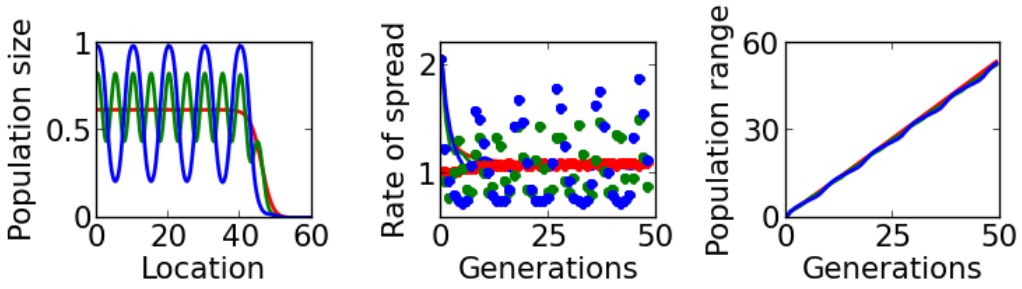

Figure 4.3: Effects of changing the environment period when the parameter values are given by: growth rates $R_1 = e^1$ and $R_2 = 1$, dispersal probabilities $d_1 = d_2 = 1$, variance of dispersal kernels $\sigma_1^2 = \sigma_2^2 = 1$. The proportion of good habitat is $p = 0.5$. The colors red, green and blue correspond to the environment period $L = 1$, $L = 5$ and $L = 10$ respectively. Left: Population size after 50 generations. Middle: Rate of spread as a function of time. Right: Population range as a function of time.

$$u(x, t+1) = \int \left[d(y)k(x-y, y) + (1-d(y))\delta(x-y)\right] R(y)u(y,t)\mathrm{d}y. \quad (4.3.1)$$

We recall that

$$g(u, x) \leq R(x)u,$$

so that the range of the population governed by the model (Eq. 4.2.6) is bounded by that of its linearisation (Eq.4.3.1).

In what follows, we use heuristic methods to find an approximation of the rate of spread of the population governed by Eq. 4.3.1. Motivated by the periodicity of the growth and dispersal parameters on one hand, and numerical observations on the other hand, we assume that when the population does not eventually become extinct, it evolves into a travelling periodic wave (Kinezaki *et al.*, 2006). In other words, there exists a number $t^* > 0$ such that

$$u(x + L, t + t^*) = u(x, t).$$

The speed of the travelling periodic wave is defined by

$$c = \frac{L}{t^*}. \quad (4.3.2)$$

Here, we seek solutions of the form

$$u(x,t) = e^{-\lambda(x-c(\lambda)t)}v(x) \tag{4.3.3}$$

for some $\lambda > 0$, where v is periodic in the space variable (x) with the same period as the habitat $(v(x+L) = v(x))$ and $v(x) \geq 0$. Inserting Eq.4.3.3 into Eq. 4.3.1 and using the fact that d, r and v are periodic, we have

$$\begin{aligned} e^{\lambda c(\lambda)}v(x) = &\sum_{n=-\infty}^{+\infty} \int_0^L d(y)k(x-y-nL,y)e^{\lambda(x-y-nL)}R(y)v(y)\mathrm{d}y \\ &+ (1-d(x))R(x)v(x). \end{aligned}$$

For exponentially bounded dispersal kernel, we invert the order of the summation and integration and get

$$\begin{aligned} e^{\lambda c(\lambda)}v(x) = &\int_0^L \left[\sum_{n=-\infty}^{+\infty} k(x-y-nL,y)e^{\lambda(x-y-nL)}\right] d(y)R(y)v(y)\mathrm{d}y \\ &+ (1-d(x))R(x)v(x). \end{aligned}$$

For L sufficiently small, we use the approximation

$$\sum_{n=-\infty}^{+\infty} k(x-y-nL,y)e^{\lambda(x-y-nL)} \approx \frac{1}{L}M(\lambda,y)$$

when x and y are fixed, where $M(\lambda,y)$ is the moment generating function of the dispersal kernel at location y given by

$$M(\lambda,y) = \int k(z,y)e^{\lambda z}\mathrm{d}z.$$

We deduce that

$$e^{\lambda c(\lambda)}v(x) = \frac{1}{L}\int_0^L M(\lambda,y)d(y)R(y)v(y)\mathrm{d}y + (1-d(x))R(x)v(x)$$

for $0 \leq x \leq L$. In particular, consider $\underline{x}$ and $\overline{x}$ such that

$$v(\underline{x}) \leq v(x) \leq v(\overline{x}). \tag{4.3.4}$$

On one hand, we have

$$e^{\lambda c(\lambda)} v(\underline{x}) \approx \frac{1}{L} \int_0^L M(\lambda, y) d(y) R(y) v(y) \mathrm{d}y + (1 - d(\underline{x})) R(\underline{x}) v(\underline{x}).$$

Assuming that $0 < v(\underline{x})$, the rate of spread $c(\lambda)$ associated to λ satisfies

$$e^{\lambda c(\lambda)} \approx \frac{1}{L} \int_0^L M(\lambda, y) d(y) R(y) \frac{v(y)}{v(\underline{x})} \mathrm{d}y + (1 - d(\underline{x})) R(\underline{x}).$$

Clearly,

$$\frac{1}{L} \int_0^L M(\lambda, y) d(y) R(y) \mathrm{d}y \leq \frac{1}{L} \int_0^L M(\lambda, y) d(y) R(y) \frac{v(y)}{v(\underline{x})} \mathrm{d}y$$

and

$$\min_{0 \leq x \leq L} (1 - d(x)) R(x) \leq (1 - d(\underline{x})) R(\underline{x}).$$

Therefore

$$\frac{1}{L} \int_0^L M(\lambda, y) d(y) R(y) \mathrm{d}y + \min_{0 \leq x \leq L} (1 - d(x)) R(x) \leq e^{\lambda c(\lambda)}. \tag{4.3.5a}$$

Similarly, one can establish that

$$e^{\lambda c(\lambda)} \leq \frac{1}{L} \int_0^L M(\lambda, y) d(y) R(y) \mathrm{d}y + \max_{0 \leq x \leq L} (1 - d(x)) R(x). \tag{4.3.5b}$$

Recall that the population from the original model (Eq. 4.2.6) does not spread faster than the linearised population. Therefore, the smallest rate of spread

$$c = \min_{\lambda \in I} c(\lambda) \tag{4.3.6}$$

from the linearised model is an upper bound of the speed of the original population, where I is the interval on which the moment generating functions $M(.,y)$ are defined for all $y \in [0,L]$. For Gaussian and Laplace dispersal kernels, I is respectively given by

$$I = (0, \infty)$$

and

$$I = \left(0, \min_{0\leq y\leq L} \frac{1}{\sqrt{\sigma^2(y)}}\right).$$

In the remainder of this chapter, we study the rate of spread given by the minimal wave seed in Eq. 4.3.6 holds. Using Eq. 4.3.5, we deduce lower and upper bounds of the the asymptotic rate of spread c.

Main result 1:

The asymptotic rate of spread c satisfies

$$\min_{\lambda\in I} c_{\min}(\lambda) \leq c \leq \min_{\lambda\in I} c_{\max}(\lambda) \tag{4.3.7a}$$

where

$$c_{\min}(\lambda) = \frac{1}{\lambda} \ln\left(\frac{1}{L}\int_0^L M(\lambda,y)d(y)R(y)\mathrm{d}y + \min_{0\leq y\leq L}(1-d(y))R(y)\right) \tag{4.3.7b}$$

and

$$c_{\max}(\lambda) = \frac{1}{\lambda} \ln\left(\frac{1}{L}\int_0^L M(\lambda,y)d(y)R(y)\mathrm{d}y + \max_{0\leq y\leq L}(1-d(y))R(y)\right). \tag{4.3.7c}$$

In particular, when the dispersal probability $d \equiv 1$, we have $c_1 = c_2$ and we obtain the relation established by Dewhirst and Lutscher (2009)

$$c = \min_{\lambda\in I} \frac{1}{\lambda} \log\left(pR_1M_1(\lambda) + (1-p)R_2M_2(\lambda)\right) \tag{4.3.8}$$

where M_1 and M_2 design the moment generating functions of the dispersal kernel from favourable and unfavourable patches respectively.

In what follows, we derive approximations of $\min_{\lambda\in I} c_1(\lambda)$ and $\min_{\lambda\in I} c_2(\lambda)$. Using the expansion of the moment generating functions

$$M(\lambda, y) \approx 1 + \frac{1}{2}\sigma^2(y)\lambda^2$$

for sufficiently small λ, we have

$$c_{\min}(\lambda) \approx \frac{1}{\lambda}\ln\left(\overline{R}_{\min} + \frac{\overline{c}^2}{4}\lambda^2\right), \text{ and } c_{\max}(\lambda) \approx \frac{1}{\lambda}\ln\left(\overline{R}_{\max} + \frac{\overline{c}^2}{4}\lambda^2\right)$$

where

$$\overline{R}_{\min} = \frac{1}{L}\int_0^L d(y)R(y)\mathrm{d}y + \min_{0\le y\le L}(1-d(y))R(y), \tag{4.3.9a}$$

$$\overline{R}_{\max} = \frac{1}{L}\int_0^L d(y)R(y)\mathrm{d}y + \max_{0\le y\le L}(1-d(y))R(y) \tag{4.3.9b}$$

and

$$\overline{c} = \sqrt{2\frac{1}{L}\int_0^L d(y)R(y)\sigma^2(y)\mathrm{d}y}. \tag{4.3.9c}$$

In particular, for periodically fragmented landscapes (that is the growth and dispersal parameters given in Eq. 4.2.7), we have

$$\overline{R}_{\min} = pd_1R_1 + (1-p)d_2R_2 + \min_{0\le y\le L}(1-d(y))R(y), \tag{4.3.10a}$$

$$\overline{R}_{\max} = pd_1R_1 + (1-p)d_2R_2 + \max_{0\le y\le L}(1-d(y))R(y) \tag{4.3.10b}$$

and

$$\overline{c} = \sqrt{2pd_1R_1\sigma_1^2 + 2(1-p)d_2R_2\sigma_2^2}. \tag{4.3.10c}$$

If $\overline{R}_{\min} > 1$, we further expand $c_{\min}$ and $c_{\max}$ and get

$$c_{\min}(\lambda) \approx \frac{1}{\lambda}\left(\ln \overline{R}_{\min} + \frac{\overline{c}^2}{4\overline{R}_{\min}}\lambda^2\right), \text{ and } c_{\max}(\lambda) \approx \frac{1}{\lambda}\left(\ln \overline{R}_{\max} + \frac{\overline{c}^2}{4\overline{R}_{\max}}\lambda^2\right)$$

with minimum

$$c^*_{\min} = \overline{c}\sqrt{\frac{\ln \overline{R}_{\min}}{\overline{R}_{\min}}}, \text{ and } c^*_{\max} = \overline{c}\sqrt{\frac{\ln \overline{R}_{\max}}{\overline{R}_{\max}}}.$$

Main result 2:

When

$$1 \leq \overline{R}_{\min} \leq \overline{R}_{\max} \leq e, \tag{4.3.11}$$

the asymptotic rate of spread c of the population generated by Eq. 4.2.6 satisfies

$$\overline{c}\sqrt{\frac{\ln \overline{R}_{\min}}{\overline{R}_{\min}}} \leq c \leq \overline{c}\sqrt{\frac{\ln \overline{R}_{\max}}{\overline{R}_{\max}}} \tag{4.3.12}$$

where $\overline{R}_{\min}, \overline{R}_{\max}$ and $\overline{c}$ are defined in Eq. 4.3.10 for periodically fragmented environment, and in Eq. 4.3.9 in general.

It is worth noting that the expressions of the asymptotic average rate of spread does not depend explicitly on the period of environmental variations (L) or the width of favourable and unfavourable patches (L_1 and L_2) but only on the proportion of favourable habitats ($p = L_1/L$). This is consistent with speculations from numerical simulations that the average rate of spread is not affected by the period of environmental variations.

The inequalities in Eq. 4.3.12 with Eq. 4.3.10 were verified with rates of spread computed from numerical simulations for various sets of parameter values. Furthermore, Fig. 4.4 suggests that the lower bound in Eq. 4.3.12 provides an approximation of the rate of spread obtained from the numerical simulations for different range of growth rate, dispersal probability and dispersal kernel. Therefore, in what follows we investigate the effects of the growth and dispersal parameters on the lower bound of the rate of spread

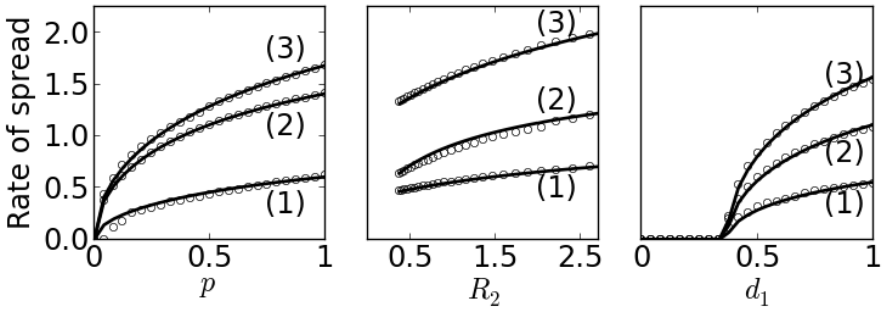

Figure 4.4: Rate of spread from Eq. 4.3.12 (solid lines) and from numerical simulations with 50 generations (open circles). Left: Rate of spread as a function of the proportion of good habitats. The parameters are (1) $R_1 = e^1, R_2 = 1$, $d_{1,2} = 0.75$ and $\sigma^2_{1,2} = 0.25$, (2) $R_1 = e^1, R_2 = 1$, $d_{1,2} = 0.75$ and $\sigma^2_{1,2} = 1$, (3) $R_1 = e^1, R_2 = 1$, $d_1 = 0.75, d_2 = 1$ and $\sigma^2_{1,2} = 2$. Middle: Rate of spread as a function of the intrinsic growth in unfavourable patches. Right: Rate of spread as a function of the emigration from favourable patches.

$$c = \overline{c}\sqrt{\frac{\ln \overline{R}_{\min}}{\overline{R}_{\min}}}. \tag{4.3.13}$$

Clearly, the rate of spread increases with the growth rates (R_1 and R_2) and the variance of the dispersal kernels (σ_1^2 and σ_2^2). The dependences of the rate of spread on the dispersal probabilities (d_1 and d_2) however are less evident due to the term $\min\{(1-d_1)R_1, (1-d_2)R_2\}$ which appears in Eq. 4.3.10a.

To elucidate the effects of the location-dependent dispersal probability, we constructed a contour plot of the rate of spread as a function of d_1 and d_2 for different proportion of favourable habitat p (Fig. 4.5). Firstly, we noticed that the rate of spread increased with the dispersal probabilities whenever $d_1 = d_2$. The slowest rate of spread was associated to the minimal dispersal probabilities ($d_1 = d_2 = 0$), and the largest rates of spread were observed when the dispersal probabilities were both at their maximal values ($d_1 = d_2 = 1$). Secondly, when $d_1 \leq d_2$, d_2 had negative influence on the rate of spread whereas d_1 yielded faster range expansion. Thirdly, when $d_1 > d_2$, emigrations from both type of habitats (favourable and unfavourable) can act to decelerate or accelerate the range expansion. On one hand, when d_1 was small the rate of spread decreased with d_2. When d_1 was sufficiently large however, the rate of spread was improved by d_2. On the other hand, the rate of spread increased with d_1 when d_1 was smaller than a threshold value beyond which the rate of spread became a decreasing function of d_1. Furthermore, we noticed that the higher the values of p and d_2, the higher the threshold at which d_1 produced negative effects on the rate of spread. As more favourable habitats became available

(larger values of p), the rate of spread increased with d_1 regardless of the values of d_2.

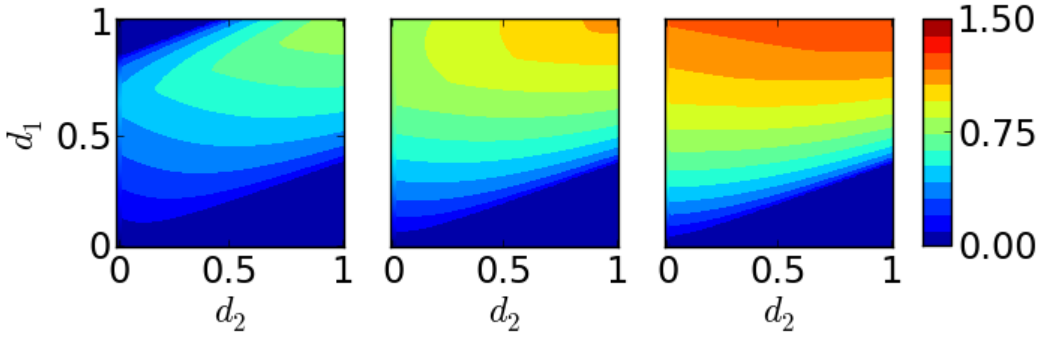

Figure 4.5: Rate of spread as a function of the dispersal probabilities. From left to right, $p = 0.25, 0.5$ and 0.75. Other parameters are $R_1 = e^1, R_2 = 1$, $\sigma^2_{1,2} = 1$.

4.3.3 Optimal proportion of favourable habitats

To investigate the proportion of favourable habitats that is optimal for the spread of an invasive species, we fix the growth and dispersal parameters ($R_{1,2}, d_{1,2}$ and $\sigma^2_{1,2}$) and consider the rate of spread as a function of the proportion of favourable habitat p

$$c(p) = \overline{c}(p)\sqrt{\frac{\log \overline{R}(p)}{\overline{R}(p)}}, \tag{4.3.14}$$

where

$$\overline{R}(p) = pd_1R_1 + (1-p)d_2R_2 + \min\{(1-d_1)R_1, (1-d_2)R_2\},$$

and

$$\overline{c}^2(p) = 2(pd_1R_1\sigma_1^2 + (1-p)d_2R_2\sigma_2^2).$$

Since c and $\frac{c^2}{2}$ assume their respective maximum at the same proportion of favourable habitat p, we study the maxima of $\frac{c^2}{2}$. Differentiating Eq. 4.3.14 with respect to p yields

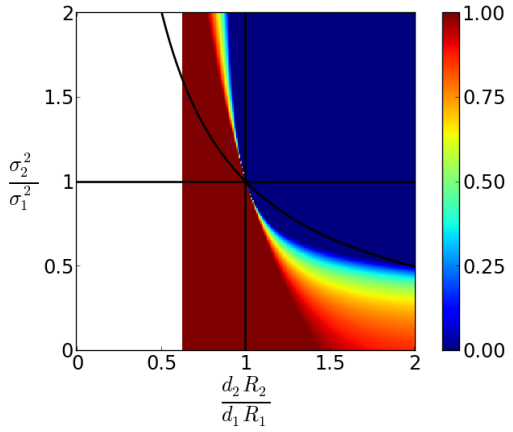

Figure 4.6: Optimal proportion of favourable habitats when $R_1 = e^1$, $d_1 = 0.5, d_2 = 1$ and $\sigma_1^2 = 1$. The white region indicates parameter values where the population did not spread ($c = 0$) regardless of the proportion of good habitat.

$$\left(\frac{c^2(p)}{2}\right)' = \frac{1}{\overline{R}^2(p)}\left((d_1R_1 - d_2R_2)\overline{c}^2(p) + (d_1R_1\sigma_1^2 - d_2R_2\sigma_2^2)m\log\overline{R}(p)\right) \tag{4.3.15}$$

One can see that when $d_1R_1 - d_2R_2 > 0$ and $d_1R_1\sigma_1^2 - d_2R_2\sigma_2^2 > 0$, the rate of spread increases with the proportion of favourable habitat p and the optimal rate of spread is attained when $p = 1$, that is when the environment is homogeneously favourable. On the other hand, when $d_1R_1 - d_2R_2 < 0$ and $d_1R_1\sigma_1^2 - d_2R_2\sigma_2^2 < 0$, we have $(c^2(p))' < 0$. In this case the rate of spread decreases with the proportion of favourable habitats and the maximal rate of spread is achieved when $p = 0$, that is when the environment consists entirely of unfavourable habitat. It is worth noting however that the population can spread in the later case only if the population can grow even in unfavourable habitats ($R_2 > 1$). Unfortunately, exact values of the optimal proportion of favourable habitats could not be derived for two cases, the first when $d_1R_1 - d_2R_2 < 0$ and $d_1R_1\sigma_1^2 - d_2R_2\sigma_2^2 > 0$, and the second when $d_1R_1 - d_2R_2 > 0$ and $d_1R_1\sigma_1^2 - d_2R_2\sigma_2^2 < 0$. Nonetheless, numerical results suggest that that the optimal proportion of favourable habitat decreases with $\frac{d_2R_2}{d_1R_1}$ and $\frac{\sigma_2^2}{\sigma_1^2}$ (Fig. 4.6).

4.3.4 Spread in a randomly fragmented environment

Since the expression of the rate of spread (Eq. 4.3.12) depends on the proportion of favourable habitats p rather than the actual width of the patches, we investigated the importance of the spatial arrangement of the favourable and unfavourable patches, that is level of fragmentation, when the proportion of favourable habitat is fixed.

To this end, we considered that the habitat consisted of a random succession of patches of length 0.1. The level of landscape fragmentation is modelled by its spatial autocorrelation I. Spatial autocorrelation near 1 indicates low level of fragmentation, that is favourable patches are likely to be grouped together and similarly for unfavourable patches. Highly fragmented landscapes on the other hand are determined by spatial autocorrelation near 0. To generate landscapes with spatial autocorrelation I and proportion of favourable habitat p, we modified the algorithm for autocorrelated data presented by Fang and Tacher (2003). Examples of the resulting habitats are shown in Fig. 4.7a for a proportion of favourable habitats $p = 0.75$.

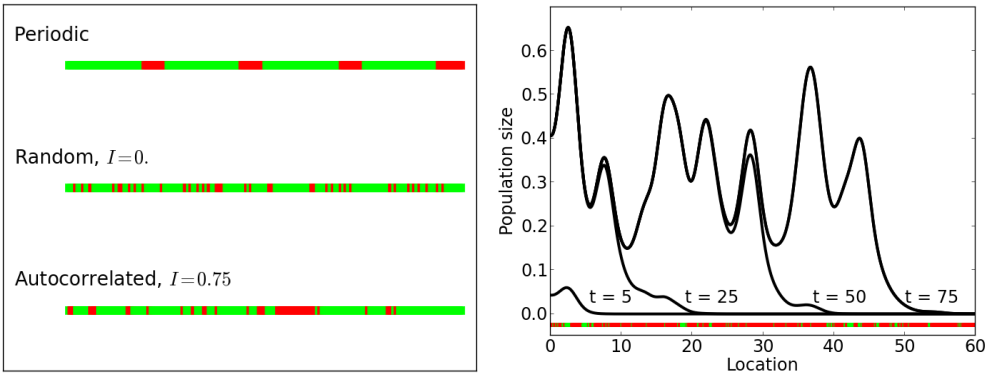

(a) Randomly generated landscapes. (b) Propagating population.

Figure 4.7: (a) Examples of non-periodic landscapes generated with prescribed spatial autocorrelation (I) and proportion of favourable habitat is $p = 0.75$. Green and red represents favourable and unfavourable patches respectively. (b) A population propagating in a non-periodic landscape. The quality of local habitats are shown at the bottom of the figure. Parameters are as in Fig. 4.3.

Snapshots of the propagating population are shown in Fig. 4.7b for the same parameter values as in Fig. 4.3 and level of fragmentation $I = 0.75$. Unlike the population invading a periodically fragmented landscape, the population densities in randomly fragmented landscapes were observed to fluctuate in space, with irregular amplitude and no apparent spatial cycles. The temporal

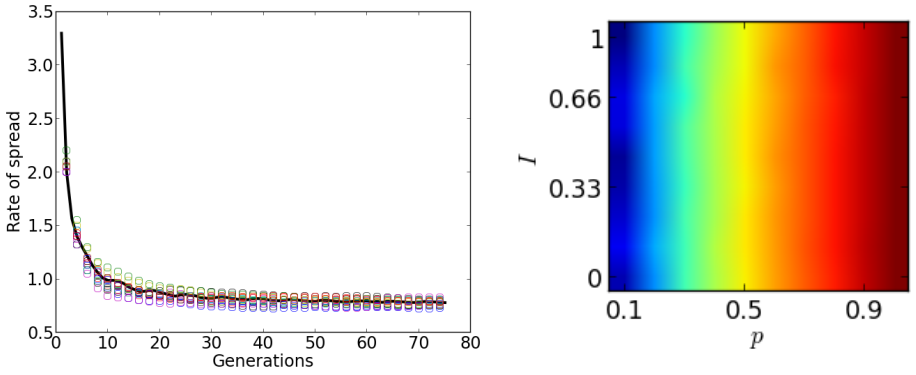

(a) Instantaneous rate of spread. (b) Asymptotic rate of spread.

Figure 4.8: (a) Rate of spread in non-periodic landscapes. Open circles indicate the rate of spread from 15 different habitat with a prescribed fragmentation level I, $p = 0.75$. For comparison, the rate of spread obtained from periodic landscape is plotted in solid line. (b) Mean asymptotic rate of spread from 15 simulations as a function of the proportion of favourable habitat p and fragmentation level I after 50 generations. In both figures, the parameters values are: Growth rates: $r_1 = 1$ and $r_2 = 0.75$, Emigration rates: $d_1 = 0.75$ and $d_2 = 1$, Dispersal rates: $\sigma_1^2 = 1$ and $\sigma_2^2 = 0.5$.

dynamics of the rate of spread however were similar for the periodic and randomly fragmented landscapes (Fig. 4.8a). In particular the rate of spread in randomly fragmented landscapes also converged to a constant value.

To elucidate the effect of the spatial arrangement favourable and unfavourable patches more accurately, we conducted exhaustive numerical simulation with different growth and dispersal parameter values (that is $R_{1,2}, d_{1,2}, \sigma_{1,2}^2$). For each set of parameter values, the landscapes were characterised the proportion of favourable habitat and fragmentation level. We run 15 simulations of the model for each pair (p, I) and collected the asymptotic rate of spread at the end of each simulation. The mean of the rates of spread from the 15 simulations are shown in Fig. 4.8b for different values of the proportion of favourable habitats p and level of fragmentation I. We observed that the mean of the rates of spread increased with the proportion of favourable habitats but was not affected by the level of habitat fragmentation.

4.3.5 Spread in a sinusoidally varying environment

To elucidate the effects of sinusoidally varying environments on the spread of a population, we carried out numerical simulations on the model Eq. 4.2.6 with the growth and dispersal parameters as defined in Eq. 4.2.8 for different

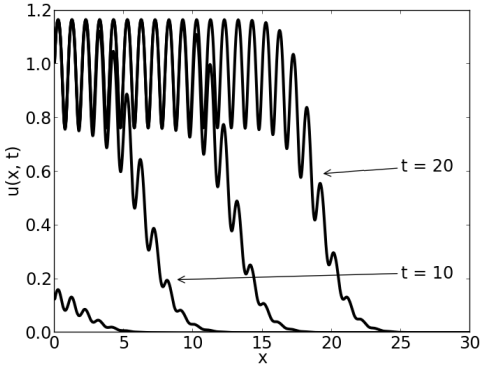

Figure 4.9: A population propagating in a sinusoidally varying environment.

sets of parameter values. We observed that when the population did not go extinct after some generations, it evolved into a periodic travelling wave and the population size oscillated in synchrony with the environment (Fig. 4.9).

Like for the case of fragmented environments, we start with the numerical investigations of the instantaneous rate of spread then move on with the asymptotic rate of spread.

When investigating the influence of the amplitude of the growth and dispersal parameters on the instantaneous rate of spread, we considered three cases:

$$\text{Case 1: } R(x) = R_m + R_a \sin\left(\frac{2\pi}{L}x\right), \sigma^2(x) = 1, d(x) = 0.75,$$

$$\text{Case 2: } R(x) = 2, \sigma^2(x) = \sigma_m^2 + \sigma_a \sin\left(\frac{2\pi}{L}x\right), d(x) = 0.75,$$

$$\text{Case 3: } R(x) = 2, \sigma^2(x) = 1, d(x) = d_m + d_a \sin\left(\frac{2\pi}{L}x\right).$$

We note that the three cases consist of evaluating the pure influence of the oscillations of the growth, dispersal kernel and dispersal probability respectively. The results are summarized in Fig. 4.10. When only the growth rate oscillated in space (Fig. 4.10, left rows), the population size also oscillated with the same wavelength. Furthermore, the oscillations became more pronounced as we increased $|R_a|$. The oscillations in the growth rate also yielded fluctuations in time of the rate of spread. Similar to the population density, the fluctuations in the rate of spread were more noticed for greater amplitude $|R_a|$ of the growth rate.

Similar behaviours were observed when only the dispersal kernels (Fig. 4.10, middle rows) or the dispersal probability (Fig. 4.10, right rows) was allowed

to oscillate in space. Namely, the population size oscillated in space with amplitude increasing with $|\sigma_a|$ and $|d_a|$. The instantaneous rate of spread in turn fluctuated in time, with amplitude growing with the amplitudes of the dispersal parameters. However, it is worth noting that the oscillations of the population size were in phase with the growth rate and out of phase with the dispersal parameters, namely the dispersal kernel and dispersal probability.

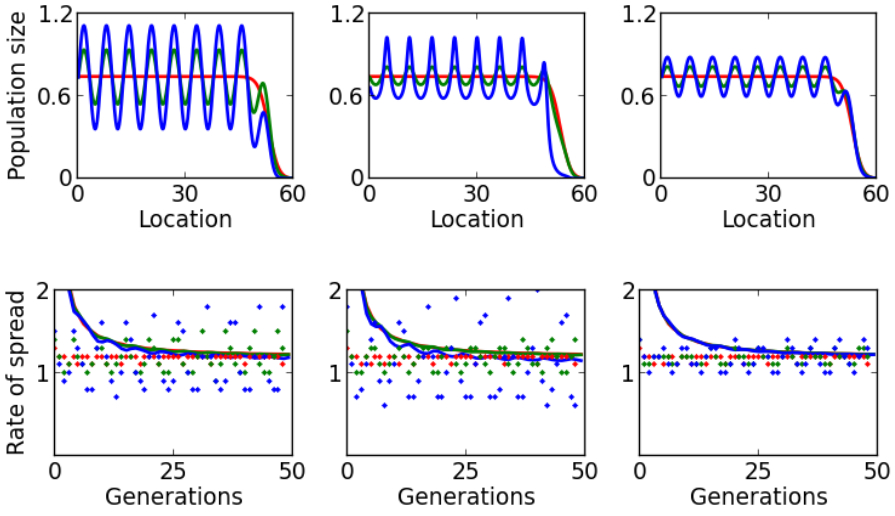

Figure 4.10: Top figures: Population size after 50 generations. Bottom figures: Instantaneous (dots) and average (solid lines) rate of spread. Left: The case where $R(x) = 2 + R_a \sin(2\pi x/L), \sigma^2(x) = 1, d(x) = 0.75$. The colors red, green and blue correspond to $R_a = 0, 1$ and 2 respectively. Middle: The case where $R(x) = 2, \sigma^2(x) = 1 + \sigma_a \sin(2\pi x/L), d(x) = 0.75$. The colors red, green and blue correspond to $\sigma_a = 0, 0.25$ and 0.5 respectively. Right: The case where $R(x) = 2, \sigma^2(x) = 1, d(x) = 0.75 + d_a \sin(2\pi x/L)$ with $d_a = 0$ (red), $d_a = 0.125$ (green) and $d_a = 0.25$ (blue).

Despite the persistent fluctuations of the rate of spread, we observed that the average rate of spread had more stable behaviour and seemed to converged to a constant value as the number of generations increased (Fig. 4.10). We numerically calculated the average rate of spread for exhaustive set of parameter values. The results are summarised in Fig. 4.11.

Firstly, Fig. 4.11c suggests that the higher the mean dispersal probability (d_m), the faster the spread of the population. Secondly, increasing the amplitude of the dispersal ability ($|d_a|$) can act to accelerate of decelerate the range expansion. Namely we found that increasing amplitude of the dispersal ability $|d_a|$ accelerated the spread of the population when the growth rate and the dispersal probability oscillate in the same phase (that is $R_a d_a > 0$ - Shown in Fig. 4.11c). When the growth rate and the dispersal probability oscillated in

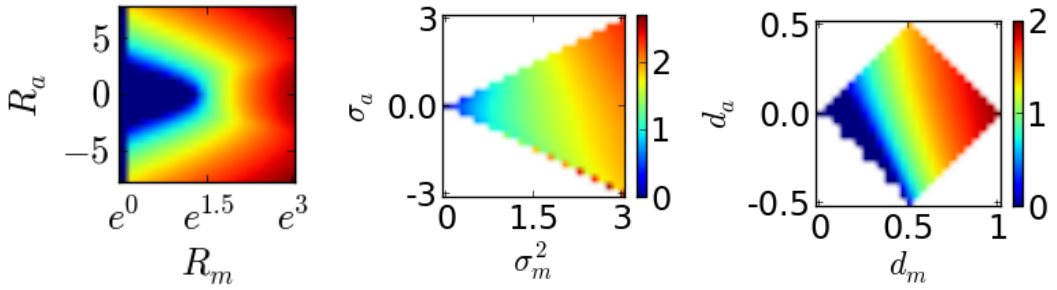

(a) (b) (c)

Figure 4.11: Parameter plans showing the asymptotic rate of spread in sinusoidally varying environments as function of (a) the mean and amplitude of the growth rate, (b) the mean and amplitude of the dispersal kernel and (c) the mean and amplitude of the dispersal probability. When not shown in the figure, the parameter values are $R_m = e, R_a = 2$, $d_m = 0.75, d_a = 0$ and $\sigma_m^2 = 2, \sigma_a = 0$.

anti-phase ($R_a d_a < 0$), the rate of spread was depreciated by increasing $|d_a|$. Finally, we observed that the rate of spread was more sensitive to the mean dispersal probability d_m than its amplitude d_a.

Similar effects were observed when the dispersal kernel oscillated in space (Fig. 4.11b). Namely increasing the mean dispersal kernel σ_m^2 yielded faster rate of spread. Higher amplitude of the dispersal kernel ($|\sigma_a|$) on the other hand had positive or negative effects on the rate of spread depending on whether the oscillations of the dispersal kernel were in phase with that of the growth rate ($|R_a\sigma_a > 0|$) or out of phase ($|R_a\sigma_a < 0|$).

We calculated the average rate of spread and found that in the long term, similar to the case of fragmented environments, the rate of spread was approximately given by

$$c = \overline{c}\sqrt{\frac{\log \overline{R}}{\overline{R}}} \tag{4.3.16}$$

when $\overline{R} > 1$ where the average growth rate $\overline{R}$ and the average rate of spread $\overline{c}$ are given by

$$\overline{R} = \frac{1}{L}\int_0^L d(x)R(x)\mathrm{d}x + \min_{0\le x\le L}(1 - d(x))R(x) \tag{4.3.17}$$

and

$$\bar{c} = \sqrt{\frac{2}{L} d(x) R(x) \sigma^2(x) \mathrm{d}x}. \tag{4.3.18}$$

4.4 Discussion

To elucidate the importance of environmental variations on the rate of spread of invasive species, we presented an IDE model in which both growth and dispersal processes are assumed to vary along with the environment. Two main environmental structures were considered, namely a patchy or fragmented environment and a sinusoidally varying environment. The first environment detail was aimed to depict the importance of environment fragmentations and the second put an emphasis on the amplitude of environmental variations on the rate of spread.

The asymptotic rate of spread

There have been different models that address the spread of a species in a spatially varying environment. In the case of continuous models, namely using PDEs, Shigesada *et al.* (1986) and Kinezaki *et al.* (2006) showed that the asymptotic rate of spread in a periodic environment may depend only space-average growth and dispersal rate. In this work, we derived an approximation of the asymptotic rate of spread in the framework of integrodifference equations. Lower and upper bounds of the rate of spread are given in Eq. 4.3.7, and the final approximation, which depends explicitly on the growth and dispersal parameters, is presented in Eq. 4.3.12. First, Eq. 4.3.7 is consistent with the results obtained by Kawasaki and Shigesada (2007) for the case where only the growth rate is spatially varying and the results derived by Dewhirst and Lutscher (2009) where both the growth rate and the dispersal kernel are location-dependent but the dispersal probability is homogeneously equal to one (in other words, all individuals migrate during the dispersal phase).

Second, although we considered in this model that part of local populations may remain sedentary during the dispersal phase depending on the quality of the local habitats, Eq. 4.3.12 suggests that the sedentary individuals also contribute to the spread of the population. The approximation advocates that the population will eventually become extinct whenever the averaged growth rate (Eq. 4.3.9a) is less than one. The expression of the average growth rate suggests that the sedentary populations contributes to the survival and growth

of local populations, hence to the spread of the overall population (Further discussed later).

Third, the derived rate of spread (Eq. 4.3.12) depends on the spatially averaged growth rate (Eq. 4.3.9a) and a "spatially averaged rate of spread" (Eq. 4.3.9c) rather than the harmonic mean of the dispersal rate as for PDE based models (Shigesada *et al.*, 1986; Kinezaki *et al.*, 2006). We speculate that this is due to the more explicit implementations of the dispersal distance in dispersal kernel models compared to the dispersal rate in their PDE counter part.

Fourth, the approximations obtained in this work were derived for small period of environmental variation. Numerical simulations (run for $L \leq 10$) however suggested that the approximations were reasonably accurate for longer period. Similar observations were made by Kawasaki and Shigesada (2007) in the case of Laplace dispersal kernels. Furthermore, one can also use a dimensionless model (see for example the work of Dewhirst and Lutscher (2009)) and assume that $L = 1$.

Finally, the approximation Eq. 4.3.12 was derived for periodically varying environments with sufficiently small period. Numerical simulations show that the approximation agree with rate of spread computed on randomly generated landscapes (Fig. 4.7b). This is due to the fact that the approximation does not depend explicitly on the period of environmental variations but rather on the availability of favourable habitats in the overall landscape.

Dispersal behaviours and the rate of spread

It is well known that the spread of a population is the result of an interplay between growth and individuals movements. Most spread models, in particular models in heterogeneous environments, have focused on different growth responses and the dispersal distance ((Kawasaki and Shigesada, 2007; Dewhirst and Lutscher, 2009)). The influence of dispersal probability in turn have received only little attention. Indeed, in a homogeneous environment, the higher the dispersal probability, the faster the spread of the population (Lutscher, 2008). In this work we investigated the effects of location-dependent dispersal behaviours.

Unlike the case of homogeneous environment, we found that spatially varying dispersal probability can have both negative and positive effects on the spread of a population (Fig. 4.5). When only a small proportion of the environments is favourable for the population's growth (Fig. 4.5 - left), the rate of spread was improved by small dispersal probability from favourable patches but decelerated by the emigrations from unfavourable patches. Indeed when

the proportion of favourable habitats is small, the local populations in the majority of the environment are open to extinction due to the low quality of the habitats. The populations from the rare favourable habitats therefore act to rescue the population from extinction and to advance the population's range. However, such rescue is beneficial to the range expansion only when the dispersal probabilities from the favourable as well as unfavourable habitats are balanced, namely both moderate or both high. Indeed, when only small proportion of the habitat is favourable for the growth, low emigration from such patches may not suffice to rescue unfavourable patches from extinction and push the range expansion. High emigration from favourable patches alone on the other hand can lead to a decline in the local "rescuer" populations and yield a slower spread. As the proportion of favourable habitats becomes higher (Fig. 4.5 - right), higher dispersal probability from the favourable and unfavourable patches can push the population's front without depleting local populations. Therefore high dispersal probabilities act to accelerate the spread of the population when a large proportion of the habitat is favourable for the population's growth.

Location-dependent dispersal probabilities also influenced the rate of spread in the sinusoidally varying environments (Fig. 4.11c). First, the rate of spread increased with the mean dispersal probability. This behaviour is consistent with the results obtained when the dispersal probability does not depend on the location (Lutscher, 2008). Second, increasing the amplitude of the variability of the dispersal probability can accelerate or decelerate the spread of the population depending on the population's growth. When the dispersal probability oscillated in the same phase as the growth rate, our results suggest that the higher the amplitude of dispersal probability, the faster the spread of the population. In this case, increasing the amplitude of the growth rate and dispersal probability improves the spread at the maxima of the growth and dispersal probability in a manner outweighing the slow spread at the less favourable locations, hence imposing an acceleration of the spread. Decelerating effects on the other hand were observed when the dispersal probability and the growth rate oscillated in anti-phase because the slow spread around the minimal dispersal probability can act to limit the overall spread of the population.

Optimal proportion of favourable habitats

As we have seen previously, the proportion of favourable habitats also influences the rate of spread even when the growth and dispersal parameters are the same. The optimal proportion of favourable habitats was determined by the ratios $\frac{\sigma_2^2}{\sigma_1^2}$ and $\frac{d_2 R_2}{d_1 R_1}$. While the first ratio compares the dispersal distance ef-

fectuated by individuals from unfavourable and favourable habitats during one dispersal phase, the second one is concerned with the size of the populations dispersing from each type of patches.

In a broad view, the optimal proportion of favourable habitats decreased with the ratios (Fig. 4.6). Indeed, when the growth and dispersal probability parameters are fixed, increasing the dispersal distance ratio $\frac{\sigma_2^2}{\sigma_1^2}$ can indicate an increase in the dispersal distance effectuated by individuals from unfavourable patches, or a decrease in the dispersal distance of individuals from favourable habitats. In both cases, the presence of unfavourable patches becomes more beneficial for the spread of the population, thereby reducing the proportion of favourable habitats that is optimal for the spread. Similarly, increasing the ratio $\frac{d_2R_2}{d_1R_1}$ suggests that individuals from unfavourable patches become more active in the dispersal process and reduces the proportion of favourable habitats required for optimal spread.

It is worth to note that homogeneously favourable environments are optimal for the spread whenever the populations from such habitats are more motile ($d_2R_2 < d_1R_1$) and accompanied with faster local spread ($d_2R_2\sigma_2^2 < d_1R_1\sigma_1^2$) even when the individuals are less prone to disperse to farther distances (that is $\sigma_1^2 < \sigma_2^2$). The extreme opposite case consists of homogeneously unfavourable environments which maximize the rate of spread whenever $d_2R_2 > d_1R_1$ and $d_2R_2\sigma_2^2 > d_1R_1\sigma_1^2$. In the latter case however, it is required that the population can grow even in the "unfavourable" habitats ($R_1 > R_2 > 1$), otherwise the population will eventually become extinct. A good balance of favourable and unfavourable habitats is necessary in order to maximaze the rate of spread when the growth rate and local rate of spread are not correlated (Fig. 4.6). This can occur for instance when there is a trade-off between growth and dispersal.

Chapter 5

Spread of a predator-prey metapopulation with density-dependent behaviours [1]

5.1 Introduction

Predation is one of the most fundamental interspecific interactions in ecology. Early theories regarding the predator-prey systems often implicitly assume well-mixed homogeneous populations in space, namely the mean-field assumption (Rosenzweig and MacArthur, 1963; Beddington *et al.*, 1975; Berryman, 1992) and thus violate the reality that the spatial distribution of species is rarely homogeneous (Kokubun *et al.*, 2008) but spatially autocorrelated (Fortin and Dale, 2005; Hui *et al.*, 2010). Furthermore, the conventional non-spatial models do not allow the implementation of different survival strategies that can lead to the spatial heterogeneity of species distribution. As such, the spatial predation models have been developed to mainly examine the effect of spatially explicit processes on the dynamics and viability of populations, such as models using partial differential equations, coupled ordinary differential equations, integrodifference equations and lattice models (Neubert *et al.*, 1995; Murray, 2002; Petrovskii and Li, 2005).

One important process that can substantially affect the spatiotemporal dynamics is dispersal (as species'behaviour strategy; (Lonsdale, 1993)). Living organisms often display a variety of behaviour strategies in nature to enhance their survival (e.g. seeking refuge and forming swarms for anti-predation; (Siegfried and Underhill, 1975; Lindén, 2007; Weng *et al.*, 2007)), where different dis-

[1] The results from this chapter has appeared in the journal of Ecological Modelling 2011.

persal (or movement) behaviours are bound to arise from the optimization of species evolutionary fitness. Consequently, different ways of capturing prey have been observed in predators. While some predators sit and wait for their prey at hidden places (e.g crab spiders; Morse (2006)), others actively change their hunting ground according to prey density (e.g. python Madsen and Shine (1996)). In contrast, prey can also improve its survival rate by actively avoiding encountering potential predators (e.g. white sharks; Weng *et al.* (2007)). Beside affecting its own survival, dispersal behaviours can also potentially affect the invasiveness and spread of non-native species (Holway and Suarez, 1999; Rehage and Sih, 2004). However, it is still unclear how species dispersal behaviours affect the speed and spatial patterns of species range expansion, especially in a predator-prey system.

Depending on the causes and the modes dispersal, the spatial patterns exhibited can vary from spatial synchrony (i.e. the dynamics of populations at different localities coincide) to a spatial chaos (Li *et al.*, 2005). While the spatial heterogeneity of species distribution enhances the survival by providing refuge and thus promoting rescue effect (Allen *et al.*, 1993; Bommarco *et al.*, 2007), spatial synchrony tends to be detrimental to the persistence of metapopulation (Matter, 2001). Studies of this kind mainly focus on (i) the effect of predator's dispersal behaviour (that depends on prey density) on the dynamics of the system (Chakraborty *et al.*, 2007; El Abdllaoui *et al.*, 2007; Ainseba *et al.*, 2008; Tao, 2010) and (ii) the effects of prey refuge and density-dependent mortality on species persistence (Gonzalez-Olivares and Ramos-Jiliberto, 2003; Forrester and Steele, 2004). An emerging question from invasion biology is how such dispersal behaviours affect the rate of spread of non-native species in novel environments (Okubu, 1988; Shigesada and Kawasaki, 1997; Sutherland *et al.*, 2002). Closely relevant to the monitoring and control of invasive species, it is only recently that this question has started to receive attention (Tsyganov *et al.*, 2004).

We here explore the effects of two density-dependent dispersal behaviours, namely prey evasion (PE) and predator pursuit (PP), on the spatiotemporal dynamics of a predator-prey using a discrete metapopulation model. Prey evasion (PE) describes the behaviour of predator avoidance in prey - that is, animals often avoid encountering their predators by actively fleeing to places with lower predator density. Predator-pursuit (PP), on the other hand, portrays the tendency of predators to pursue prey by moving from their current location to high-prey density areas Tsyganov *et al.* (2004). The effects of PE and PP have been investigated in a semi-discrete framework (Li *et al.*, 2005), showing that these dispersal behaviours can alter the spatial synchrony in a predator-prey system and promote population persistence.

Our model is based on the model published by Beddington *et al.* (1975) and

adapted to incorporate PE and PP. A similar model was used by McCann *et al.* (2000) for building a three-patch model to investigate the outbreak of populations in a discrete system. Our metapopulation model consists of predator-prey systems in different habitat patches which are spatially linked by nonlinear density-dependent dispersals. We focus on the effects of PE and PP on the metapopulation persistence and the rate of spread when a species expand, both of which are of crucial importance for controlling the spread of invasive species and conserving endangered species.

5.2 Models

5.2.1 Dispersal-reproduction model

We assume a dispersal-growth model, that is , the model consists of two phases. During the dispersal phase, a fraction of prey and predators move from their location to more suitable surrounding patches according to density-dependent dispersals, namely dispersal due to random walk, PE and PP. During the growth phase, populations within a patch undergo growth and experience predation. In the following, we let $N_{i,t}$ and $P_{i,t}$ denote the density of the prey and predator populations in the patch i at time t respectively.

The dispersal phase includes three components: random-walk, PE and PP. Firstly, individuals undergo random-walk which leads to individuals diffusing from crowded patches to less-crowded adjacent patches. We assumed that the patches were homogeneous and that the prey and predators had the same sighting range so that individuals can compare equal amount of neighbouring patches. The net number of prey individuals $RW(N_{i,t})$ gained by patch i due to random walk between the patch and its neighbouring patches can be depicted as follows:

$$RW(N_{i,t}) = \frac{1}{\sharp\zeta_i}\sum_{j\in\zeta_i}\left(\frac{\max(0, N_{j,t}-N_{i,t})}{N_{i,t}+N_{j,t}}N_{j,t} - \frac{\max(0, N_{i,t}-N_{j,t})}{N_{i,t}+N_{j,t}}N_{i,t}\right) \tag{5.2.1}$$

where ζ_i designates the set of patches surrounding the patche i, and $\sharp\zeta_i$ is the number of patches surrounding the patch i. We used the Moore neighbourhood which consists of all patches sharing and edge or corners with the patch. The random walk of the predator species was defined analogously.

Secondly, the movement of individuals between cells (patches) can also be affected by the dispersal behaviours (i.e PE and PP). We modified the form of

PE and PP previously presented by McCann *et al.* (2000) and Li *et al.* (2005) to ensure the solutions are positive, and derived the following revised forms for the net number of prey gained in patch i (PE_i) due to the effect of PE (i.e the number of prey fled to patch i from its neighbouring patches):

$$PE_i = \frac{1}{\sharp\zeta_i}\sum_{j\in\zeta_i}\left(\frac{\max(0, P_{j,t} - P_{i,t})}{P_{j,t} + P_{i,t})}N_{j,t} - \frac{\max(0, P_{i,t} - P_{j,t})}{P_{j,t} + P_{i,t})}N_{i,t}\right) \tag{5.2.2}$$

Similarly, we can define the net number of predators gained in patch i due to the effect of PP (i.e. the number of predators following prey from neighbouring patch to patch i minus the number of predators following prey from patch i to its neighbouring patch):

$$PP_i = \frac{1}{\sharp\zeta_i}\sum_{j\in\zeta}\left(\frac{\max(0, N_{i,t} - N_{j,t})}{N_{i,t} + N_{j,t}}P_{j,t} - \frac{\max(0, N_{j,t} - N_{i,t})}{N_{i,t} + N_{j,t}}P_{i,t}\right). \tag{5.2.3}$$

Let ν and β denote the intensity of PE and PP respectively, μ and α the maximum dispersal rate of the prey and predators, and $\widetilde{N_{i,t}}$ and $\widetilde{P_{i,t}}$ the post-dispersal prey and predator population densities of patch i at time t. We thus have the population dynamics for the dispersal phase:

$$\begin{aligned}\widetilde{N_{i,t}} &= N_{i,t} + \frac{\mu}{1+\nu}(RW(N_{i,t}) + \nu PE_i)\\ \widetilde{P_{i,t}} &= P_{i,t} + \frac{\alpha}{1+\beta}(RW(P_{i,t}) + \beta PP_i)\end{aligned} \tag{5.2.4}$$

The coefficients of the dispersal behaviours of the prey were chosen such that (i) when the PE intensity ν is negligible, in the absence of predators for instance, the dispersal of prey is driven completely by random walk with a dispersal rate μ, (ii) where ν is large, the dispersal of prey is dominated by PE with the same dispersal rate μ. The coefficients of the dispersal of predators were defined analogously.

The reproduction phase includes population growth and predation (Beddington *et al.*, 1975), adjusted to incorporate the above dispersal phase:

$$\begin{aligned}N_{i,t+1} &= \widetilde{N_{i,t}}e^{b\left(1-\frac{\widetilde{N_{i,t}}}{K}\right)-a\widetilde{P_{i,t}}}\\ P_{i,t+1} &= c\widetilde{P_{i,t}}(1 - e^{-a\widetilde{P_{i,t}}})\end{aligned} \tag{5.2.5}$$

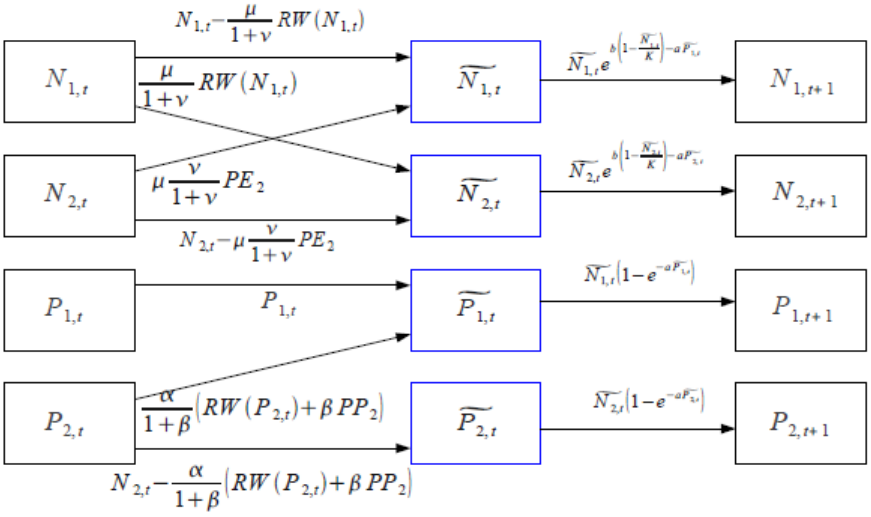

Figure 5.1: A step of the two-patch model. Fluxes are shown for $N_{1,t} > N_{2,t}$ and $P_{1,t} < P_{2,t}$ in the illustration.

with positive initial distribution $N_{i,0} \geq 0, P_{i,0} \geq 0, i = 0, 1, \ldots n$, where b is the intrinsic growth rate of prey, K is the carrying capacity of prey per patch, a is the predator's attach rate and c is the efficiency of conversion of prey into predators. The population flow is show in Fig. 5.1 when $N_{1,t} > N_{2,t}$ and $P_{1,t} < P_{2,t}$. In the figure, PE and PP occur from the first patch to the second one. A summary of the parameters and variables used in this model is given in Table 5.1. It is worth to noting that with positive initial population density, the solution to the above model remains positive and is bounded for all time t.

5.2.2 Numerical simulations

In most cases in the simulation, we used the same set of parameters ($b = 0.5, c = 1, a = 0.5, K = 15, \mu = 0.75$ and $\alpha = 0.75$) and only changed the intensity of PE and PP (i.e. ν and β). to investigate their effects on the spatiotemporal dynamics of the predator-prey system. Both the prey and the predators were initially located in the centre of the lattice, leaving other patches empty. Reflective boundaries were used (i.e. individuals which move out of the lattice will be located back to their pre-dispersal locations). We studied the effects of different levels of PE and PP on the metapopulation persistence, the spatiotemporal dynamics of the predator-prey metapopulation, specifically spatial synchrony and the rate of spread.

Variable / Parameter	Description
$N_{i,t}$	Prey population size before migration in patch i at time t
$\widetilde{N_{i,t}}$	Prey population size after migration in patch i at time t
$P_{i,t}$	Predator population size before migration in patch i at time t
$\widetilde{P_{i,t}}$	Predator population size after migration in patch i at time t
PE_i	Prey evasion between a patch i and its neighbours
ν	Intensity of PE
PP_i	Predator pursuit between a patch i and its neighbours
β	Intensity of PP
μ	Maximum migration rate of preys
α	Maximum migration rate of predators
a	Predators attack rate
c	Conversion efficiency of preys into predators
K	Prey's carrying capacity per patch
b	Prey's intrinsic growth rate
ζ_i	Set of neighbours of a patch i
$\sharp\zeta_i$	Number of neighbours of a patch i

Table 5.1: Description of parameters and variables for the spread of a predator-prey metapopulation.

To investigate the effects of PE and PP on the persistence of the metapopulation, we started by exploring the effects of PE and PP on the stability of a two-patch model. We then undertook extensive numerical simulations to investigate the effects of PE and PP on the persistence of the metapopulation on a large lattice. The persistence of the metapopulation was measured by the mean population density over the occupied patches. Non-symmetric steady states which may arise in large lattices were not captured in the study.

Spatial synchrony depicts the coincidence in the temporal fluctuations in local population size and can be measured using the method *based on change* described by Buonaccorsi *et al.* (2001). For two patches i and j, the level of synchrony is given by

$$s_{ij} = 2\frac{A_{ij}}{t-1} - 1 \tag{5.2.6}$$

where A_{ij} is the number of times that the population size in the patches i and j fluctuate in the same direction. The level of synchrony for the lattice was

then defined as the mean synchrony of all pairs of patches in the lattice.

To calculate the rate of spread, we adopted the method used by Kawasaki and Shigesada (2007) for a discrete-time one-dimensional model to the two-dimensional lattice. The rate of spread is given by

$$r(t) = \frac{1}{t}\sum_{\tau=1}^{t}(R(\tau) - R(\tau-1)) = \frac{R(t) - R(0)}{t},\ t > 0 \tag{5.2.7}$$

where $R(t)$ is the approximate radius occupied by the species at time t. Here, *occupied patch* refers to a patch with a population size higher than a threshold of detection σ. If we denote the area occupied by the species, that is also the number of occupied patches, by $S(t)$, the the approximate radius is given by

$$R(t) = \frac{S(t)}{\pi}.$$

5.3 Results

5.3.1 Asymptotic behaviour

The two-patch model has three steady states, including a trivial steady state $(N_1 = 0, N_2 = 0, P_1 = 0, P_2 = 0)$, a semi-trivial steady state $(K, K, 0, 0)$ and a non-trivial steady state (N^*, N^*, P^*, P^*) where N^* is a solution of

$$\frac{b(1 - N^*/K)}{aN^*} = 1 - e^{-b(1-N^*/K)}$$

with $0 < N^* < K$ and P^* is given by

$$P^* = \frac{b}{a}\left(1 - \frac{N^*}{K}\right).$$

The trivial steady state is stable regardless of the parameter values. The stability region of the non-trivial steady state became largest in the parameter plane when there was no PE and PP in the system (See Fig. 5.2). the population started to oscillate for high prey carrying capacity (K), and the predators became instinct for low prey carrying capacity and prey intrinsic growth rate (b). The stability region of the non-trivial steady state shrank for high prey intrinsic growth rate, driving the system to oscillate. The asymptotic mean

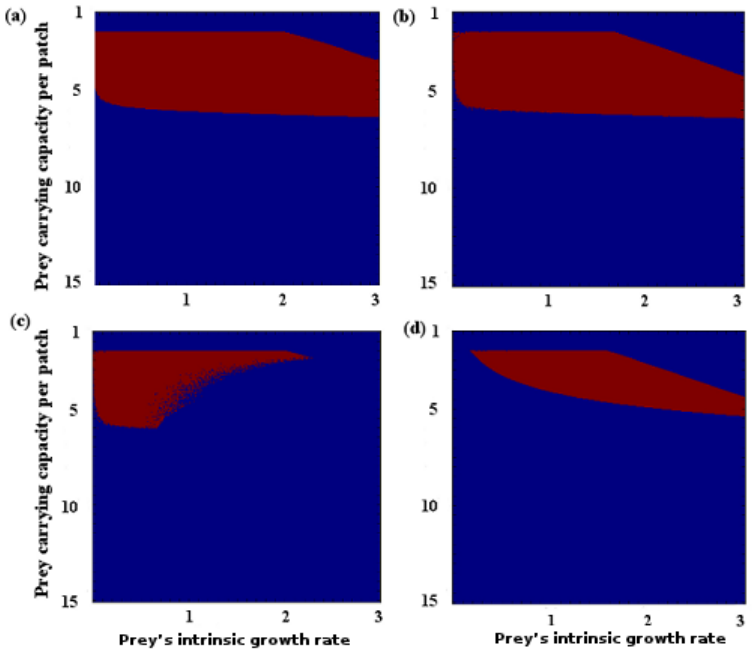

Figure 5.2: Stability switch of the two patch-model. The non-trivial steady state is stable in the region in red and unstable otherwise. (a) When there is no prey evasion (PE) or predator pursuit (PP). (b) Strong PE ($\nu = 30$) but no PP. (c) Strong PP ($\beta = 30$) but no PE. (d) Strong PE and PP with $\nu = \beta = 30$.

population size of the prey is shown in Fig. 5.3 for $K = 4$ and $b = 0.5$, representing a stable non-trivial steady-state (Fig. 5.2). The mean population size is low when PE and PP are small, and strong PE and PP lead to high population size. However, the effect of PP on the mean population size is much less than the effect of PE.

5.3.2 Spatial distribution and rate of spread

Spatial distributions of the prey after 120 time steps are presented in Fig. 5.4 under different intensities of PE and PP. When PE and PP were weak, the prey population expanded in circular waves and distributed evenly over the occupied patches. This uniform distribution of the population was gradually deteriorated as we increased the intensities of PE and PP either independently or simultaneously. When the intensity of PE was disproportionately higher than the intensity of PP, the prey population propagated in circular waves and accumulated in a circular ring front. When PP was stronger than PE, directional (anisotropic) expansions of the prey appeared and gave rise to a heterogeneous but symmetric distribution of the population. When both

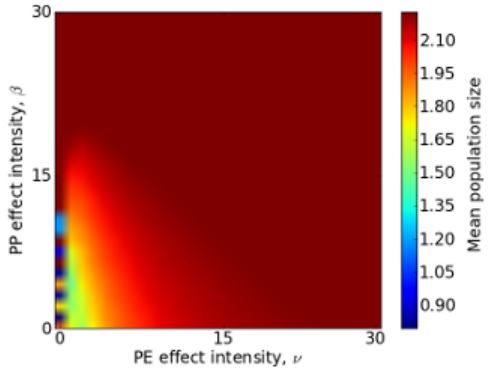

Figure 5.3: A parameter plane showing the mean prey population size as a function of density-dependent prey evasion (PE) and predator pursuit (PP). Parameter values are set as $K = 4, b = 0.5, a = 0.5, \mu = 0.75, \alpha = 0.75$. PE and PP are increased in steps of 1 from 0 to 30.

PE and PP were strong, the circular ring front associated with a strong PE became thinner and the directional expansion associated with a strong PP became more isotropic.

The spatial synchrony of the prey is presented as a function of the intensities of PE and PP in Fig. 5.5, showing an asynchronous behaviour of the populations in the lattice. Highly synchronised dynamics was observed for weak PE and PP. Both PE and PP had a desynchronizing effect on the spatial dynamics. Furthermore, the level of synchrony was more sensitive to PE than PP. The spatial synchrony remained with the increase of PP intensity (β) only, whereas the synchrony declined with the increase of PE intensity (ν). The least synchrony was reached for strong PE and PP simultaneously.

The rate of spread of the prey and predators were calculated according to the radius at the 120 time step with a threshold of detection of 0.01 (Fig. 5.6). The rate of spread for prey was correlated with the rate of spread of predators. The range expansion became faster with the increase of PE intensity but only when the PE intensity was below a certain threshold ($\nu^*(\beta)$), beyond which the rate of spread started to decline with the PE intensity ν. Similarly, the rate of spread was an increasing function of the PP intensity when $\beta < \beta^*(\nu)$, beyond which the rate of spread became a decreasing function of the PP intensity.

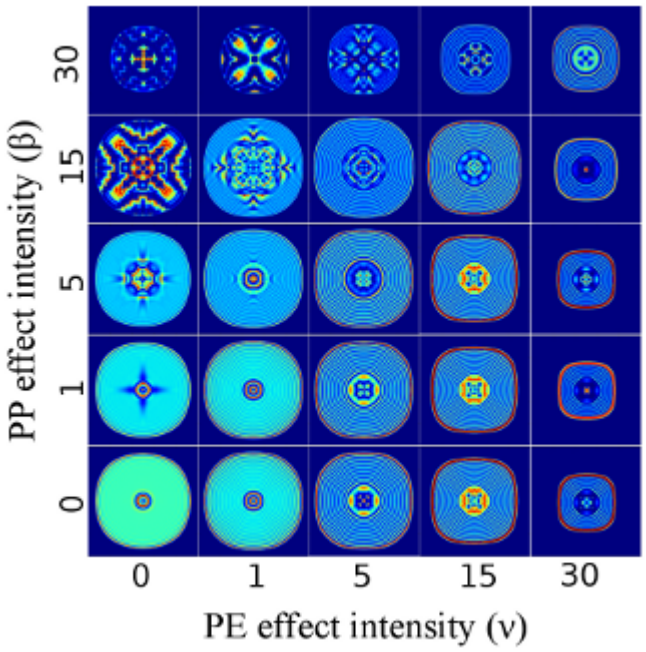

Figure 5.4: Spatial distribution of the prey population after 120 generations on a 250×250 lattice. Parameter values are set as $b = 0.5, c = 1, a = 0.5, K = 15, \mu = 0.75, \alpha = 0.75$. In the patterns, red refers to high population size and dark blue reflects low population size.

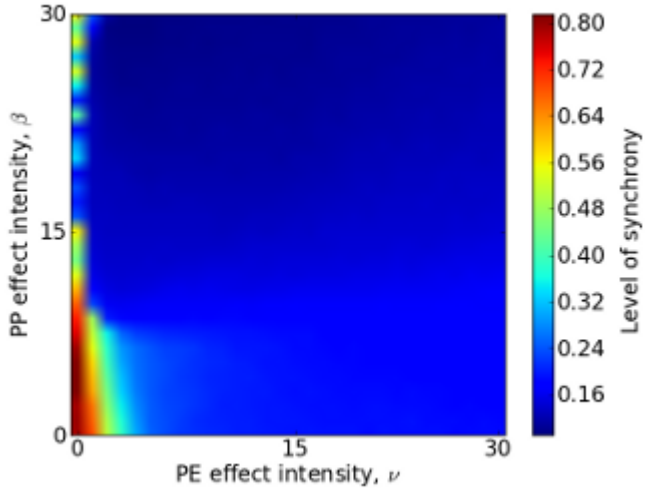

Figure 5.5: A parameter plan showing the level of spatial synchrony of the prey population as a function of prey evasion and predator pursuit, calculated on a 20×20 lattice. Parameter values are set $K = 4, b = 0.5, a = 0.5, \mu = 0.75, \alpha = 0.75$. PE and PP are increased from 0 to 30 in steps of 1.

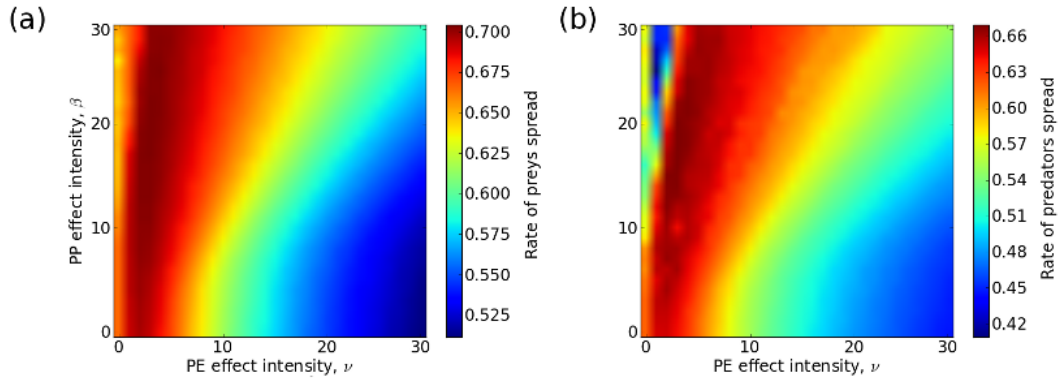

Figure 5.6: A parameter plan showing the rate of species spread as a function of prey evasion and predator pursuit, calculated on a 250×250 lattice. Parameter values are set as $K = 15, b = 0.5, a = 0.5, \mu = 0.75, \alpha = 0.75$. PE and PP are increased from 0 to 30 in steps of 1. (a) Rate of prey spread. (b) Rate of predator spread.

5.4 Discussion

5.4.1 Dispersal behaviour and spatial distribution

Spatial synchrony in population dynamics is mainly caused by three factors - (i) spatial autocorrelation inherent in the environment (Moran, 1953; Gao *et al.*, 2007), (ii) interspecific density regulation through predation and parasitism (Ims and Andreassen, 2000; Gonzalez-Olivares and Ramos-Jiliberto, 2003) and (iii) density-dependent dispersal (Jansen, 2001). For a predator-prey system in particular, even a small dispersal rate can lead to synchrony if the environment is homogeneous (Jansen, 2001). In contrast, we studied the effect of two density-dependent dispersals (PE and PP) on the spatial synchrony of the predator-prey systems. The spatial synchrony reached peaks when the dispersals were only motivated by random walk and reduced whenever PE and PP were present. This is consistent with the results from a two-patch semi-discrete model (Li *et al.*, 2005). Moreover, PP alone has a less desynchronizing effect than PE. When PE is strong, however, prey can move to 'refuge' patches with low predator densities and thus grow in abundance before being detected by predators. This allows the growth of prey in 'refuge' patches while the remaining prey in the original patch is being depleted by predators, inducing a spatial asynchrony between refuge and original patches. Moreover, the decline of synchrony caused by the density-dependent dispersal was more severe in predator-prey systems than in single-species systems (Münkemüller and Johst, 2008).

Numerical simulation on the 250×250 lattices further confirmed that density-dependent dispersal is a force of asynchrony: an even spatial distribution of the prey population was observed when the patches are connected only via density-dependent random walk (Fig. 5.4), consistent with Nguyen-Huu *et al.* (2006) results. The prey with strong PE is mainly driven by fear of predators and thus takes minimal-effort evasion strategy (Oshanin *et al.*, 2009). This potentially explains the high concentration of prey in the range front for prey when there is high PE intensity (the red ring front in Fig. 5.4). In contrast, predators with a strong PP ability can quickly move into patches with a high prey density and deplete the local prey while the prey population in other patches expands, giving rise to the anisotropic expansion (Fig. 5.4). When PE and PP are both strong, the minimal-effort evasion of prey is interfered with by the anisotropic expansion, leading to strong asynchrony and spatial chaos (Li *et al.*, 2005).

5.4.2 Dispersal behaviour and the rate of spread

Elucidating the effect of biotic interactions on the spread of invasive species is important for mitigating the detrimental impact of biological invasions on the recipient ecosystem (Petit *et al.*, 2008). The rate of spread has been shown to be more sensitive to long distance dispersal (Lewis, 1997; Shigesada and Kawasaki, 1997). Predation, on the other hand, has been speculated to be able to slow down the expansion of a prey species (Owen and Lewis, 2001). Our results suggest (i) that the velocity of range expansion for predators is closely tied with the velocity of prey range expansion (Fig. 5.6) and (ii) the rate of spread of both species is an increasing function of weak PE and PP but a decreasing function of strong PE and PP. The results are consistent with the results from Tsyganov *et al.* (2004) for a continuous one-dimensional model with weak PE and PP. When PE becomes more dominant (compared to PP and random walk), however, the prey avoid mainly predator-crowded areas. This implies a lack of prey for the predators and slows down the range expansion of the species. This further reduces the movement of the prey once the prey passed the area occupied by the predators, and slows down the range expansion (Fig. 5.6). On the other hand, when the PP is strong, pursuiting success of predators is improved, which increases the chance of encountering prey. This will promote predation success and suppress the prey population from rapid range expansion. Therefore, density-dependent dispersal behaviour is indeed a factor that can change the speed of range expansion (Owen and Lewis, 2001; Petrovskii and Li, 2005).

5.4.3 Dispersal behaviour and metapopulation persistence

The idea that dispersal between different patches may favour the persistence of metapopulations has its origin in the 1990s. Predator-prey systems, where in particular non-spatial models tend to be unstable or lead to population extinction (Taylor, 1990) have been shown to be able to persist spatially even if local populations in different patches fluctuate (Wilson *et al.*, 1993). In our case, the coexistence of the prey and predators was strongly mediated by the density-dependent dispersal behaviours of PE and PP. The stability diagram in Fig. 5.2 shows that, for the two patch model, the prey and predators can stably coexist when the carrying capacity of the prey is low and when the PE and PP are weak. This stable coexistence was disturbed by the introduction of density-dependent dispersal behaviours (PE and PP). For instance, an increase in the PE intensity could lead to the extinction of predators when the prey carrying capacity is low. This is because PE can affect the prey population by providing local refuges and thus induces lack of prey for the predators.

Beside their effects on the asymptotic behaviour of the population dynamics, PE and PP can also influence the population size. Low population size can be expected when the patches are connected only by random-walk. Although prey does not go extinct in the system, small prey population was indeed observed when only PP was present in the model. This is expected since the pursuit of predators can bring the system to a spatially evenly distribution in the absence of PE and PP. However, the mean population increased whenever PE was present in the model. The evasiveness of the prey does not only save local prey populations from predation, but also promotes rescue effect between prey populations. Furthermore, an increase in the population size is also associated with a decrease in the level of spatial synchrony (Figs. 5.3 and 5.5)., consistent with the idea that spatial synchrony reduces the persistence of the population (Lloyd and May, 1999; Matter, 2001).

Overall, our findings suggest that the two density-dependent dispersal behaviours, PE and PP, can provoke asynchronous dynamics even in the absence of environmental heterogeneity, and thus both can improve the metapopulation persistence. Specifically, PE has a stronger desynchronizing effect on the dynamics than PP. Furthermore, weak density-dependent dispersal behaviours promote the spread of the prey and predator. However, when one of the two density-dependent dispersal PE and PP is strong, the range expansion will slow down. The results provide theoretical clues for reducing the rate of spread of problematic invasive species by choosing appropriate biological agents that can provoke strong density-dependent dispersal of either the agent or targeted species.

Chapter 6

Conclusion

After the establishment of a viable population of an exotic species, the next stage of the invasion process is the spread across the available environment (Blackburn *et al.*, 2009). Forecasting regions that are susceptible to the invasion as well as predicting the rate of spread therefore become crucial as any delay in response to the spread of an invasive species may render its control or eradication less successful if not impossible.

Theoretical investigations of the range expansion and rate of spread of an invasive species have made great progresses since the works of Fisher (1937) and Skellam (1951). While some works focus on providing estimates of the rate of spread, others made previous results more clear for applied and theoretical purposes (Mollison, 1991; Kot *et al.*, 1996; Weinberger *et al.*, 2002; Hui *et al.*, 2011). Several investigations, both empirical and theoretical, have pointed out a positive correlation between the rate of spread on the one hand, and the population's growth and dispersal on the other hand.

The focus of Chapter 3 is on the role of propagule pressure on the spread of an invasive species. Propagule pressure, also known as introduction effort, describes the number of individuals released at the introduction (propagule size) and the number of releases (propagule number) (Lockwood *et al.*, 2005). Different observations have reported that the propagule pressure can promote not only the establishment of an invasive species in a novel area, but also the rate of the subsequent range expansion or rate of spread (Lockwood *et al.*, 2005; Colautti *et al.*, 2006; Wilson *et al.*, 2007; Simberloff, 2009). Indeed, a large propagule is less vulnerable to demographic stochasticity and is more likely to establish in the novel area (Lande, 1993; Allen, 2003). Furthermore, more individuals in the initial propagule can improve the chance of having individuals with higher reproductive rate or stronger dispersal ability. Ignoring the number as well as the properties of individuals in the initial propagule can

lead to an underestimation of the population's rate of spread. The importance of the propagule pressure however has not been theoretically investigated.

This issue was approached in this chapter by considering a different measure of the propagule pressure. We considered not only the propagule size, but also a propagule composition which consists of individuals with different dispersal abilities in the initial propagules. For a given propagule size, three cases of propagule composition can occur. First, the individuals in the initial propagule have the same dispersal ability. In the second case, the initial propagules consist of most individuals sharing common dispersal ability, and the rest of individuals being significantly better dispersers. In the third case, many dispersal abilities are present in the initial population. The first case is the focus of most models for studying the spread of a single species and has been investigated in continuous - and discrete - time using PDE and IDE respectively (Fisher, 1937; Skellam, 1951; Kot *et al.*, 1996). The second and third cases were investigated in this chapter using a system of IDE in which each equation depicts the spread of individuals with a given dispersal ability (Eq. 3.2.4).

Overall, each case of propagule composition leads to a different pattern of range expansion. As previously shown by different models (Skellam, 1951; Kot *et al.*, 1996), the first case of propagule composition yields a linear range expansion, that is the type 1 pattern according to the classification by Shigesada *et al.* (1995). From the second and third cases of propagule composition, we obtained the type 2 and type 3 range expansion patterns respectively, that is a biphasic and a continuously accelerating range expansion.

The increase in the rate of spread was observed from our model until a maximal rate, which corresponds to the maximal dispersal ability in the initial population, was reached. Once the maximal rate of spread was reached, the range expansion became linear with a constant asymptotic rate of spread. In the case of log-normally distributed initial population, we derived an expression of the asymptotic rate of spread (Eq. 3.3.18) and found that it increases with the propagule size as well as the propagule diversity (Fig. 3.6). Although log-normal distributions were used to model the distribution of dispersal abilities in the initial propagule, the rate of spread associated to other distributions can be obtained simply by using the corresponding cumulative probability function in Eq. 3.3.16. It is worth noting however that the use of log-normal distributions in this work to model the initial propagule was founded on the growing evidence that species-abundance relationships follow the same distribution (Limpert *et al.*, 2001; May and McLean, 2007).

Indeed, when there is no trade-off between reproduction and dispersal ability, individuals with weaker dispersal abilities are bound to occupy the core of the invaded range, leaving individuals with stronger dispersal abilities to occupy the front of the invasion and lead the range expansion (Fig. 3.3c). Such spa-

tial sorting of dispersal abilities, which has been observed in different taxa (Simmons and Thomas, 2004; Phillips *et al.*, 2007; Berthouly-Salazar *et al.*, 2012), is associated with a dynamic dispersal kernel (Fig. 3.4) and yields an accelerating range expansion in a mixed population, as speculated by (Phillips *et al.*, 2008). From our model however, the rate of spread does not increase indefinitely as the dispersal abilities are bounded from the initial propagule.

The spatial sorting of dispersal abilities and accelerating range expansions may also be linked to the evolution of dispersal related traits which occur at much faster paces than usual (Hughes *et al.*, 2007; Shine *et al.*, 2011). Our models do not take into account possible mutations of dispersal abilities. However, we suspect that incorporating evolutionary processes in the model will amplify the acceleration of the population's spread, and transform the asymptotic linear range expansion obtained from the current model into an accelerating invasion (Bouin *et al.*, 2012) specially in the absence of demographic responses such as Allee effect which can reduce the rate of spread despite the strong dispersal abilities of the frontal population (Lewis and Kareiva, 1993). Evolutionary trade-offs between reproduction and dispersal also need to be considered in this case as potential advantages resulting from increased dispersal abilities may be balanced if not outweighed by reduced reproductive processes (Hughes *et al.*, 2003; Shine *et al.*, 2011).

In addition to the initial population, spatial variations of the environment can also influence the spread of an invasive species (With, 2002). Such influences are the focus Chapter 4. The impacts of spatial heterogeneity is unavoidable because the quality of local habitats affect both demographic processes and individual movements (With and King, 2001; With, 2002). The invasion of heterogeneous environments by continuously moving and reproducing species have been investigated by Shigesada *et al.* (1986) and Kinezaki *et al.* (2006) using PDEs. In this case the rate of spread was determined by the spatial averages of the growth and dispersal rates. In this chapter, we studied the spread of a population modelled by IDEs. IDEs are commonly used to model the spatiotemporal dynamics of populations with non-overlapping generations. They are also usually preferred to PDEs due to their flexibility to incorporate different dispersal kernels (Kot *et al.*, 1996). In addition to spatially varying growth rate, we considered the spatial-dependence of two aspects of the dispersal process. The first consists of the dispersal kernel which models the probability distribution of the dispersal distance effectuated by individuals during the dispersal stage. The dispersal kernel is influenced by the local habitat for example when individuals from low quality habitats disperse farther in a quest of more favourable habitats. Spatially varying dispersal kernels have been investigated for particular environment structure by Kawasaki and Shigesada (2007) and Dewhirst and Lutscher (2009). The second aspect of the dispersal process is the dispersal probability. Dispersal probability can depend on the local habitat

for example when individuals prefer staying in favourable habitats Hui *et al.* (2012).

In homogeneous environments, population growth, dispersal distance (dispersal kernel) and the dispersal probability all influence the spread of a population in a positive manner (Skellam, 1951; Kot *et al.*, 1996; Lutscher, 2008). Previous studies have shown that population growth and dispersal distance also improve the spread of invasive species in heterogeneous environments (Kawasaki and Shigesada, 2007; Dewhirst and Lutscher, 2009). This work highlights the impacts of spatially varying dispersal probability. Overall, our results suggest that spatially varying dispersal probability can yield faster or slower spread depending on the availability of favourable habitat (Fig. 4.5). When only a small proportion of the environment is favourable for the growth of the population, lower dispersal from the favourable habitats lead to faster overall spread of the species. Indeed, in metapopulation dynamics, dispersal can reduce the probability of local extinctions (Gotelli, 1991). High dispersal probability from favourable habitats however could depress the overall population as the dispersing individuals are likely to land in unfavourable habitats. Lower dispersal probability on the other hand can lead to faster spread as the sedentary population acts as reservoir and allow the populations in favourable patches to grow and rescue unfavourable patches from extinction. As the amount of favourable habitats increases however, the spread of the population benefits from dispersal as the dispersing individuals push the front of the invasion without leading the population to extinction. In a sinusoidally varying environment, increasing variability in the dispersal probability was found to benefit the spread when the dispersal probability oscillate in phase with the population growth. In a sinusoidally varying environment, increasing variability in the dispersal probability was found to benefit the spread when the dispersal probability oscillate in phase with the population growth.

The impacts of the dispersal probability is linked with the availability of favourable habitats. For fragmented environment, the asymptotic rate of spread depends on the availability, or proportion, of favourable habitats in the landscape rather than the actual sizes of the patches (Eq. 4.3.12). This dependence on the proportion of favourable habitats was observed in periodically as well as in randomly generated landscape (Fig. 4.8b). We investigated the relation between the rate of spread and the favourable habitats and found that the optimal proportion of favourable habitats decreases with the ratio of the growth of population emigrating from favourable and unfavourable patches as well as the ratio of their dispersal distance (namely the variances of the dispersal kernels) (Fig. 4.6). Homogeneous environments are optimal for the spread when the population growth and local spread are correlated. Otherwise, a good balance of favourable and unfavourable habitats is necessary (Fig. 4.6).

In this work, we assumed that the distribution of the dispersal distance (dispersal kernel) is only affected by the origin of the dispersal event. However, the dispersal distance may also be affected by the environmental heterogeneity. Indeed migrating individuals may explore and settle in favourable habitats that are on their dispersal path (Schliehe-Diecks *et al.*, 2012), or may adopt directed dispersal when the quality of potential dispersal target sites are known (Bossenbroek *et al.*, 2001). Such behaviour may influence the distribution of dispersal distance.

In its current form, the model incorporates two type of habitats, namely favourable and unfavourable habitats. Populations in favourable habitats are accompanied with fast growth rate when the population size is small. Unfavourable habitats on other hands resemble to sink patches where the population size always declines. A variant of the spatially varying growth can allow for an Allee effect in the entire region, or in unfavourable habitats only. Dewhirst and Lutscher (2009) have provided some insights on the role of Allee effects when the dispersal probability is not spatially varying. The combined effects of an Allee effect and dispersal probability, which can also model residence time favourable and unfavourable habitats, is still unknown.

Chapter 5 investigates the spread of a predator-prey system with density-dependent dispersal behaviour. The spatiotemporal dynamics of predator-prey systems have been investigated in different framework (Dunbar, 1983, 1984; Owen and Lewis, 2001). It has been suggested that while the rate of spread of a predator species increases with the availability of a prey population, predation can slow down the expansion of its prey. It is worth to note that these speculations were based on density-independent behaviours. Living organisms however often display density-dependent strategies in order to improve their survival. In particular, different ways of capturing prey or avoiding predators have been observed in different predators and prey respectively (Madsen and Shine, 1996; Morse, 2006; Weng *et al.*, 2007). The influence of such behaviours were investigated in this thesis. Namely, we used a metapopulation model to explore the effects of prey evasion and predator pursuit. Prey evasion (PE) describes the predator-avoiding dispersal of prey - that is, prey often avoid encountering their predators by fleeing to places with lower predator density. Predator-pursuit (PP), on the other hand, portrays the tendency of predators to pursue prey by moving from their current location to high-prey density areas (Tsyganov *et al.*, 2004; Li *et al.*, 2005). The local populations were described by the predation model introduced by Beddington *et al.* (1975) (Eq. 5.2.5). The different patches on the other hand were linked by PE, PP in addition to random walk (Eq. 5.2.4, Fig. 5.1). The density-dependent behaviours affected different aspects of the spatiotemporal dynamics of both species.

First, The density-dependent dispersal affected the persistence of the popula-

tions. In other words, the dispersal behaviours influenced the success of the invasion. Dispersal has been known to favour the persistence of a metapopulation even when local populations fluctuate and may appear to be extinct at some generations (Taylor, 1990; Wilson *et al.*, 1993). In this study however, the coexistence of the prey and predators was only promoted by the density-dependent dispersal behaviours when PE and PP are weak. The persistence of the mepatopulation was deteriorated by density-dependent dispersal for example when PE was intensified.

Second, when the population persists, the spatial distributions of both species, in particular the front of the invasion, were strongly influenced by PE and PP (Fig. 5.4). The populations were evenly distributed in space when the patches are connected only by density-dependent random walk. Such distribution have been predicted also previously (Nguyen-Huu *et al.* (2006)). When PE is intensified, the front of the invasion was circular. However the population was oddly distributed with a high population density at the edge of the invasion. On the other hand, anisotropic expansion were observed when PP was strong compared to PE. Indeed, in this case the predators can quickly move into patches with a high prey density and deplete the local prey while the prey population in other patches expands. Cancelling effects were observed when PE and PP where equally strong.

Finally, PE and PP also affected the rate of spread of the prey and predators species. The rate at which the prey and predator spread were found to be closely tied (Fig. 5.6). Indeed in this model, as the prey tries to evade the predators, the latter engages in a pursuit of the prey which yields the correlations between the rate of spread of the species. Both density-dependent behaviours were found to accelerate the spread of both species when they occur both at low intensity. A decrease in the rate of spread however were observed when PE and PP were both strong. This effect has also been speculated by Tsyganov *et al.* (2004) for a continuous one-dimensional model with weak PE and PP. When PE becomes significantly dominant (compared to PP and random walk), however, the dispersal of the prey are mainly due to avoid predator-crowded areas. This slows the spread of the predators due to a lack of prey. The spread of the prey is also slowed down once the prey passed the area occupied by the predators. In other words, significantly stronger PE can act to decelerate the spread of the predator as well as the prey even though predation did not necessarily take place due to the highly evasive prey strategy. On the other hand, when the PP is strong, pursuiting success of predators is improved, which increases the chance of encountering prey. This will promote spread of the predators while limiting the expansion of the prey population. This result is consistent with the speculation from density-independent dispersal that predation can slow down the spread of a prey population.

Overall, this thesis provides a possible explanation to the patterns of range expansion reported by Shigesada *et al.* (1995) (Chapter 3). The importance of varying dispersal probability is also highlighted whether it is due to environmental heterogeneity (Chapter 4) or density-dependent dispersal strategies (Chapter 5). In particular, the current work points out that while the spread of an invasive species is positively correlated with the dispersal distance, the influence of dispersal probability in heterogeneous environment depends on the availability of favourable habitats. Finally, this study also advises the importance of census locations when collecting data to estimate dispersal parameters. The rate of spread of the population was determined by the frontal population and can be underestimated by the population at the core of the invasion. Possible extensions and challenges from the current works are discussed, including, the role of evolutionary changes in range expansion patterns, as well as the interference between Allee effect and dispersal probability in heterogeneous environments.

List of References

Ainseba, B., Bendahmane, M. and Noussair, A. (2008). A reaction-diffusion system modeling predator-prey with prey-taxis. *Nonlinear Analysis: Real World Applications*, vol. 9, pp. 2086–2105.

Allee, W.C. (1931). *Animal aggregations*. The University of Chicago Press.

Allee, W.C. and Bowen, E.C. (1932). Studies in animal aggregations: Mass protection against colloidal silver among goldfishes. *Journal of Experimental Zoology*, vol. 61, pp. 185–207.

Allen, E.J., Allen, L. and Gilliam, X. (1996). Dispersal and competition models for plants. *Journal of Mathematical Biology*, vol. 34, pp. 455–481.

Allen, J.C., Schaffer, W.M. and Rosko, D. (1993). Chaos reduces species extinction by amplifying local population noise. *Nature*, vol. 364, pp. 229–232.

Allen, L.J. (2003). Risk of population extinction due to demographic stochasticity in population models. *Comments on Theoretical Biology*, vol. 8, pp. 433–454.

Andow, D.A., Kareiva, P.M., Levin, S.A. and Okubo, A. (1990). Spread of invading organisms. *Landscape Ecology*, vol. 4, pp. 177–188.

Andow, D.A., Kareiva, P.M., Levin, S.A. and Okubo, A. (1993). *Evolution of insect pests: The pattern of variations*, chap. Spread of invading organisms: Patterns of spread, pp. 219–242. Wiley, New York.

Béchinou, O., Calvez, V., Meunier, N. and Voituriez, R. (2012). Front acceleration by dynamic selection in fisher population waves. *Physical Review E*, vol. 86, pp. 041908 1–5.

Beddington, J.R., Free, C.A. and Lawton, J.H. (1975). Dynamic complexity in predator-prey models framed in difference equations. *Nature*, vol. 255, pp. 58–60.

Bell, G. (2000). The distribution of abundance in neutral communities. *The American Naturalist*, vol. 155, pp. 606–617.

Bengtsson, G., Hedlund, K. and Rundgren, S. (1994). Food- and density-dependent dispersal: Evidence from a soil collembolan. *Journal of animal ecology*, vol. 63, pp. 513 –520.

Bengtsson, J. (1989). Interspecific competition increases local extinction rate in a metapopulation system. *Nature*, vol. 340, pp. 713–715.

Berec, L. (2002). Techniques of spatially explicit individual-based models: construction, simulation, and mean-field analysis. *Ecological Modelling*, vol. 150, pp. 55–81.

Berestycki, H., Hamel, F. and Roques, L. (2005). Analysis of the periodically fragmented environment model. *Journal de Mathematiques Pures et Appliquees*, vol. 84, pp. 1101–1146.

Berryman, A.A. (1992). The orgins and evolution of predator-prey theory. *Ecology*, vol. 73, pp. 1530–1535.

Berthouly-Salazar, C., van Rensburg, B.J., Le Roux, J.J., van Vuuren, B.J. and Hui, C. (2012). Spatial sorting drives morphological variation in the invasive bird, acridotheris tristis. *PLos ONE*, vol. 7, p. e38145.

Beverton, R.J.H. and Holt, S.J. (1957). *On the Dynamics of Exploited Fish Populations*. Fishery Investigations Series II Volume XIX.

Birch, C.P.D., Oom, S.P. and Beecham, J.A. (2007). Rectangular and hexagonal grids used for observation, experiment and simulation in ecology. *Ecological Modelling*, vol. 206, pp. 347–359.

Blackburn, T.M., Lockwood, J.L. and Cassey, P. (2009). *Avian Invasions: The Ecology and Evolution of Exotic Birds*. Oxford Avian Biology Series.

Bommarco, R., Firle, S.O. and Ekbom, B. (2007). Outbreak suppression by predatorsdepends on spatialdistribution of prey. *Ecological Modelling*, vol. 201, pp. 163–170.

Bossenbroek, J.M., Kraft, C.E. and Nekola, J.C. (2001). Predition of long-distance dispersal using gravity models: Zebra mussel invasion of inland lakes. *Ecologal Applications*, vol. 11, pp. 1778–1788.

Bouin, E., Calvez, V., Meunier, N., Mirrahimi, S., Perthame, B., Raoul, G. and Voituriez, R. (2012). Invasion fronts with variable motility: Phenotype selection, spatial sorting and wave acceleration. *Comptes Rendus de l'Académie des Sciences, Série I*, vol. 350, pp. 761–766.

Boukal, S.D. and Berec, L. (2002). Single-species Models of the Allee Effect: Extinction Boundaries, Sex Ratios and Mate Encounters. *Journal of Theoretical Biology*, vol. 218, pp. 375–394.

Buonaccorsi, J.P., Elkinton, J.S., Evans, S.R. and Liebhold, A.M. (2001). Measuring and testing for spatial synchrony. *Ecology*, vol. 82, pp. 1668–1679.

Chakraborty, A., Singh, M., Lucy, D. and Ridland, P. (2007). PredatorâĂŞpreymodel with prey-taxis and diffusion. *Mathematical and Computer Modelling*, vol. 46, pp. 482–498.

Clark, J.S., Fastie, C., Hurtt, G. and Jackson, S.T. (1998). Reid's paradox of rapid plant migration. *Bioscience*, vol. 48, pp. 13–24.

Clark, J.S., Lewis, M. and Horvath, L. (2001). Invasion by extrems: Population spread with variation in dispersal and reproduction. *American Naturalist*, vol. 157, pp. 537–554.

Cohen, A.N. and Carlton, J.T. (1998). Accelerating invasion rate in a highly invaded estuary. *Science*, vol. 279, pp. 555–558.

Colautti, R.I., Grigorovich, I.A. and MacIsaac, H.J. (2006). Propagule pressure: a null model for biological invasions. *Biological invasions*, vol. 8, pp. 1023–1037.

Coulson, T. and Godfray, H.C.J. (2007). *Theoretical ecology: Theoretical Ecology: Principles and Applications*, chap. Single-species dynamics. Oxford University Press.

Davis, M.A. (2009). *Invasion biology*. Oxford University Press.

Denno, R.F. and Peterson, M.A. (1995). *Population Dynamics: New Approaches and Synthesis*, chap. Density-dependent dispersal and its consequences for population dinamics. Elsevier Science.

Dewhirst, S. and Lutscher, F. (2009). Dispersal in heterogeneous habitats: thresholds, spatial scales, and approximate rates of spread. *Ecology*, vol. 90, pp. 1338–1345.

Dunbar, S.R. (1983). Travelling wave solutions of diffusive lotka-volterra equations. *Journal of Mathematical Biology*, vol. 17, pp. 11–32.

Dunbar, S.R. (1984). Traveling wave solutions of diffusive lotka-volterra equations: a heteroclinic connection in $\mathbb{R}^4$. *Transactions of the American Mathematical Society*, vol. 286, pp. 557–594.

Dunning Jr., J.B., Stewart, D.J., Danielson, B.J., Noon, B.R., Root, T.L., Lamberson, R.H. and Stevens, E.E. (1995). Spatially explicit population models: Current forms and future uses. *Ecological Applications*, vol. 5, pp. 3–11.

El Abdllaoui, A., Auger, P., Kooi, B.W., Bravo de la Parra, R. and Mchich, R. (2007). Effects of density dependent migrations on the dynamics of a predator prey model. *Mathematical Bioscience*, vol. 210, pp. 335–354.

Fahrig, L. (2007). Non-optimal animal movement in human-altered landscapes. *Functional Ecology*, vol. 21, pp. 1003–1015.

Fang, J. and Tacher, L. (2003). An efficient and accurate algorithm for generating spatially-correlated random fields. *Communications in numerical methods in engineering*, vol. 19, pp. 801–808.

Ferrer, X., Motis, A. and Peris, S.J. (1991). Changes in the breeding range of starlings in the iberian peninsula during the last 30 years: Competition as a limiting factor. *Journal of Biogeography*, vol. 18, pp. 631–636.

Fisher, R.A. (1937). The wave advance of advantageous genes. *Annals of Eugenics*, vol. 7, pp. 355–369.

Flinn, K.M., Gouhier, T.C., Lechowicz, M.J. and Waterway, M.J. (2010). The role of dispersal in shaping plant community composition of wetlands within an old-growth forest. *Ecology*, vol. 98, pp. 1292–1299.

Forrester, G.E. and Steele, M.A. (2004). Predators, prey refuges, and the scaling of density-dependent prey mortality. *Ecology*, vol. 85, pp. 1332–1342.

Fortin, M.-J. and Dale, M.R.T. (2005). *Spatial Analysis: A Guide for Ecologists*. Cambridge University Press.

Fraser, D.F. and Gilliam, J.F. (1992). Nonlethal impacts of predator invasion: Facultative suppression of growth and reproduction. *Ecology*, vol. 73, pp. 959–970.

Gaines, D.S. and Bertness, M. (1993). The dynamics of juvenile dispersal: Why field ecologists must integrate. *Ecology*, vol. 74, pp. 2430–2435.

Gao, M., Li, W., Li, Z., Dai, H. and Liu, H. (2007). Spatial synchrony in host-parasitoid populations. *Ecological Modelling*, vol. 204, pp. 29–39.

Geller, J., Sotka, E., Kado, R., Palumbi, S. and Schwindt, E. (2008). Sources of invasions of a northeastern pacific acorn barnacle, balanus glandula, in japan and argentina. *Marine Ecology Progress Series*, vol. 358, pp. 211–218.

Gertzen, E.L., Leung, B. and Yan, N.D. (2011). Propagule pressure, Allee effects and the probability of establishment of an invasive species (bythotrephes longimanus). *Ecosphere*, vol. 2, pp. 1–17.

Gonzalez-Olivares, E. and Ramos-Jiliberto, R. (2003). Dynamic consequences of prey refuges in a simple model system: more prey, fewer predators and enhanced stability. *Ecological Modelling*, vol. 166, pp. 135–146.

Gotelli, N.J. (1991). Metapopulation models: The rescue effect, the propagule rain, and the core-satellite hypothesis. *The American Naturalist*, vol. 138, pp. 768–776.

Gruntfest, Y., Arditi, R. and Domrovsky, Y. (1997). A Fragmented Population in a Varying Environment. *Journal of Theoretical Biology*, vol. 185, pp. 539–547.

Gurney, W. and Nisbet, R. (1975). The regulation of inhomogeneous populations. *Journal of theoretical biology*, vol. 52, pp. 441–457.

Hadeler, K.P. (1981). *Numerical treatments of free boundary value problems*, chap. Travelling fronts and free boundary value problems. Bassel: Birkhaouser.

Hanski, I. (1998). Metapopulation dynamics. *Nature*, vol. 396, pp. 41–49.

Hassell, M.P., Comins, H.N. and Mayt, R.M. (1991). Spatial structure and chaos in insect population dynamics. *Nature*, vol. 353, pp. 255–258.

Hastings, A. (1996). Models of spatial spread: A synthesis. *Biological Conservation*, vol. 78, pp. 143–148.

Hastings, A., Cuddington, K., Davies, K.F., Dugaw, C.J., Elmendorf, S., Freestone, A., Harrison, S., Holland, M., Lambrinos, J., Malvadkar, U., Melbourne, B.A., Moore, K., Taylor, C. and Thomson, D. (2005). The spatial spread of invasions: new developments in theory and evidence. *Ecology Letters*, vol. 8, pp. 91–101.

Hengeveld, R. (1989). *Dynamics of biological invasions*. Chapman & Hall, London.

Holmes, E.E., Lewis, M.A., Banks, J.E. and Veit, R.R. (1994). Partial differential equations in ecology: Spatial interactions and population dynamics. *Ecology*, vol. 75, pp. 17–29.

Holway, D.A. and Suarez, A.V. (1999). Animal behavior: an essential component of invasion biology. *Trends in Ecology and Evolution*, vol. 14, pp. 328–330.

Hosono, Y. (1998). The minimal speed of travelling fronts for a diffusive Lotka-Volterra competition model. *Bulletin of Mathematical Biology*, vol. 60, pp. 435–448.

Hughes, C.L., Dytham, C., and Hill, J.K. (2007). Modelling and analysing evolution of dispersal in populations at expanding range boundaries. *Ecological Entomology*, vol. 32, pp. 437–445.

Hughes, C.L., Hill, J.C. and Dytham, C. (2003). Evolutionary trade-offs between reproduction and dispersal in populations at expanding range boundaries. *Proceedings of the Royal Society London B*, vol. 270, pp. S147–S150.

Hui, C., Krug, R.M. and Richardson, D.M. (2011). *Fifty years of invasion ecology*, chap. Modelling spread in invasion ecology: a synthesis, pp. 329–344. Wiley-Blackwell.

Hui, C., Roura-Pascual, N., Brotons, L., Robinson, R.A. and Evans, K.L. (2012). Flexible dispersal strategies in native and non-native ranges: environmental quality and the 'good-stay, bad-disperse' rule. *Ecography*, vol. Early View, p. 1024âĂŞ1032.

Hui, C., Veldtman, R. and McGeoch, M.A. (2010). Measures, perceptions and scaling patterns of aggregated species distributions. *Ecography*, vol. 33, pp. 95–102.

Ims, R. and Andreassen, H.P. (2000). Spatial synchronization of vole population dynamics by predatory birds. *Nature*, vol. 408, pp. 194–196.

Ims, R.A. and Andreassen, H.P. (2005). Density-dependent dispersal and spatial population dynamics. *Prococedings of the Royal Society B*, vol. 272, pp. 913–918.

Jansen, V.A. (2001). The dynamics of two diffusively coupled predator-prey populations. *Theoretical Population Biology*, vol. 59, pp. 119–131.

Jenkins, D.G., Brescacin, C.R., Duxbury, C.V., Elliott, J.A., Evans, J.A., Grablow, K.R., Hillegass, M., Lyon, B.N., Metzger, G.A., Olandese, M.L., Pepe, D., Silvers, G.A., Suresch, H.N., Thompson, T.N., Trexler, C.M., Williams, G.E., Williams, N.C. and Williams, S.E. (2007). Does size matter for dispersal distance? *Global Ecology and Biogeography*, vol. 16, pp. 415–425.

Kawasaki, K. and Shigesada, N. (2007). An integrodifference model for biological invasions in a periodically fragmented environment. *Japan Journal of Industrial and Applied Mathematics*, vol. 24, pp. 3–15.

Kinezaki, N., Kawasaki, K. and Shigesada, N. (2006). Spatial dynamics of invasion in sinusoidally varying environments. *Population Ecology*, vol. 48, pp. 263–270.

Klaassen, R.H.G., Nolet, B.A. and Bankert, D. (2006). Movement of foraging tundra swans explained by spatial pattern in cryptic food densities. *Ecology*, vol. 87, pp. 2244–2254.

Kokubun, N., Iida, K. and Mukai, T. (2008). Distribution of murres (Uriaspp.) and their prey south of St. George Island in the southeastern Bering Sea during the summers of 2003-2005. *Deep Sea Research*, vol. 55, pp. 1827–1836.

Kolmogorov, A., Petrovskii, I. and Piscounov, N. (1991). *Selected Works of A.N. Kolmogorov*, chap. A study of the diffusion equation with increase in the amount of substance, and its application to a biological problem, pp. 248–270. Kluwer.

Korsu, K. and Huusko, A. (2009). Propagule pressure and initial dispersal as determinants of establishment success of brook trout (*Salvelinus fontinalis* Mitchill 1814). *Aquatic invasions*, vol. 4, pp. 619–626.

Kot, M. (1992). Discrete-time travelling waves: Ecological examples. *Mathematical Biology*, vol. 30, pp. 413–436.

Kot, M., Lewis, M. and van den Driessche, P. (1996). Dispersal data and the spread of invading organisms. *Ecology*, vol. 77, pp. 2027–2042.

Kramer, A.M., Dennis, B., Liebhold, A.M. and Drake, J.M. (2009). The evidence for Allee effects. *Population Ecology*, vol. 51, pp. 341–354.

Krebs, C.J., Gaines, M., Keller, B.L., Myers, J. and Tamarin, R.H. (1973). Population cycles in small rodents. *Science*, vol. 179, pp. 35–41.

Lande, R. (1993). Risks of population extinction from demographic and environmental stochasticity and random catastrophes. *The American Naturalist*, vol. 142, pp. 911–927.

Lawrence, D.J. and Cordell, J.R. (2010). Relative contributions of domestic and foreign sourced ballast water to propagule pressure in puget sound, washington, usa. *Biological Conservation*, vol. 143, pp. 700–709.

Levine, J.M. and Murrell, D.J. (2003). The community level consequences of seed dispersal patterns. *Annual Review of Ecology, Evolution, and Systematics*, vol. 34, pp. 549–574.

Levins, R. (1969). Some demographic and genetic consequences of environmental heterogeneity for biological control. *Bulletin of the Ecological Society of America*, vol. 15, pp. 237–240.

Lewis, M. and Kareiva, P. (1993). Allee dynamics and the spread of invading organisms. *Theoretical Population Biology*, vol. 43, pp. 141–158.

Lewis, M.A. (1997). *Spatial Ecology: The Role of Space in Population Dynamics and Interspecific Interactions*, chap. Variability, patchiness and jump dispersal in the spread of an invading population, pp. 46–69. Princeton University Press.

Li, K. and Li, X. (2012). Asymptotic behavior and uniqueness of travelling wave solution in ricker competition system. *Journal of Mathematical Analysis and Applications*, vol. 389, pp. 486–497.

Li, Z., Gao, M., Hui, C., Han, X. and Shi, H. (2005). Impact of predator pursuit and prey evasion on synchrony and spatial patterns in metapopulation. *Ecological Modelling*, vol. 185, pp. 245–254.

Liebhold, A.M. and Tobin, P.C. (2008). Population ecology of insect invasions and their management. *Annual review of entomology*, vol. 53, pp. 387–408. ISSN 0066-4170.

Limpert, E., Stahel, W.A. and Abbt, M. (2001). Log-normal distributions across the sciences: Keys and clues. *Bioscience*, vol. 51, pp. 341–352.

Lindén, E. (2007). The more the merrier: Swarming as an antipredator strategy in the mysid neomysis integer. *Aquatic Ecology*, vol. 41, pp. 299–307.

Lloyd, A.L. and May, R.M. (1999). Synchronicity, chaos and population cycles: spatial coherence in an uncertain world. *Trends in Ecology and Evolution*, vol. 14, pp. 417–418.

Lockwood, J.L., Cassey, P. and Blackburn, T. (2005). The role of propagule pressure in explaining species invasions. *Trends in Ecology and Evolution*, vol. 20, pp. 223–228.

Lonsdale, W.M. (1993). Rates of spread of an invading species–mimosa pigra in northern Australia. *Ecology*, vol. 81, pp. 513–521.

Lutscher, F. (2007). A short note on short dispersal events. *Bulletin of mathematical biology*, vol. 69, p. 1615.

Lutscher, F. (2008). Density-dependent dispersal in integrodifference equations. *Journal of Mathematical Biology*, vol. 56, pp. 499–524.

Lutscher, F. and Petrovskii, S.V. (2008). The importance of census times in discrete-time growth-dispersal models. *Journal of Biological Dynamics*, vol. 2, pp. 55–63.

Mack, R.N., Simberloff, D., Londsale, W.M., Evans, H., Cout, M. and Bazzaz, F. (2000). Biotic invasions: causes, epidemiology, global consequences and control. *Ecological applications*, vol. 10, pp. 689–710.

Madsen, T. and Shine, R. (1996). Seasonal migration of predators and prey–a study of pythons and rats in tropical Australia. *Ecology*, vol. 77, pp. 149–156.

Magurran, A.E. (1988). *Ecological Diversity and its Measurement*. London: Croom Helm.

Malthus, T.R. (1798). An essay on the principle of population.
Available at: `http://www.econlib.org/library/Malthus/malPop.html`

Matter, S.F. (2001). Synchrony, extinction, and dynamics of spatially segregated, heterogeneous populations. *Ecological Modelling*, vol. 141, pp. 217–226.

Matthysen, E. (2005). Density-dependent dispersal in birds and mammals. *Ecography*, vol. 28, pp. 403–416.

May, R.M. and McLean, A.R. (2007). *Theoretical Ecology: Principles and Applications*. Oxford University Press.

McCann, K., Hastings, A., Harrison, S. and Wilson, W. (2000). Population outbreaks in a discrete world. *Theoretical Population Biology*, vol. 57, pp. 97–108.

Meyer, P.S. and Ausubel, J.H. (1999). Carrying capacity: A model with logistically varying limis. *Technolotical Forecasting and Social Change*, vol. 61, pp. 209–2014.

Mikheyev, A.S., Tchingnoumba, L., Henderson, A. and Alonso, A. (2008). Effect of propagule pressure on the establishment and spread of the little fire ant *Wasmannia auropunctata* in a Gabonese oil field. *Diversity and Distributions*, vol. 14, pp. 301–306.

Miller, T.E. and Tenhumberg, B. (2010). Contributions of demography and dispersal parameters to the spatial spread of a stage-structured insect invasion. *Ecological Applications*, vol. 20, pp. 620–633.

Mollison, D. (1977). Spatial contact models for ecological and epidemic spread. *Journal of the Royal Statistical Society. Series B*, vol. 39, pp. 283–326.

Mollison, D. (1991). Dependence of epidemic and population velocities on basic parameters. *Mathematical Bioscience*, vol. 107, pp. 255–287.

Moran, P. (1953). The statistical analysis of the canadian lynx cycle. *Australian Journal of Zoology*, vol. 1, pp. 291 – 298.

Morse, D.H. (2006). Fine-scale substrate use by a small sit-and-wait predator. *Behavioral Ecology*, vol. 17, pp. 405–409.

Morse, D.H. and Schmitt, J. (1985). Propagule size, dispersal ability, and seedling performance in *Asclepias syriaca*. *Oecologia*, vol. 67, pp. 372–379.

Münkemüller, T. and Johst, K. (2008). Spatial synchrony through density-independent versus density-dependent dispersal. *Journal of Biological Dynamics*, vol. 2, pp. 31–9.

Murray, J.D. (2002). *Mathematical Biology*. Springer.

Murrell, D.J., Travis, J.M.J. and Dytham, C. (2002). The evolution dispersal of population in spatially structured populations. *OIKOS*, vol. 97, pp. 229–236.

Neubert, M.G. and Caswell, H. (2000). Demography and dispersal: Calculation and sensitivity analysis of invasion speed for structured populations. *Ecology*, vol. 81, pp. 1613–1628.

Neubert, M.G., Kot, M. and Lewis, M. (1995). Dispersal and pattern formation in a discrete-timepredator-preymodel. *Theoretical Population Biology*, vol. 48, pp. 7–43.

Nguyen-Huu, T., Lett, C., Auger, P. and Poggiale, J. (2006). Spatial synchrony in host-parasitoid models using aggregation of variables. *Mathematical Biosciences*, vol. 203, pp. 204–221.

Nowicki, P. and Vrabec, V. (2011). Evidence for positive density-dependent emigration in butterfly metapopulations. *Oecologia*, vol. 167, pp. 657–665.

Okubo, A., Maini, P.K., Williamson, M.H. and Murray, J.D. (1989). On the spatial spread of the grey squirrel in britain. *Proceedings of the Royal Society London B*, vol. 238, pp. 113–125.

Okubu, A. (1988). *Acta XIX Congressus Internationalis Ornithologici*, vol. 1, chap. Diffusion-type models for avian range expansion, pp. 1038–1049. Ottawa Press.

Oshanin, G., Vasilyev, O., Krapivsky, P.L. and Klafter, J. (2009). Survival of an evasive prey. *PNAS*, vol. 106, pp. 13696–13701.

Owen, M.R. and Lewis, M.A. (2001). How predation can slow, stop or reverse a prey invasion. *Bulletin of Mathematical Biology*, vol. 63, pp. 655–684.

Pärn, H., Ringsby, T.H., Jensen, H. and Saether, B.E. (2012). Spatial heterogeneity in the effects of climate and density-dependence on dispersal in a house sparrow metapopulation. *Proceedings of the Royal Society London B*, vol. 279, pp. 144–152.

Pearson, R.G. and Dawson, T.P. (2005). Long-distance plant dispersal and habitat fragmentation: identifying conservation targets for spatial landscape planning under climate change. *Biological Conservation*, vol. 123, pp. 389–401.

Petit, J.N., Hoddle, M.S., Grandgirard, J., Roderick, G.K. and Davies, N. (2008). *Tahiti: Implications for its use as a biological control agent against Homalodisca vitripennis (Hemiptera: Cicadellidae)*, vol. 45, chap. Short distance dispersal behavior and establishment of the parasitoid Gonatocerus ashmeadi (Hymenoptera: Mymaridae), pp. 344–352. Biological Control.

Petrovskii, S.V. and Li, B.L. (2005). *Exactly Solvable Models of Biological Invasion*. Chapman & Hall/CRC.

Phillips, B., Brown, G., Geenlees, M., Webb, J. and Shine, R. (2007). Rapid expansion of the cane toad (bufo marinus) invasion front in tropical Australia. *Austral Ecology*, vol. 32, pp. 169–176.

Phillips, B., Brown, G. and Shine, R. (2010). Life-history evolution in range-shifting populations. *Ecology*, vol. 91, pp. 1617–1627.

Phillips, B.L., Gregory, P.B., Travis, J.M.J. and Shine, R. (2008). Reid's paradox revisited: The evolution of dispersal kernels during range expansion. *The American Naturalist*, vol. 172, pp. S34–S48.

Pielou, E.C. (1969). *An introduction to Mathematical Ecology*. Wiley, New York.

Pielou, E.C. (1977). *Mathematical Ecology*, chap. Population dynamics. John Wiley and Sons Inc, Canada.

Pielou, E.C. (1979). *Biogeography*. Wiley, New York.

Pimentel, D., Zuniga, R. and Morrison, D. (2005). Update on the environmental and economic costs associated with alien-invasive species in the united states. *Ecological Economics*, vol. 52, pp. 273–288.

Preston, F.W. (1962). The canonical distribution of commonness and rarity. *Ecology*, vol. 43, pp. 185–215.

Rabinowitz, D. (1978). Dispersal properties of mangrove propagules. *Biotropica*, vol. 10, pp. 47–57.

Ramanantoanina, A., Hui, C. and Ouhinou, A. (2011). Effects of density-dependent dispersal behaviours on the speed and spatial patterns of range expansion in predator-prey metapopulations. *Ecological Modeling*, vol. 222, pp. 3524–3530.

Rehage, J.S. and Sih, A. (2004). Dispersal behavior, boldness, and the link to invasiveness: a comparison of four gambusia species. *Biological Invasion*, vol. 6, pp. 379 – 391.

Ricker, W.E. (1954). Stock and recruitment. *Journal of the Fisheries Research Board of Canada*, vol. 11, pp. 559–623.

Rosenzweig, M.L. and MacArthur, R.H. (1963). Graphical representation and stability conditions of predator-prey interactions. *The American Naturalist*, vol. 97, pp. 209–223.

Sanchez-Garduno, F. and Maini, P.K. (1994). Existence and uniqueness of a sharp travelling wave in degenerate non-linear diffusion fisher-kpp equations. *Journal of Mathematical Biology*, vol. 33, pp. 163–192.

Sanchez-Garduno, F., Maini, P.K. and Kappos, E. (1997). A review of travelling wave solutions of one-dimensional reaction-diffusion equations with non-linear diffusion term. *FORMA*, vol. 11, pp. 45–59.

Sattenspiel, L. (2012). *The Geographic Spread of Infectious Diseases: Models and Applications*. Princeton series in Theoretical and Computational Biology.

Savidge, I.R. (1974). Social factors in dispersal of deer mice (Peromyscus maniculatus) from their natal site. *American Midland Naturalist*, vol. 91, no. 2, pp. 395–405.

Savidge, J.A. (1987). Extinction of an island forest avifauna by an introduced snake. *Ecology*, vol. 68, pp. 660–668.

Schliehe-Diecks, S., M., E. and Kappeler, P.M. (2012). Walk the line-dispersal movements of gray mouse lemurs (microcebus murinus). *Behavioral Ecology and Sociobiology*, vol. 66, pp. 1175–1185.

Seward, N.W., VerCauteren, K.C., Witmer, G.W. and Engeman, R.M. (2004). Feral swine impacts on agriculture and the environment. *Sheep & Goat Research Journal*, vol. 19, pp. 34–40.

Shigesada, N. and Kawasaki, K. (1997). *Biological Invasions: Theory and Practice*. Oxford University Press.

Shigesada, N., Kawasaki, K. and Takeda, Y. (1995). Modeling stratified diffusion in biological invasions. *The American Naturalist*, vol. 146, pp. 229–251.

Shigesada, N., Kawasaki, K. and Teramoto, E. (1986). Traveling periodic waves in heterogeneous environments. *Theoretical Population Biology*, vol. 30, pp. 143–160.

Shine, R., Brown, G. and Phillips, B. (2011). An evolutionary process that assembles phenotypes through space rather than through time. *PNAS*, vol. 108, pp. 5708–5711.

Siegfried, W.R. and Underhill, L.G. (1975). Flocking as an anti-predatorstrategy in doves. *Animal Behaviour*, vol. 23, pp. 504–508.

Simberloff, D. (2009). The role of propagule pressure in biological invasions. *Annual Review of Ecology, Evolution, and Systematics*, vol. 40, pp. 81–102.

Simmons, A.D. and Thomas, C.D. (2004). Changes in dispersal during species' range expansions. *The American Naturalist*, vol. 164, pp. 378–395.

Skalski, G.T. and Gilliam, J.F. (2000). Modeling Diffusive Spread in a Heterogeneous Population: A Movement Study with Stream Fish. *Ecology*, vol. 81, no. 6, pp. 1685–1700.

Skellam, J.G. (1951). Random dispersal in theoretical populations. *Biometrika*, vol. 38, pp. 196–218.

Skellam, J.G. (1973). *The Mathematical Theory of the Dynamics of Biological Population*, chap. The Formulation and Interpretation of Mathematical Models of Diffusionary Processes in Population Biology. New York Academic Press.

Sutherland, W.J., Gill, J.A. and Norris, K. (2002). *Dispersal ecology*, chap. Density-dependent dispersal in animals: concepts, evidence, mechanisms and consequences, pp. 134–151. Blackwell, Oxford, UK.

Talavera, M., Arista, M. and Ortiz, P.L. (2012). Evolution of dispersal traits in a biogeographical context: a study using the heterocarpic rumex bucephalophorus as a model. *Ecology*, vol. 100, pp. 1194–1203.

Tao, Y. (2010). Global existence of classical solutions to a predatorâĂŞprey model with nonlinear prey-taxis. *Nonlinear Analysis: Real World Applications*, vol. 11, pp. 2056–2064.

Taylor, A.D. (1990). Metapopulations, dispersal, and predator-prey dynamics: An overview. *Ecology*, vol. 71, pp. 429–433.

Taylor, C.M. and Hall, R.J. (2012). Metapopulation models for seasonally migratory animals. *Biology Letters*, vol. 8, pp. 477–480.

Travis, J.M.J. and Dytham, C. (2002). Dispersal evolution during invasions. *Evolutionary Ecology Research*, vol. 4, pp. 1119–1129.

Travis, J.M.J., Mustin, K., Benton, T.G. and Dytham, C. (2009). Accelerating invasion rates results from evolution of density dependent dispersal. *Journal of theoretical biology*, vol. 259, pp. 151–158.

Tsyganov, M.A., Brindley, J., Holden, A.V. and Biktashev, V.N. (2004). Soliton-like phenomena in one-dimensional cross-diffusion systems: a predator-prey pursuit and evasion example. *Physica D: Nonlinear Phenomena*, vol. 197, pp. 18–33.

Veit, R.R. and Lewis, M.A. (1996). Dispersal, population growth, and the Allee effect: dynamics of the house finch invasion of eastern north america. *American Naturalist*, vol. 148, pp. 255–274.

Verhulst, P.F. (1838). *Correspondance mathématique et physique*, vol. 10, chap. Notice sur la loi que la population poursuit dans son accroissement, pp. 113–121. Societe Belge de librairie.

Wang, M.H., Kot, M. and Neubert, M.G. (2002). Integrodifference equations, Allee effects, and invasions. *Journal of Mathematical Biology*, vol. 44, pp. 150–168.

Weinberger, H.F. (1982). Long-time behavior of a class of biological models. *SIAM Journal on Mathematical Analysis*, vol. 13, pp. 353–396.

Weinberger, H.F., Kawasaki, K. and Shigesada, N. (2008). Spreading speeds of spatially periodic integro-difference models for populations with nonmonotone recruitment functions. *Journal of Mathematical Biology*, vol. 57, pp. 387–411.

Weinberger, H.F., Lewis, M.A. and Li, B. (2002). Analysis of linear determinacy for spread in cooperative models. *Journal of Mathematical Biology*, vol. 45, pp. 183–218.

Weng, K.C., Boustany, A.M., Pyle, P., Anderson, S.D., Brown, A. and Block, B.A. (2007). Migration and habitat of white sharks (*Carcharodon carcharias)* in the eastern Pacific Ocean. *Marine Biology*, vol. 152, pp. 877–894.

Wilson, J.R., Richardson, D.M., Rouget, M., Proches, S., Amis, M.A., Henderson, L. and Thuiller, W. (2007). Residence time and potential range: crucial considerations in modelling plant invasions. *Diversity and Distributions*, vol. 13, pp. 11–22.

Wilson, W.G., Deroos, A.M. and Mccauley, E. (1993). Spatial instabilities within the diffusive lotka-volterra system: Individual-based simulation results. *Theoretical Population Biology*, vol. 43, pp. 91–127.

With, K.A. (2002). The landscape ecology of invasive spread. *Conservation Biology*, vol. 16, pp. 1192–1203.

With, K.A. and King, A.W. (2001). Analysis of landscape sources and sinks: the effect of spatial pattern on avian demography. *Biological Conservation*, vol. 100, pp. 75–88.

Yamamura, K. (2002). Dispersal distance of heterogeneous populations. *Population Ecology*, vol. 44, no. 2, pp. 93–101.

Zalewski, M. and Ulrich, W. (2006). Dispersal as a key element of community structure: the case of ground beetles on lake islands. *Diversity and Distributions*, vol. 12, pp. 767–775.